

ESTIMATE OF MUSCLE CONTRIBUTION TO SPINAL LOADS DURING
CONTINUOUS PASSIVE MOTION FOR LOW BACK PAIN

APPROVED BY SUPERVISORY COMMITTEE

John J. Triano, D.C., Ph.D.

Robert C. Eberhart, Ph.D.

C.J. Chuong, Ph.D.

DEDICATION

I want to express my greatest respect and admiration for my advisor Dr. John J. Triano for his guidance and encouragement during my entire thesis. I would also like to thank my committee members Dr. C. J. Chuong and Dr. Robert C. Eberhart for their recommendations on my thesis. Next, I want to give a special thank you to Dr. Marion McGregor for her support and direction in statistical analysis. Last, I would like to convey my love and appreciation for the unending encouragement and faith of my family and friends.

This work was supported in part by

The Spinal Health Group

Leader Health Technologies

ESTIMATE OF MUSCLE CONTRIBUTION TO SPINAL LOADS DURING
CONTINUOUS PASSIVE MOTION FOR LOW BACK PAIN

by

JENNIFER MARIE DIEDERICH

THESIS

Presented to the Faculty of the Graduate School of Biomedical Sciences

The University of Texas Southwestern Medical Center at Dallas

And

The University of Texas at Arlington

In Partial Fulfillment of the Requirements

For the Degree of

MASTER OF SCIENCE IN BIOMEDICAL ENGINEERING

The University of Texas Southwestern Medical Center at Dallas

Dallas, Texas

May, 2005

Copyright

by

Jennifer Marie Diederich, 2005

All Rights Reserved

ESTIMATE OF MUSCLE CONTRIBUTION TO SPINAL LOADS DURING
CONTINUOUS PASSIVE MOTION FOR LOW BACK PAIN

Publication No. _____

Jennifer Marie Diederich, M.S.

The University of Texas Southwestern Medical Center at Dallas, 2005

John J. Triano, D.C., Ph.D.

This research is a first approximation model for determining the active loads in the lumbar spine during continuous passive motion (CPM) in the prone position. The study consisted of two groups' five healthy subjects and four subjects with the diagnosis of mechanical low back pain (LBP) at L4/L5/S1. Solutions to the issues in this investigation were sought in three stages. First was the introduction and synchronization of a number of sensors for making valid, time-linked observations of kinematic variables during CPM. Second, a root mean square myoelectric signal (RMS-MES) model was needed to calibrate muscle activation levels during feasible standardized tasks to be performed by low back pain

patients. Such a model must be able to partition passive and active load components acting on the lumbar spine and to estimate equivalent muscle loads from activity observed during CPM. Finally, biomechanical models are necessary for estimating the passive, active and total loads transmitted through the trunk during CPM.

Testing consisted of three calibration stances: upright, weighted holding 3lb weights in hands extended 90° at the shoulder and CPM at intermediate speed 11.5 degrees, fast speed 11.5 degrees, and intermediate speed at 20 degrees. Measurements recorded: 8 myoelectric signals (MES) of paired muscles (latissimus dorsi, multifidus, gluteus maximus, and hamstring femoris), 4 Polhemus Fastrak electromagnetic positioning sensors (lumbar, sacrum, 10cm posterior to center of knee, and table), linear accelerometer, uniaxial load cell, and modified treatment table with AMTI force plate.

Results demonstrate consistent repeatable measurements from the instrumented treatment table. The active loads created during CPM are minimal in comparison to the passive loads for both groups and therefore the muscle loads are not counteracting the implied therapy.

TABLE OF CONTENTS

List of FIGURES	ix
List of TABLES	xiii
List of APPENDICES	xiv
List of ABBREVIATIONS	xv
CHAPTER ONE - INTRODUCTION.....	1
Anatomy and Biomechanics of the Spine	3
Continuous Passive Motion Therapy	8
Purpose.....	12
CHAPTER TWO - PRELIMINARY STUDIES	13
Instrumentation	13
Validation of Kinematic Measures	15
Accelerometry	16
Consistency of Table Motion.....	18
Uniaxial Load Cell.....	18
Myoelectric Calibrations.....	20
CHAPTER THREE - EXPERIMENTAL METHODS	23
Table Foundation	23
Volunteer Selection.....	26
MES Calibration Testing	27
CPM Testing	29
Biomechanical Modeling.....	32

Data Reduction.....	43
Statistical and Data Analysis	44
CHAPTER FOUR - RESULTS	45
Validation of Kinematic Measures	45
Accelerometry	49
Generalizability of Table Motion.....	53
Uniaxial Load Cell.....	56
Subjects	57
Validation of the Biomechanical Model	58
MES-RMS Predicted Loads.....	59
Inverse Dynamics Model of CPM	60
Overview of MES-RMS Activity	63
Low Back CPM Transmitted Loads	69
CHAPTER FIVE - DISCUSSION.....	81
CHAPTER SIX - CONCLUSIONS.....	82
CHAPTER SEVEN - RECOMMENDATIONS FOR FUTURE WORK	84
APPENDIX A - CONSENT FORM.....	- 85 -
APPENDIX B - MATLAB PROGRAMS.....	92
BIBLIOGRAPHY	115
Vitae	119

LIST OF FIGURES

Figure 1:	Spinal Pain Generators - Common Tissue Sources of Low Back Pain Within the Functional Spinal Unit (Fsu).	2
Figure 2:	Functional Spinal Unit (FSU) - Two Vertebrae and the Intervening Disc with Ligaments Between Constitute the Smallest Functional Unit of the Spine Under Equilibrium Conditions for Upright Posture.....	4
Figure 3:	Lumbopelvis - The Lumbar Spine And Pelvis are a Mechanical Linkage That Forms a Concave Curvature Posteriorly. Downward Load Bearing (White Arrows) is Distributed to the Legs Through the Pelvis. The Oval Locates the L5/S1 Segment and the Black Area Overlays the Multifidus Muscle as it Crosses the L5/S1 Transverse Plane.	5
Figure 4:	Immobilized Facet Joint.....	10
Figure 5:	Schematic of Instrumentation Input into Motion Monitor and Output of Filtered Data.	14
Figure 6:	Linear accelerometer Attached to the Pendulum on the Treatment Table.....	17
Figure 7:	Load Cell in the Modified Cam-Drive.....	19
Figure 8:	Instrumented treatment table – ACC = Pylon Supporting Accelerometer and Table Position Sensor, FP = AMTI Force Plate, Gap = Table Support Gap, LC = Uniaxial Load Cell, MES = BIOPAC 8 Channel EMG, MM = Motion Monitor, P = Polhemus Magnetic Transmitter.	25

Figure 9: Subject Positioned on the CPM Table at Table Stroke of 11.5°. Sensors for Measuring the MES and Position can be Observed Attached at their Sites in Relation to Anatomical Landmarks.	31
Figure 10: Calibration model - Free Body Diagrams and Equilibrium Equations for the Standardized Postures.	36
Figure 10-a: Upright Stance.....	36
Figure 10-b: Weighted Stance	37
Figure 10-c: Flexion Stance.....	38
Figure 11: CPM Experimental Environment.....	39
Figure 12: Free Body Diagram and Equilibrium Equations for the Constrained Inverse Dynamics Model.....	41
Figure 13-a: Comparison of Polhemus Transmitter Height in Relation to Percent Error of Measured Distance in X-Axis to Data Collected for Sensors.....	46
Figure 13-b: Comparison of Polhemus Transmitter Height in Relation to Percent Error of Measured Distance in Y-Axis to Data Collected for Sensors.....	47
Figure 13-c: Comparison of Polhemus Transmitter Height in Relation to Percent Error of Measured Distance in Z-Axis to Data Collected for Sensors	48
Figure 14: Linear Acceleration Profiles, Double Differentiated Marker Versus Accelerometer Output, for Intermediate Setting at 0.245 Hz	50
Figure 15: Linear Acceleration Profiles, Double Differentiated Marker Versus Accelerometer Output for Higher Setting at 0.5 Hz	51

Figure 16: Theoretical Sine Function Estimation of the Table Angular Acceleration Compared to the Calculated Angular Acceleration from the Linear Accelerometer	52
Figure 17: Acceleration Profiles Comparing Performance of Eight Commercial Tables with that of the Instrumented Table for this Study Set at Approximately 0.5 Hz	54
Figure 18: Data From the Subject in Figure 14 is Plotted in Conjunction with a Second Subject of Smaller Stature	55
Figure 19: Displacement of Lower Body Segments and Table in the Vertical (Z) Axis ...	62
Figure 20-a: Variability of Lag to Greatest and Least RMS Amp with Table Position Between Healthy and LBP Groups During CPM at Intermediate Speed	66
Figure 20-b: Variability of Lag to Greatest and Least RMS Amp with Table Position Between Healthy and LBP Groups During CPM at Fast Speed	67
Figure 20-c: Variability of Lag to Greatest and Least RMS Amp with Table Position Between Healthy and LBP Groups During CPM at Intermediate Speed with 20 Degrees	68
Figure 21-a: Intermediate Speed Grand Mean of Healthy Active and Passive Sagittal CPM Loads 11.5 Degree Angular Motion	73
Figure 21-b: Intermediate Speed Grand Mean of LBP Active and Passive Sagittal CPM Loads 11.5 Degree Angular Motion	74
Figure 21-c: Fast Speed Grand Mean of Healthy Active and Passive Sagittal CPM Loads 11.5 Degree Angular Motion	75

Figure 21-d: Fast Speed Grand Mean of LBP Active and Passive Sagittal CPM Loads 11.5

Degree Angular Motion 76

Figure 21-e: Intermediate Speed Grand Mean of Healthy Active and Passive Sagittal CPM

Loads at 20 Degree Angular Motion 77

Figure 21- f: Intermediate Speed Grand Mean of LBP Active and Passive Sagittal CPM

Loads at 20 Degree Angular Motion 78

Figure 22: Active Loads for Healthy and LBP Groups During CPM at Intermediate Speed,

Fast Speed, and Intermediate Speed at 20 Degrees 80

LIST OF TABLES

Table 1: Inclusion / Exclusion Criteria for LBP Group	27
Table 2: MES Sensor Placement.....	28
Table 3: MES Calibration Stance Testing.....	29
Table 4: CPM Testing.....	32
Table 5: Moment Arms for Biomechanical Models	35
Table 6: Comparison of Load Cell Output with Output From Factory Calibration, and Following Adjusted Calibration with Known Static Loads Stacked In-Line on the Load Cell and Force Plate.....	57
Table 7: Comparison of Mean Force and Moment Estimations Between the 3D Commercial Model and the 2D Static Model Developed for this Project.....	59
Table 8: Calculation of Table Angular Displacement From Peak Marker Vertical Displacements and Mean Distance of Marker Site Along the Table Length (Y- Axis).....	63
Table 9: Greatest RMS Amplitude, Cycle Lag, and Predicted Load for Healthy and LBP Groups.....	65
Table 10: Mean MES-RMS Values per Full Cycle	69
Table 11: Regression Equation Coefficients and Associated Significance Values	73

LIST OF APPENDICES

APPENDIX A - CONSENT FORM.....	85
APPENDIX B - MATLAB PROGRAMS.....	92

LIST OF ABBREVIATIONS

CPM – Continuous passive motion

LBP – Low back pain

FSU – Functional spine unit

MES – Myoelectric signal

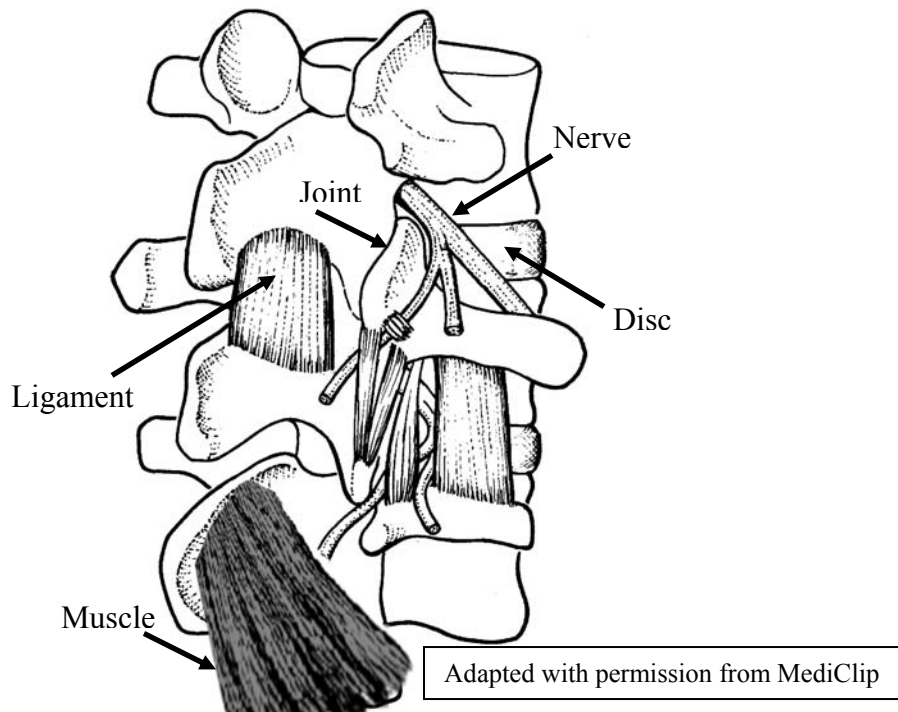
RMS – Root mean square

CHAPTER ONE

INTRODUCTION

Continuous passive motion (CPM) is a method of treatment originating in the 1970s for rehabilitation of knee joints, post-operatively¹. Since that time, application has been extended to other joints and most recently has been employed in the non-operative care of patients with low back pain. CPM is the passive cycling of a joint or joints through a specified range of motion at a predetermined rate by a motorized device. Experimental evidence from animal and human studies¹⁻⁴, shows CPM has several beneficial effects including the reduction of edema⁵ from the joint or periarticular tissues, prevention or disruption of adhesions and promotion of cartilage repair. In non-operative low back care, it has the additional intent to reduce joint stiffness and alter local joint stresses⁶. Various sources of low back pain are known to exist^{7,8} and include the disc, facet joint, ligaments, nerve and muscle spasm (Figure 1). Damage to any of these tissues can result in local edema and clinical symptoms defined by the tissue source. Edema in the facet joint space, for example, may be caused by an acute injury or repetitive overloading of the functional spinal unit (FSU)⁹. The therapeutic mechanism of action for CPM is a time-dependent mechanical stimulation of the tissues¹⁰ with small amplitude loads. CPM is believed to invoke viscoelastic properties of the tissues, resulting in creep deformity and the dispersion of fluid from tissue compartments.

Figure 1: Spinal Pain Generators - Common Tissue Sources of Low Back Pain Within the Functional Spinal Unit (FSU).



While the use of CPM as a therapeutic method for low back pain has increased, little is known about its biomechanics. Two studies have been conducted using CPM in seated configuration^{10;11}, however, most clinical applications are recumbent. While limited descriptive data⁶ suggests that the loads transmitted through the torso are small, no information is available on load control parameters. The therapeutic treatment has not been defined in relation to the duration, amplitude, or velocity in which CPM is applied. The loads being transmitted to the lumbar spine is a summation of the inertial load from the body segments being in motion, and if any, tension from the paraspinal muscles¹². The phase and

intensity of muscle activation within the CPM cycle also are unknown and may alter the therapeutic action in unpredictable ways.

The intent of this project is to quantify the biomechanics of continuous passive motion and, specifically to test two hypotheses related to its control parameters:

Hypothesis 1: Muscle activation during CPM is sufficiently small as to be negligible in the estimation of loads acting through the torso.

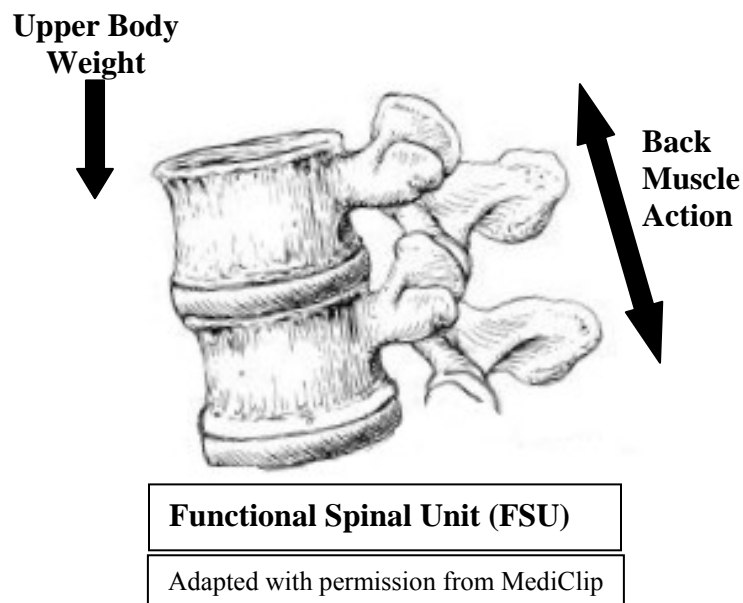
Hypothesis 2: Passive loads transmitted through the torso at the targeted spinal level are a function of the patient's stature and CPM speed.

Anatomy and Biomechanics of the Spine

The spinal column performs three basic functions: 1) it sustains loads and moments from the mass of the head, trunk, and weight placed above the pelvis; 2) it allows motion between the main segments of the body; and 3) it protects contents of the spinal cord from trauma⁷. The spine is a complex interlinked mechanical system with elements acting the role of levers, pivots, passive restraints, and activators. The basic linkage of the spine is called a functional spine unit (FSU) (Figure 2). Generally, the FSU is composed of the superior vertebrae, intervertebral disc, inferior vertebrae, and supporting ligamentous tissues. Anteriorly, the vertebral bodies and disc support the majority of the body weight. Posteriorly, the facet joints provide resistance to shear loads. The facet or zygapophyseal joints and discs act both as passive kinematic restraints and as pivots. The bony processes of the vertebrae are the levers in the overall mechanical system of the spine. The ligamentous tissues act as

passive range limiters giving support for the spine while the surrounding musculature is responsible for structural stability¹³ by stiffening the series of FSUs and act as actuators for motion in the spine⁹.

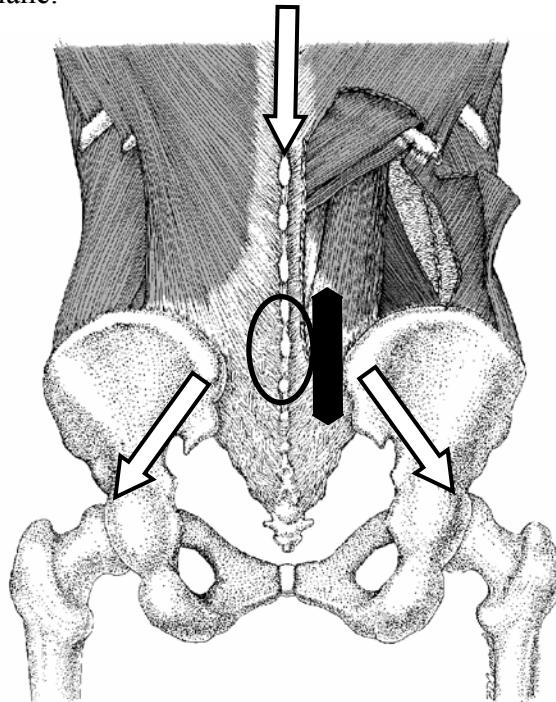
Figure 2: Functional Spinal Unit (FSU) - Two Vertebrae and the Intervening Disc with Ligaments Between Constitute the Smallest Functional Unit of the Spine Under Equilibrium Conditions for Upright Posture.



The lumbar region of the spine consists of a linkage of five vertebrae and discs that form a segmented beam-column on top of the pelvis⁷. Acting as a reinforced structural arch, the pelvis distributes the postural load downward to the legs. When the spine is viewed from a lateral aspect, the lumbar region forms a posterior concave curve (Figure 3). The thorax above the lumbar spine is relatively stiff owing to the interconnection of the thoracic

vertebrae, rib cage and sternum¹⁴. For purposes of this work, the thorax and pelvis will be considered rigid structures.

Figure 3: Lumbopelvis - The Lumbar Spine and Pelvis are a Mechanical Linkage That Forms a Concave Curvature Posteriorly. Downward Load Bearing (White Arrows) is Distributed to the Legs Through the Pelvis. The Oval Locates the L5/S1 Segment and the Black Area Overlays the Multifidus Muscle as it Crosses the L5/S1 Transverse Plane.



Adapted with permission from MediClip

The intervertebral discs act as pressure vessels consisting of three regions; cartilaginous end plates above and below, an outer laminated wall called the annulus fibrosis, and a central nucleus pulposus contained within. The nucleus is composed of fibrous strands

in a hydrophilic mucoprotein gel having a water content of 70-90%¹⁴. The annulus is made of individual laminar elements tightly bound together. Each lamina is constructed with collagen fibers oriented 30° to the disc plane and 120° from each other in alternating directions, moving radially from inside to outside of the disc¹⁵. The vertical dimensions undergo viscoelastic creep deformity with cycles of weight bearing. The fluid transfer between tissue compartments during load cycles contributes to nutritional support of the disc itself, as the adult disc is avascular. Nutrients transport in and metabolic wastes out with the tide of fluid flow. The cartilaginous endplates of the vertebra above and below the disc form the vertical boundaries for the disc and is composed of hyaline cartilage and acts as a shock absorber. Endplates are highly vascular, form tufts of capillaries at the upper and lower disc boundaries, supplying gradient concentrations of nutrients and waste to promote transfer to and from the disc material. The vertebrae bodies have the role of supporting the majority of postural load and as acting as connection points for forces transmitted by ligaments and muscle. Through the progression from the head downward to the pelvis there is a proportionate increase in vertebral size and mass to support the increasing load¹⁵. Extending posteriorly from the vertebral body are two bridging structures, the pedicles that, with the articular processes and laminae form the posterior arch. The arch encloses the spinal canal and the neural contents. Extending laterally are the transverse processes and posteriorly, the spinous processes that serve as primary levers for muscle attachments. The superior and inferior of the articular processes terminate in facet joint surfaces. Two posterior, inferior articular facets of the vertebra above interact with the superior articular facets of the vertebra below to form the zygapophyseal joints. The facet joints have a complex load sharing

interaction with the disc, providing for stabilization and motion control of the spine, and can be a direct source of pain¹⁴.

The pelvis forms a skeletal ring with the lumbar spine attaching through the lowest disc to the sacral bone centrally. The sacrum, acting as the keystone for the pelvic ring, is bounded laterally by two large bony structures through the sacroiliac joints. The pelvis closes its ring anteriorly at the symphysis pubis. Approximately two-thirds around the ring, on each side, is the acetabulum that articulates with the femur, the uppermost bone of the leg. Postural loads transmitted downward and distribute through the pelvic ring to the legs.

The ligaments connect the linkage of the individual bony segments. They function both as motion limiters, energy absorbers and as kinematic sensors that reflexively advise the nervous system of spinal status⁸. There are seven common ligaments which extend the length of the spine, connecting at each FSU. Ligaments are considered passive restraints because they are only active in tension and buckle in compression. The active direction is along the axis of the fibers and therefore each ligament is engaged depending on the combination of bending or twisting motions that a subject assumes.

The anterior longitudinal ligament attaches broadly over the front portion of each vertebra with a narrower section over the disc. The posterior longitudinal ligament attaches to the back of the vertebral body with wider section over the disc¹⁴. Intertransverse ligaments interconnect the transverse processes. Ligamenta flava extend from the anteroinferior laminae to the superior border of the adjacent laminae above. These ligaments contain a high proportion of elastic fibers that are under preload at rest. Through their inherent elastic tension, they provide a positive resting intradiscal pressure even when the subject is

reclining¹⁵. Interspinous ligaments connect between the adjacent spinous processes while the supraspinous ligament attaches to the posterior aspect of the spinous processes. Finally, the capsular ligament attaches adjacent articular process with fibers running perpendicular to the facet joints. They enclose the joint and help to contain the low viscosity synovial fluid that serves as an effective lubricant for the cartilaginous surfaces. The osseo-ligamentous spine, stripped of muscles, is a very unstable structure. The maximum compressive load on a spine that can be sustained without stabilizing action of the musculature is 20 N (4 lbf). The neuromuscular components are necessary for stability and physiologic function. Stabilizing muscles surround the spine. The posterior muscles are divided into deep, intermediate, and superficial groups. The deep muscles include interspinous, intertransverse and rotatores. The multifidus is an intermediate muscle that attaches the transverse processes of a vertebra to the spinous process of the above vertebra. The superficial muscles as a group are referred to as erector spinae and are subdivided from furthest lateral to medial as the iliocostalis, longissimus, and spinalis. The anterior muscles consist of four abdominal muscles: external oblique, internal oblique, transverses abdominis, and rectus abdominis.

Statistically, the majority of low back pain problems are associated with the lower lumbar spine and lumbopelvic junction¹⁶.

Continuous Passive Motion Therapy

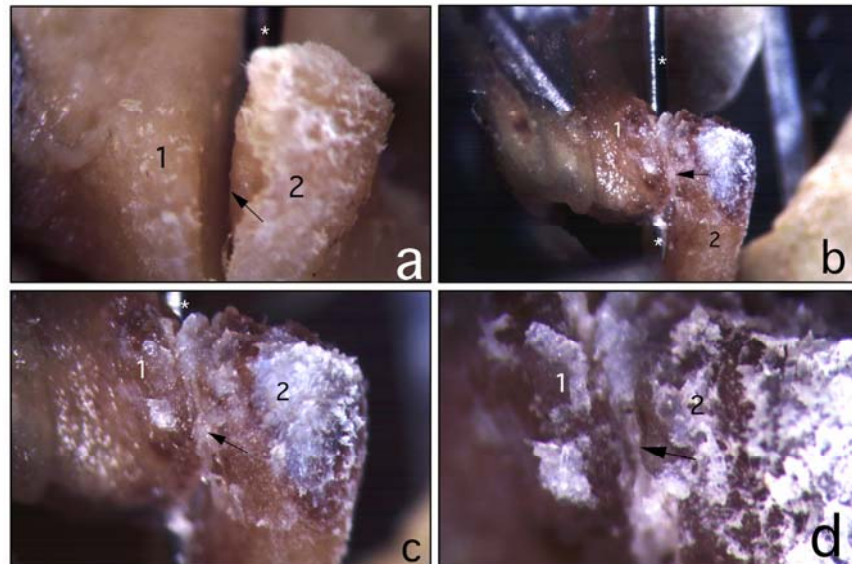
CPM was developed initially by Salter based on clinical observation and basic science research¹. The results of joint immobilization include stiffness, pain, muscle atrophy,

arthritis with reuse of joint, and disuse osteoporosis. Empirically, the fact that injured tissue can effectively repair while still bearing loads during function is evident from both musculoskeletal and cardiac examples. After cardiac surgery, even if the heart has undergone direct trauma, the tissue cannot be immobilized. On closure of any wounds, the heart continues to beat despite its wounds, distributing blood throughout the body. Similarly, regular respiration is necessary for adequate oxygen exchange supporting life. Injury to the costovertebral articulation or rib fractures may be supported but the thorax respiratory function is never immobilized following trauma. The joints themselves are seldom inflicted with degenerative changes¹.

Working with experimental cartilage defects in rabbit knees, Salter¹ hypothesized that movement passively applied to a joint in a non-weight bearing posture might be useful. He contrasted the effects on healing of the knee cartilage with three different types of rehabilitation: immobilization, intermittent activity within a cage, and CPM. The rabbits given 1 to 4 weeks of CPM showed the greatest healing of soft tissues, higher material strength of repaired tissue, and greater improvement in the range of motion. O' Driscoll, Salter, et al^{1;2;17} evaluated the effects of CPM acute joint hemarthrosis and edema, noting more rapid resolution and prevention of adhesion formation. Figure 4 shows the effects of experimental immobilization of the zygapophyseal joint in the lumbar spine using a rat animal model. Restricted movement in the facet results in the formation of adhesions between the cartilage surfaces and beginning of bone spur or osteophyte formation within twelve weeks.

Figure 4: Immobilized Facet Joint - Animal Model of Restricted Joint Movement Where “1”

is the Inferior Articular Process From the Bone Above and “2” is the Superior Articular Process From the Bone Below. A) Normal Gapping of the Facet Joint (Arrow) by Probe Insertion into the Articulation From Behind. B), C), D) Progressive Adhesion Formation Between the Joint Surfaces Over a 12 Week Interval. D) Shows a Small Osteophyte Beginning to Form (“1”) By 12 Weeks. (Courtesy of Charles Hendersen, DC, PhD Palmer University)



Spurred by Salter’s work, Coutts experimented with CPM in patients having total knee replacements³, which flaunted the accepted post-surgical practice to completely immobilize the leg for several days. These earlier practices resulted in increased joint stiffness as bleeding and edema settled within the knee⁵. Physical therapy, applied later, had

to overcome both the debilitating effects of the condition leading up to surgery but also the compounded effect of adhesions from the restricted joint movement following the procedure. Coutts used a control group of immobilization and an experimental group consisting of CPM, beginning immediately post-op³. The results demonstrated a greater range of motion at the time of release from the hospital (102° to 80°), reduction in pain medication (2.8 to 3.3 times/day), and decrease in hospital stay (11.6 to 13.6 days)³.

Salter's idea of applying motion to injured joints ran counter to prevailing practices; "the vast majority of physicians and surgeons throughout the world have advocated rest rather than movement. They have embraced the time-honored but unproved principle that diseased or injured tissues must be put to rest in order to heal"^{1;2}. The same logic of rest had been applied to patients with back pain and only recently has it been found that returning patients more rapidly to normal daily activities may be more effective. The only spinal studies of CPM have induced movement in the lumbar spine during seated tasks. Reinecke et al used a cyclic lumbar support in an automobile to determine if adjusting seated lordosis prevented low back pain during extended driving¹¹. van Deursen found significant reduction in chronic low back pain patients after engineering chairs with seat pans that induced axial spine rotation, using small motions (<2°) at a frequency of one cycle per 10 to 12 seconds.

While CPM has begun to be used widely as a recumbent treatment method for both acute and chronic low back pain⁶, little is known of the underlying biomechanics. Based on the cited earlier work in other joints and the apparent clinical response, CPM is now promoted for reducing joint edema, increasing intervertebral motion and enhancing the transport of nutrients and biological waste.

Purpose

This research is to my knowledge, the first study of the dynamics of prone, spinal CPM. It evaluates the consistency and reliability of applied therapeutic table motions and loads. Further, it begins the assessment of relationships between passive loads transmitted through the lumbar spine and patient stature, as well as exploring the relative contribution of spine loading by paraspinal muscle contraction during CPM.

There are three main objectives of this research: 1) to develop adequate instrumentation of a typical treatment table to quantify CPM input loads and kinematic behavior; 2) to examine the feasibility of a simple system to calibrate myoelectric activity from relevant muscles in a first approximation; and 3) to develop biomechanical and statistical models that give predictive load equivalents acting on the spine from muscle activation during prone CPM loading.

Completion of these objectives will permit the two main hypotheses of this work to be tested. The first proposes that the magnitude of passive loads acting through the lumbar spine during CPM can be accurately predicted, based on a subject's stature and the motion control parameters (speed, displacement) of the treatment table motion. The second hypothesis is that muscle responses to motion will vary minimally between healthy individuals and patients with mechanical low back pain and are negligible. Should muscle action be adequately strong, it may alter the intended therapeutic loads by changing direction, magnitude or both in an unknown manner.

CHAPTER TWO

PRELIMINARY STUDIES

Solutions to the issues in this investigation were sought in three stages. First was the introduction and synchronization of a number of sensors for making valid, time-linked observations of kinematic variables during CPM. Second, a root mean square myoelectric signal (RMS-MES) model was needed to calibrate muscle activation levels during feasible standardized tasks to be performed by low back pain patients. Such a model must be able to partition passive and active load components acting on the lumbar spine and to estimate equivalent muscle loads from activity observed during CPM. Finally, biomechanical models are necessary for estimating the passive, active and total loads transmitted through the trunk during CPM.

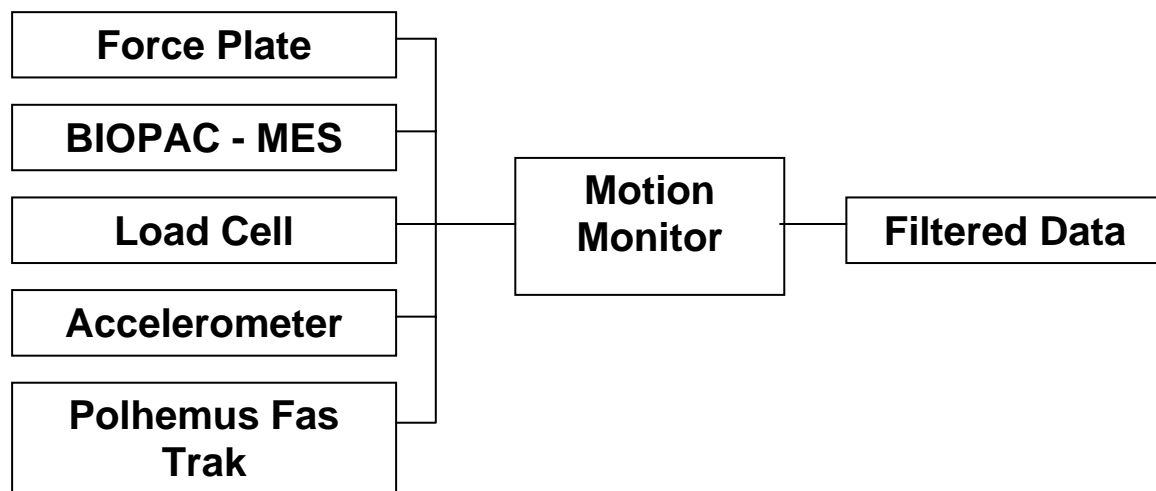
In the section that follows, a brief description of each preliminary study is given along with a summary of results. Details of important results are provided in the Results Section.

Instrumentation

New instrumentation augmenting the original load sensing table evaluated by Rogers and Triano¹⁸ was necessary to derive input values for the biomechanical models. Detection of the involved body segment relative to table motion was achieved by including an electromagnetic multi-body positional sensing system (Polhemus FasTrak 3SF0002). A

pendulum-mounted, linear accelerometer (Entran EGCS-D1S) was attached to the table to directly monitor acceleration components. Driving force creating the CPM motion itself was monitored with an in-line uniaxial load cell (Futek L1665 Universal Load Cell) sensitive to both compressive and tensile loading. Finally, a set of 8 myoelectric signal ,MES, electrode pairs (BIOPAC EMG100B) served to monitor key muscles of the torso and lower extremities during calibration tasks and CPM. Linking of all electronic inputs through the Motion Monitor (Innovative Sports Training, Inc - Chicago IL), a real time data collection system, enabled simultaneous recording through coaxial cables on a 16-channel patch panel to the A/D board or via USB port connections as shown in Figure 5.

Figure 5: Schematic of Instrumentation Input into Motion Monitor and Output of Filtered Data.



Validation of Kinematic Measures

The planned experimental configuration held two potentially challenging features that could significantly influence measurement accuracy or complicate biomechanical model development. While the commercial Polhemus tracking system has been commonly used for kinematic measures with good accuracy (0.0002 cm / cm), its proximity in this study to the metallic mass of the sensing table and its motorized drive system posed potential distortion of the magnetic fields ¹⁹. Two assumptions were made and tested in an effort to validate the accuracy of measurements under this configuration. The first approach was based on the premise that the electromagnetic field transmitter could be positioned so that the calibrated space (76 cm X 91.5 cm) defining sensor precision was outside the influence of the table mass. In the second, the motions of the table ($\Theta = 11.5^\circ$) were expected to be sufficiently small so as to result in negligible distortion as the moving sensors interacted with the field flux lines.

Verification of reported positions by the Polhemus system was performed in several stages. An electromagnetic field sensor, (CellSensor, Tec-Health.com) was used to identify the distance from the table motor that minimized the effect of EMF (59.3cm above the floor). A grid pattern of four sensors (rectangular 12.7 cm X 15.2 cm) was constructed on a non-magnetic material base and the measured distances between markers were compared with those calculated from the sensors signals. The electromagnetic sensor grid was fixed on the table surface at 61.3 cm (5.1 cm above the table surface) and tested at various distances from

the transmitter to minimize error in the relative intermarker position vectors reported. An optimal height for the transmitter was determined to be 98.4 cm.

Commercial biomechanical analysis software (Motion Monitor Innovative Sports Training, Inc - Chicago IL) provided numerical analysis from the electromagnetic sensor position data to obtain linear and angular velocities and acceleration for three points on the body and one point on the treatment table.

Accelerometry

Accurate determination of lower body accelerations is important to the understanding of the table motion consistency and for validating the derivation of linear and angular accelerations from position data. They may also be used in developing alternative models to the quantitative estimation of loads transmitted through the body section containing the targeted FSU. Accelerations also can be estimated by double differentiation of the kinematic data, but with progressively increasing artifact from displacement signal noise.

Accelerometry was selected as a means of direct measure and to estimate measurement error caused from the double derivative approach.

Since treatment table motion consisted of rotation about a fixed point, the linear accelerometer (Entran model EGCS-D1S; +/- 5g range, 40 mV/g sensitivity, $f_n = 300$ Hz) was fixed to a pendulum, that in turn, was rigidly attached to the moving table which effectively transformed angular to linear accelerations (Figure 6). Geometric relations were

used to quantitatively convert between linear and angular accelerations according to the formula:

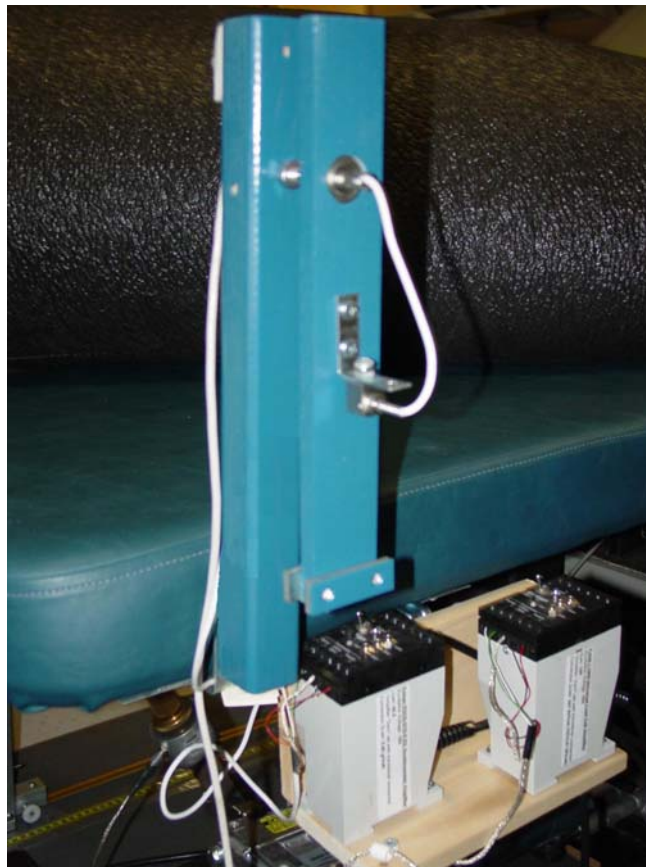
$$a_t = r\alpha \quad \text{Eq. 2.1}$$

a_t = tangential acceleration of the pendulum

r = the radius of the arc path

α = the angular acceleration of the rigid body

Figure 6: Linear accelerometer Attached to the Pendulum on the Treatment Table.



Using a sine function, a simple theoretical model of table motion was created and used to validate accelerometer output through numerical differentiation. To determine the parameters for the theoretical sine wave, estimates for the period of table motion were made by determining the time necessary to complete 3 cycles.

Consistency of Table Motion

Representation of typical CPM dynamics by the instrumented treatment table presumes that there is consistency of periodic motion both within the instrumented table and across a sample of commercial tables. Consistency was evaluated by conducting a series of tests comparing the performance of the instrumented table and 8 commercial tables (Leander 900Z) in clinical use under varying mass loads (0 Kg, 4.5 Kg, 9.1 Kg and 13.6 Kg) and at cycle frequencies (0.103 Hz, 0.245 Hz, 0.500 Hz).

Uniaxial Load Cell

The cam-drive train of the instrumented table was modified to accept an in-line uniaxial load cell (Futek - model L1665: capacity of 2224N; 2mV/V sensitivity) to directly measure force input as shown in Figure 7. The load cell accuracy was tested as an isolated instrument and again in its installed position within the drive chain.

Figure 7: Load Cell in the Modified Cam-Drive.



Manufacturer calibration of the load cell was confirmed by a series of static compression and tension tests over a range of 2.27 Kg to 13.6 Kg, three times. The loads were applied in series to the load cell, which was resting on the AMTI force plate. Output of the force plate and the load cell were directly compared with the known loads and calibration settings adjusted as necessary.

Tensile test calibrations were performed using a pulley system. Absolute value of the output from the known load (2.27 Kg to 9.1 Kg), attached by cable to the fixation point on the force transducer, was compared to the results from the compression load testing.

The load cell was then placed in line of the drive chain and tested in both static and dynamic modes. Static testing was performed with the table in its rest (horizontal) position with the drive chain push arm at a 73.1 degree angle. As the table moves through the CPM cycle the angle of engagement of the push arm to the table is 69.6 to 76.6 degrees with negligible impact, therefore a mean angle of 73.1 degrees was used during analysis. The masses used during testing were of 4.5 Kg, 9.1 Kg and 13.6 Kg.

Myoelectric Calibrations

Use of myoelectric measures of muscle activity to estimate muscle tension and loads acting on joints is a common technique in biomechanical modeling. Most muscle calibration methods, however, depend on calibration of activities in comparison to graded exertions up to and including maximal voluntary effort (MVE). The reported muscle activity is then compared with the loads acting on the joint of interest using some form of regression modeling. Thus, calibration has three necessary elements. They are: 1) a sequence of feasible and reproducible exertion tasks; 2) quantification of myoelectric activities; and 3) knowledge of the moments acting on the target joint of interest.

As the work designed here was intended for use with patients with lower back pain, MVE exertions may unacceptably load the painful area and potentially be uncomfortable or

harmful. In addition, it was anticipated from observation of patient muscle tone during clinical CPM that myoelectric activities to be observed would be small. As a result, a more relevant calibration method was sought.

Based on the work of Finneran²⁰ and Pease et al²¹, a sequence of standardized up-right tasks were identified that were designed for use in populations of low back pain patients. These tasks consisted of erect stance, trunk flexion of 20°, and erect stance with three pound weights held at full forward arm reach. Existing applications broadly monitor muscle activities of the low back from the thoracolumbar junction to the sacrum.

In addition, the work of Chaffin et al^{22;23} has resulted in commercial software that predicts lumbar spine loads from patient anthropometry, applied weights and quantification of patient posture. As a part of the data reported by this three dimensional static biomechanical model, the relative contribution of equivalent muscle tension developed to maintain static equilibrium is quantitatively reported. The overall model has been tested and validated in the literature²³.

Using the sagittally symmetric tasks^{20;21;22} a two-dimensional sagittal plane biomechanical model was constructed to partition passive loads acting at the L5/S1 disc level. Modeling details are given in the section Experimental Methods: Biomechanical Modeling. The model was validated by comparing output from the commercial 3D model for passive loads acting at the disc. Having good agreement with the 3D model on passive loads, the muscle generated loads opposing the postural moments from the calibration tasks were used to develop a regression equation based on the recorded myoelectric (MES-RMS) signals.

Equations may be developed using either moment or compression force measures. Both approaches were used and the method accounting for the greatest variability in the data (highest R^2) was selected. Two equations were then developed with that method; one for the healthy volunteers and one for the low back pain subjects, looking for systematic differences. The equation from the healthy volunteers was later used to estimate the multifidus muscle tensions from MES-RMS behavior during CPM.

Because the 3D model considered the total erectors spinae muscle action to support the torso in an upright posture and the 2D static model considered the multifidus as the primary loading factor for prone CPM; an adjustment was necessary to accommodate the difference in muscle cross-sectional area. Anatomically, the multifidus is a subcomponent of the erector spinae and is independently commensurable at the level of the L5/S1. As a result, the multifidus load represents a percentage of the load born by the erector spinae as a whole. Schultz demonstrated the cross sectional area of the erector spinae as a function of A-P and lateral torso measurements²⁴, allowing its size to be estimated independently for each subject. McGill, on the other hand, has shown that the cross-sectional area of the multifidus is a 12.44% of the erector spinae²⁵. The load produced by a muscle is directly related to its cross sectional area. The percentage of cross-sectional area can be used to calculate the contribution of muscle load.

CHAPTER THREE

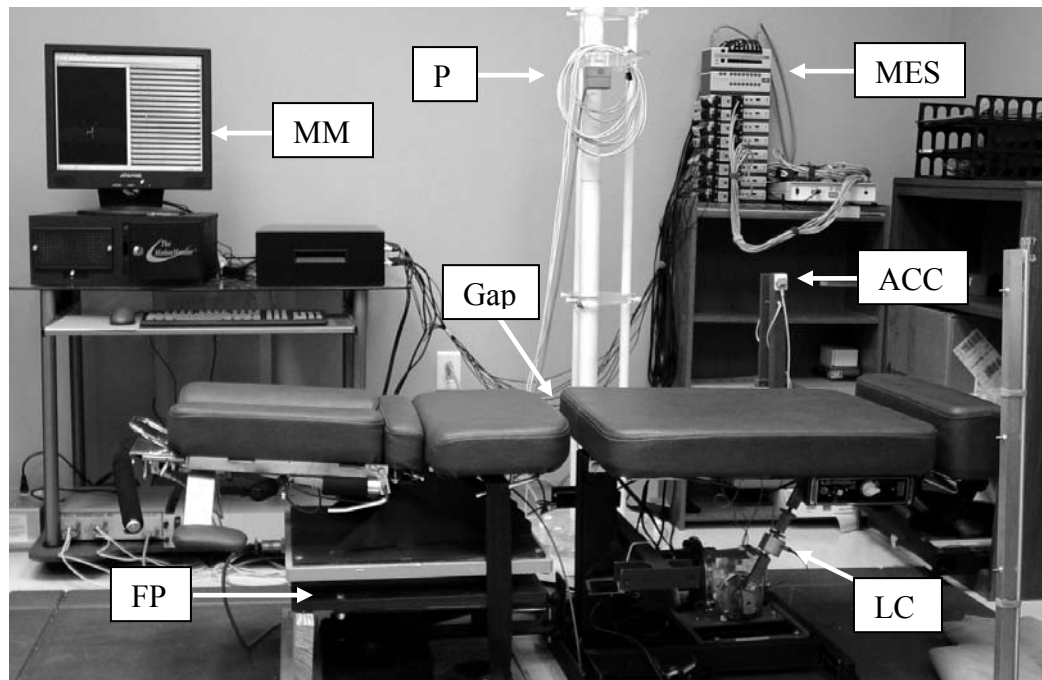
EXPERIMENTAL METHODS

Table Foundation

This work builds on the earlier instrumentation developed by Rogers and Triano¹⁸. In that study, a commercial treatment table (Leander 900 Z Series - Leader Health Technologies Corporation, Port Orchard, Washington) was modified by adding an AMTI force plate (Watertown, Massachusetts - model number OR6-7-2000). The sensing table system (Figure 8) was shown to be capable of measuring static and dynamic loads with high fidelity. Briefly in review, the table system has three basic elements necessary for accurate estimation of the passive loads transmitted through the torso at the target spinal segment. They are 1) applied loads at a single known site where all forces and moments must pass through the target segment, 2) constraint of the upper body mass to prevent motion (deformation being ignored), and 3) isolation of the upper body above the targeted segment level from the lower body where CPM motions are applied. This was accomplished through structural modification of the table. First, the table was separated into two isolated sections; a cephalad piece instrumented with the AMTI force plate and caudal piece that cycles under controlled speeds driven by a motorized cam and push rod system. The cephalic section of the table supports the head, thorax, upper extremities and upper abdomen. The caudal section supports the lower abdomen, pelvis and lower extremities. The modified table permits the lower section to be fixed, manually adjusted, or oscillated through an arc from 0° horizontal

to 11.5° degrees downward, a distance approximately one-half that permitted by the commercial table. Using cushions on the table surface, an additional range of body position in (e.g. 11.5° to 20°) can be tested. The separation between the cephalad and caudal surfaces accomplished two tasks. First, it isolated the force plate from the lower section, effectively preventing base motion vibration and artifact from confounding the resultant loads reported by the plate. Secondly, it forced all input loads to the spine to pass through the cross-section of the torso and spine that lay across the gap separating the table sections. In this way, all CPM passive loads are forced to traverse the segments of interest before passing to the sensing table for recording.

Figure 8: Instrumented treatment table – ACC = Pylon Supporting Accelerometer and Table Position Sensor, FP = AMTI Force Plate, Gap = Table Support Gap, LC = Uniaxial Load Cell, MES = BIOPAC 8 Channel EMG, MM = Motion Monitor, P = Polhemus Magnetic Transmitter.



For this project, the table was further modified to permit kinematic and force measures as described in the section on Preliminary Studies. The series of preliminary studies were undertaken to validate the accuracy of the input measures before actually testing volunteers.

Quantifying CPM dynamics in the lumbar spine requires an estimation of the passive loads transmitted through the torso cross-section of interest and the muscular tensions developed by reactions within muscles traversing the cutting plane. If muscle action is too

variable or is too strong compared to the loads caused by the CPM table motions, the intended clinical effects may be altered or obviated.

A two-phase investigation was initiated. In the first phase, the loading of the low back during a series of standardized tasks was partitioned into active and passive components. The active component from muscle activation was used to create a linear regression to predict equivalent loads due to muscle activity. In the second phase, muscle activity during common CPM settings for treatment of low back pain was measured in a group of healthy subjects and a second group of low back pain subjects. The active and passive loads acting on the spine during CPM were then evaluated.

Volunteer Selection

Project protocols and recruitment materials were submitted to the Presbyterian Hospital system IRB for review. Once approval was obtained, recruitment of healthy and low back pain volunteers was begun. A total of 5 healthy and 4 low back pain subjects meeting inclusion and exclusion criteria (Table 1) agreed to participate and signed the informed consent form.

Table 1: Inclusion / Exclusion Criteria for LBP Group.

Inclusion Criteria	Exclusion Criteria
▪ Age 18 to 50 years of age	▪ Degenerative disease on x-ray
▪ Ability to perform calibration tasks	▪ Signs of nerve injury
▪ Clinically diagnosed mechanical pain of facet origin at L4/L5/S1 defined as:	▪ Bone disease, cancer, or infection
1. Low back pain with or without buttock or posterior thigh pain.	▪ Previous spine surgery
2. Kemp's test or prone facet loading positive	▪ Pregnancy
3. Symptom stability during sit/stand rising from a chair.	▪ History of adhesive tape sensitivity
▪ VAS pain scores ≥ 3.0 of 10.0	▪ Active in any other research

MES Calibration Testing

Anthropometric data (age, height, weight) and torso segment measures (anteroposterior and transverse diameters) along with longitudinal distance from the bottom of the foot to the palpable joint line of the knee were obtained in the standing position. Data served both to assist in landmark identification and for input variables to biomechanical models during data analysis.

Myoelectric (MES) signal calibration was performed through measurement of MES from selected muscles (Table 2) bilaterally during the performance of three standardized tasks. Muscle pairs sampled were the multifidus, latissimus dorsi, gluteus maximus and

hamstring femoris. The selected pairs of muscles allowed an overview of each subjects' muscular response to CPM at the different velocity settings. The table below describes the electrode placement for the specified muscles²⁶.

Table 2: MES Sensor Placement.

Muscle	Location of EMG sensor
Latissimus Dorsi	3 fingerbreadths distal to and along the posterior axillary fold
Multifidus	Halfway point between the posterior superior iliac spine and midline
Gluteus Maximus	Midpoint of the line connecting the posterior inferior iliac spine and greater trochanter
Hamstring Femoris	At midhigh there is a palpable groove from the iliotibial band between vastus lateralis and the external hamstring and electrode is placed just posterior to the groove

The electromyography system included eight EMG100B amplifier modules by BIOPAC Systems, Inc. Each module is a single channel, high-gain, differential input, biopotential amplifier for monitoring muscle. The EMG100B modules were connected in series to UIM100A and then HLT100C is connected to the MP100A-CE. Each of the eight modules is connected from the HLT100C through a HLT100 to the Motion Monitor patch panel.

With the subjects prone, bipolar surface electrodes (10 mm diameter, Ag-AgCl) were placed over the muscles at the specified locations after preparing the skin with isopropyl alcohol and mild skin abrasion. The interelectrode distance was 35mm. Signals were visually inspected for absence of noise and for response from isometric contraction. Subjects resumed an upright stance and calibration tasks were performed. The sequence of testing progressively increased the demand on the musculature of the lower back to offset postural

loads (Table 3). The tasks selected were those reported in the literature to be associated with negligible abdominal muscle recruitment and only sagittally symmetric flexion moments acting on the spine^{20;21}. They included 1) upright relaxed stance, 2) weight holding 3 lb in each hand at full reach, shoulders at 90 degrees flexion, and 3) 20° torso flexion. The flexed posture task was determined by inclinometer measure taken at the T12/L1 landmark. Each position was held for 10 seconds during MES sampling.

Table 3: MES Calibration Stance Testing.

MES Calibration Stance	Duration
Upright	10 sec
Weighted – 3lb each hand, 90° at shoulder	10 sec
Flexion – 20°	10 sec

Anthropometric and postural data were entered into both the commercial 3D model to predict the moments and resultant MES forces generated to maintain postural equilibrium. A linear regression equation was determined relating the mean sum of the root mean square (RMS) of the right and left multifidus MES signal values in mV to the erector spinae loads predicted by the 3D model. Multifidus muscles were selected as the muscle equivalent as they directly cross the cutting plane through the L5/S1 disc levels.

CPM Testing

Three CPM conditions were tested. They included 11.5° angular table displacement at 1) the more common intermediate speed (0.245 Hz) and 2) the maximum speed (0.5 Hz).

The third condition tested an increased displacement from 11.5° to 20° at 0.245 Hz. Speed control settings are set by adjusting a rotary potentiometer to settings marked at half and full turn. The sequence of testing was prospectively randomized.

On completion of the calibration tasks, the force plate strain gages were balanced for the unloaded table. The load cell and accelerometer were similarly calibrated. All 28 data parameters (force plate - 6, load cell, accelerometer, electromagnetic markers – 12, myoelectric signals – 8) were time linked and set for capture through the Motion Monitor multiplexer. The volunteer then assumed a prone recumbent position on the CPM table with the pelvic crest aligned to the cephalad edge of the lower table support surface to standardize relative position of the targeted spine segment within the gap between the upper and lower table support sections. The Polhemus FasTrak electromagnetic sensors (Figure 9) were placed on the subject in three locations (L4/L5, second sacral tubercal, and 10mm inferior to the left knee joint line) using anatomical landmarks. The fourth sensor was rigidly fixed to the post supporting the accelerometer pendulum on the caudal section of the table.

Figure 9: Subject Positioned on the CPM Table at Table Stroke of 11.5°. Sensors for Measuring the MES and Position can be Observed Attached at their Sites in Relation to Anatomical Landmarks.



Once all sensors were attached the subject was aligned symmetrically in the middle of the table and the sandbags (combined weight of 19 lbs) were placed at the sides of the subject's legs to constrain inadvertent repositioning of the lower body. Location of the joint line on the lateral surface of the left knee was determined in all three axes (± 0.5 cm) with respect to the force plate, allowing for definition of all relevant body segment mass centers based on anthropometric relationships.

Data collection commenced with testing the sequence of conditions in random order (Table 4). The intermediate speed tests required 60 seconds while the fast speed completed in

30 seconds. Subjects were given 5 minutes in between tests when they were asked to return to an upright posture and walk or bend *ad libitum*. Visual analog, 10 cm line pain scales were completed by the subject at the outset and after the calibration tasks and each CPM condition.

Table 4: CPM Testing.

CPM	Duration
Intermediate speed 11.5°	60 seconds
Fast speed 11.5°	30 seconds
Intermediate speed 20°	60 seconds

Biomechanical Modeling

Modeling methods are commonly used to estimate the internal loads on soft tissue and joint structures during various tasks. The use of models is necessary because direct measurement is too invasive, causing potential harm to volunteers. For the purposes of this work, two biomechanical models were necessary. In the static model, the passive loads acting on the spine during calibration tasks were estimated and validated by comparison with commercially available software. Additionally, the commercial model partitioned the loads into active and passive components allowing for calibration of myoelectric activity. The dynamic model was used to estimate the passive loads acting on the lumbar spine during continuous passive motion. MES-RMS values from the simultaneous muscle activity of the multifidus group served to estimate active loading during CPM.

For the static model, three calibration tasks were performed: 1) erect stance; 2) trunk flexion of 20° ; and 3) erect stance, weight holding (3 lbs in each hand) at full arm reach at shoulder level. Anthropometric values (height, weight) on subject stature along with quantitative, standardized postures and hand loads were used as input to a multisegment biomechanical static model to estimate the compressive force and moments acting at the level of the lumbosacral (L3 – S1) spine. This model results were corroborated by comparing them to those for the passive postural loads from commercially available and validated software (3DSSPP, University of Michigan). In addition to providing a realistic estimate of passive loads, the “3D” also estimates the muscle tension components necessary to maintain stable, upright postures. The output from the 3D modeling program includes moments as well as passive (upper body weight and hand loads), active (from internal muscle tensions), and total (passive + active) forces that account for the compressive, shear and moment components at the L5/S1 spine level²⁷. The partitioning of active and passive loads is very useful. For sagittally symmetric tasks, the muscle activity can be combined into a single muscle equivalent, providing a means to calibrate muscle activity for the postural tasks as is discussed under the section on myoelectric calibrations. Figure 10 shows a diagram of the calibration tasks and the biomechanical model equations for passive load estimates.

The literature base for the 3D model assumes a sacral base angle for the L5/S1 disc at 40 degrees²². Radiographs available from examination of twenty patients, taken as a lateral view in the upright posture, were digitized. Bony landmarks were identified using a back lighted 2D digitizing table (CalComp model 813, Columbia MD) and measured in AutoCAD.

The mean value (40°) from the sample confirmed the generalizability for the biomechanical model developed for comparison.

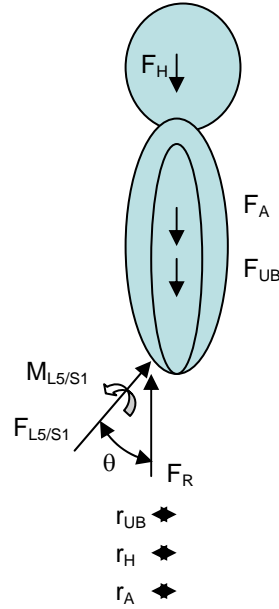
The length of moment arms is dependent on the individual subjects and there were several methods used in determining the appropriate moment for body segments and muscles. Table 5 gives the particular moment arm and reference of how it was obtained.

Table 5: Moment Arms for Biomechanical Models.

Moment Arm	Definition	Reference
Weighted Posture - r_{UB} , r_H	L5/S1 to COM of Upper Body	3DSSPP
Weighted Posture - r_A	0.413*(Upper Arm Length+ Lower Arm & Hand Length)	3DSSPP
Weighted Posture - r_W	Arm Length + COM of Hand Length	3DSSPP
Flexion Posture - r_{UB}	L5/S1 to COM of Upper Body Length	3DSSPP
Flexion Posture - r_H	L5/S1 to COM of Head Length	3DSSPP
Flexion Posture - r_A	L5/S1 to Shoulder Length	3DSSPP
Dynamic Model Multifidus - r_M	$[(\text{Erector Spinae x-axis})^2 + (\text{Erector Spinae y-axis})^2]^{1/2}$	3DSSPP
Dynamic Model - r_{UBy}	0.72*Ht – (Force plate to knee COJ + Floor to Knee COJ)	Occupational Biomechanics ²² and measurements during testing
Dynamic Model - r_{UBz}	Force plate to table top + (knee COJ to table)*1.2	Measurements during testing
Dynamic Model – $r_{L5/S1y}$	Force plate to knee COJ – (0.583*Ht – knee COJ to floor)	Occupational Biomechanics ²² and measurements during testing
Dynamic Model - $r_{L5/S1z}$	Force plate to table top + (knee COJ to table)*1.2	Measurements during testing

Figure 10: Calibration model - Free Body Diagrams and Equilibrium Equations for the Standardized Postures, a) Upright Stance, b) Weighted Stance and c) Flexed Stance.

Figure 10-a: Upright Stance.



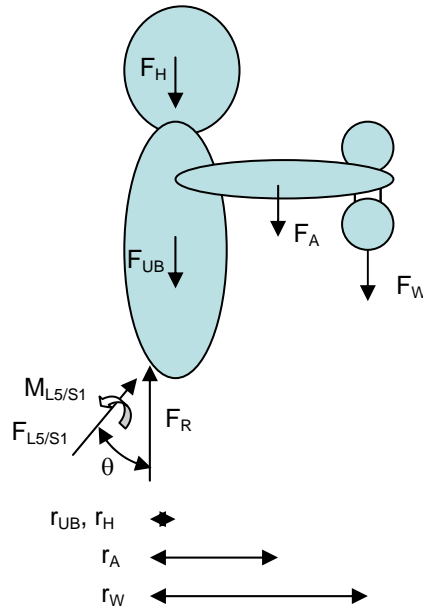
$$\Sigma F = 0: \quad F_R = F_H + F_{UB} + F_A \quad \text{Eq 3.1}$$

$$F_{L5/S1} = F_R \cos \theta \quad \text{Eq 3.2}$$

$$\theta = 40^\circ ;$$

$$\Sigma M = 0: \quad M_{L5/S1} = r_H F_H + r_{UB} F_{UB} + r_A F_A \approx 0 \quad \text{Eq 3.3}$$

Figure 10-b: Weighted Stance.



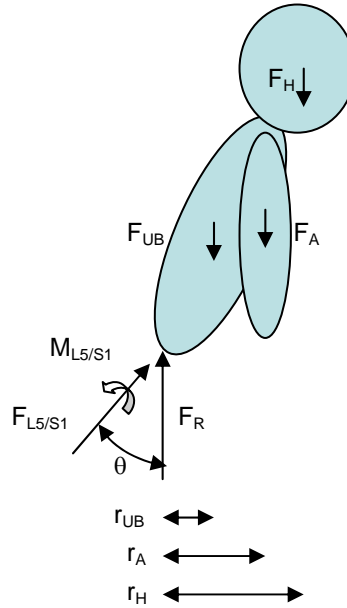
$$\Sigma F = 0 \quad F_R = F_H + F_{UB} + F_A + F_W \quad \text{Eq 3.4}$$

$$F_{L5/S1} = F_R \cos \theta \quad \text{Eq 3.5}$$

$$\theta = 40^\circ$$

$$\Sigma M = 0 \quad M_R = r_A F_A + r_W F_W \quad \text{Eq 3.6}$$

Figure 10-c: Flexion Stance.



$$\Sigma F = 0 \quad F_R = F_H + F_{UB} + F_A + F_W \quad \text{Eq 3.7}$$

$$F_{L5/S1} = F_R \cos \theta \quad \text{Eq 3.8}$$

$$\theta = 45^\circ$$

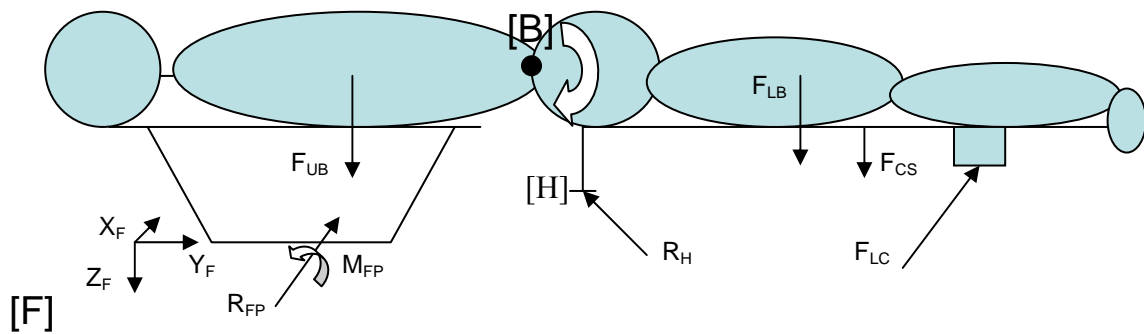
$$\Sigma M = 0 \quad M_R = r_A F_A + r_W F_W + r_H F_H \quad \text{Eq 3.9}$$

The equations for flexion are similar to upright and weighted conditions except for the angle of L5/S1. During flexion L5/S1 accounts for twenty-five percent of the angular motion in the lumbar spine²⁸. Subjects were standing with 20° flexion and therefore the angle used in calculating the force at L5/S1 was 45 degrees.

The dynamic model builds upon the basic static model but assumes relevant body postures for prone recumbency used in CPM. The appropriate additional computational phrases are added to account for inertial loading associated with body segment motions.

Figure 11 shows the complete experimental environment from which the model for the present work was isolated.

Figure 11: CPM Experimental Environment.



Where the curved arrow indicates CPM movement about [B], the targeted L5/S1 disc level, as the table pivots on the hinge [H]. [F] = Global reference coordinate system of the force plate, [B] = Body fixed reference system at the targeted spinal joint (L5/S1), F_{UB} = Action of the upper body weight, R_{FP} = Reaction force measured at the force plate, M_{FP} = Moment measured at the force plate, R_H = Reaction force at the hinge on the caudal section, F_{LB} = Action of the lower body weight, F_{CS} = Force of the caudal section weight, F_{LC} = Driving force measured at the load cell.

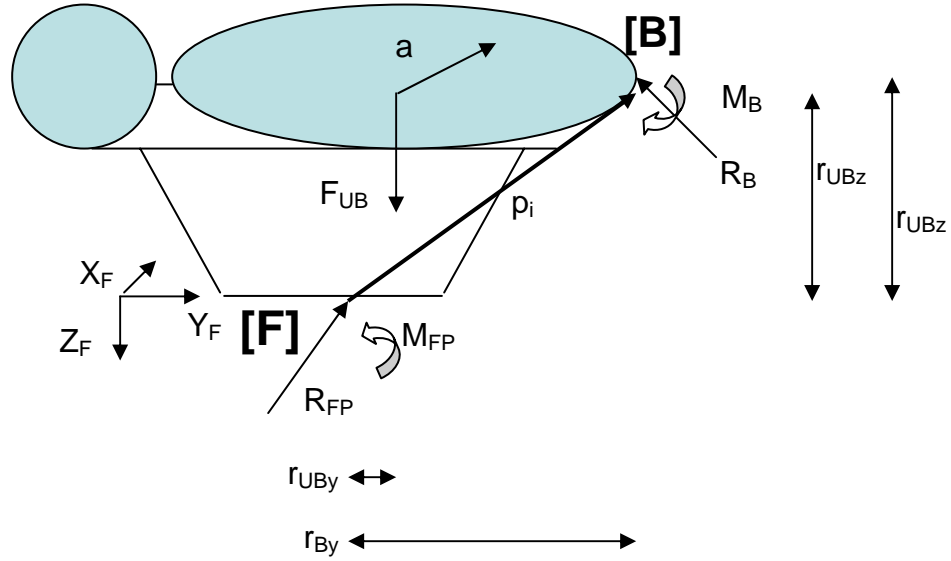
Input variables to the dynamic model include the reaction forces measured by the force plate imbedded within the table under the upper body, motions of the upper body

determined from electromagnetic sensors positioned on the surface of the back and anthropometric measures. The subject anatomical landmarks and dimensions were measured and used to determine the appropriate moment arms, as a ratio to stature^{22;29} necessary for model computations. Because the table is split into an upper sensing support and a lower passive support that drives lower body motions, the loads transmitted through the torso at the level of the target segment at [B] can be estimated using an inverse dynamics approach. In general, a load transformation equation estimates the forces and moments at [B] from those reported at [F]. These are combined with the inertial forces from the acceleration of the upper body under the constraints imposed by the sensing table support.

The free body diagram for the dynamic model is shown in Figure 12 where “a” represents the upper body mass center linear acceleration. M_B and R_B are the moment and force loads transmitted through the lower torso at the target segment of the L5/S1 disc.

Figure 12: Free Body Diagram and Equilibrium Equations for the Constrained Inverse

Dynamics Model.



$$\Sigma F=0$$

$$R_B = a \cdot UBmass - R_{FP} \quad \text{Eq 3.10}$$

$$\Sigma M=0$$

$$r_B = [r_{Bx} \ r_{By} \ r_{Bz}]$$

$$r_{Bx} = 0$$

$$r_{UB} = [r_{UBx} \ r_{UBy} \ r_{UBz}]$$

$$r_{UBx} = 0$$

$$M_B = -M_{FP} - (r_B \times R_B) - (r_{UB} \times UBmass) \quad \text{Eq 3.11}$$

Equation 3.12 Transforming and estimating the loads at [B] is given below as:

$$\begin{bmatrix} \overline{M_{x_B}} \\ \overline{M_{y_B}} \\ \overline{M_{z_B}} \\ \overline{R_{x_B}} \\ \overline{R_{y_B}} \\ \overline{R_{z_B}} \end{bmatrix} = \begin{bmatrix} n1 & n2 & n3 & pn1 & pn2 & pn3 \\ o1 & o2 & o3 & po1 & po2 & po3 \\ a1 & a2 & a3 & pa1 & pa2 & pa3 \\ 0 & 0 & 0 & n1 & n2 & n3 \\ 0 & 0 & 0 & o1 & o2 & o3 \\ 0 & 0 & 0 & a1 & a2 & a3 \end{bmatrix} \begin{bmatrix} \overline{M_{x_F}} \\ \overline{M_{y_F}} \\ \overline{M_{z_F}} \\ \overline{R_{x_F}} \\ \overline{R_{y_F}} \\ \overline{R_{z_F}} \end{bmatrix}$$

Where n_i , o_i , a_i are the direction cosine vectors defining the orientation of [B] with respect to [F], p_i is the vector locating [B] in [F] and pn_i , po_i , pa_i are the results of cross product computations between vectors p_i and n_i , o_i , a_i , respectively.

The total load transmitted through the target segment of the torso is the sum of the passive loads applied by motion of the CPM table and any derived from the activation of muscles acting across the cutting plane at that level. Determination of the total loads, then, requires the calculation of the active loads throughout the CPM cycles. The regression equation relating multifidus load to MES-RMS of the multifidus is used in determining the active loads at each time interval as shown in Eq.3.13 and Eq. 3.14.

$$\text{Active Force (t)} = (\text{regintercept} + c * (\text{MES-RMS})(t)) * \text{percentmult} \quad \text{Eq. 3.13}$$

$$\text{Active Moment x (t)} = r_M * \text{Active Force (t)} \quad \text{Eq. 3.14}$$

regintercept = x intercept of the regression equation

c = x variable of the regression equation

(t) = at each time interval

Data Reduction

The section on Preliminary Studies and the subsection above on *Biomechanical Modeling* have provided a number of details on how raw kinematic, myoelectric and load data were preprocessed. To simplify representation of the results, all data was truncated after the first cycle and before the final CPM cycle. Variability in lag time of parameters, and particularly for MES activity across each period within a test, for each subject, was evaluated by calculating the mean percent of CPM period at which the event occurred. The range of lag times and mean amplitudes were then displayed as a superimposed interval on the table motion period.

Purely kinematic variables were evaluated numerically and then compared to theoretical or independently measured values for validation.

Passive and active loads acting through the lumbar spine-targeted level of interest were developed as load-time histories, through inverse dynamics methods. Inverse dynamics is modeling a given system and solving for the unknown loads. Mean and standard deviations were computed on a point-by-point basis to accurately describe the behavior of the models representing the two study groups. These were displayed as typical load-time histories superimposed on the CPM angular displacement cycle.

Statistical and Data Analysis

To test the hypotheses of this project, a number of secondary analyses were conducted. Pearson-r correlation, regression analysis, Student-t test and ANOVA from a commercial statistical program (STATA Corp, College Station Texas) were all used to confirm foundational work. The primary analysis concerned the answers to the two primary hypotheses:

- 1: Muscle activation during CPM is sufficiently small as to be negligible in the estimation of loads acting through the torso.
- 2: Passive loads transmitted through the torso at the targeted spinal level are a function of the patient's stature and CPM speed.

For the first, comparison of load-time histories was sufficient. The F test for variability was used to evaluate the range of intervals over which activity occurred. For the second, regression analyses were performed with critical significance adjusted to accommodate the small sample size.

CHAPTER FOUR RESULTS

Validation of Kinematic Measures

Figures 13 a-c show the percentage error in relative position coordinates. Greater percent error was noted when the sensors are located on the table surface and closer to the metallic undercarriage and motor than positioned above it for coordinates in the plane (x-y) parallel to the table as well as those in the vertical (y-z) plane.

Figure 13-a: Comparison of Polhemus Transmitter Height in Relation to Percent Error of Measured Distance in X-Axis to Data Collected for Sensors.

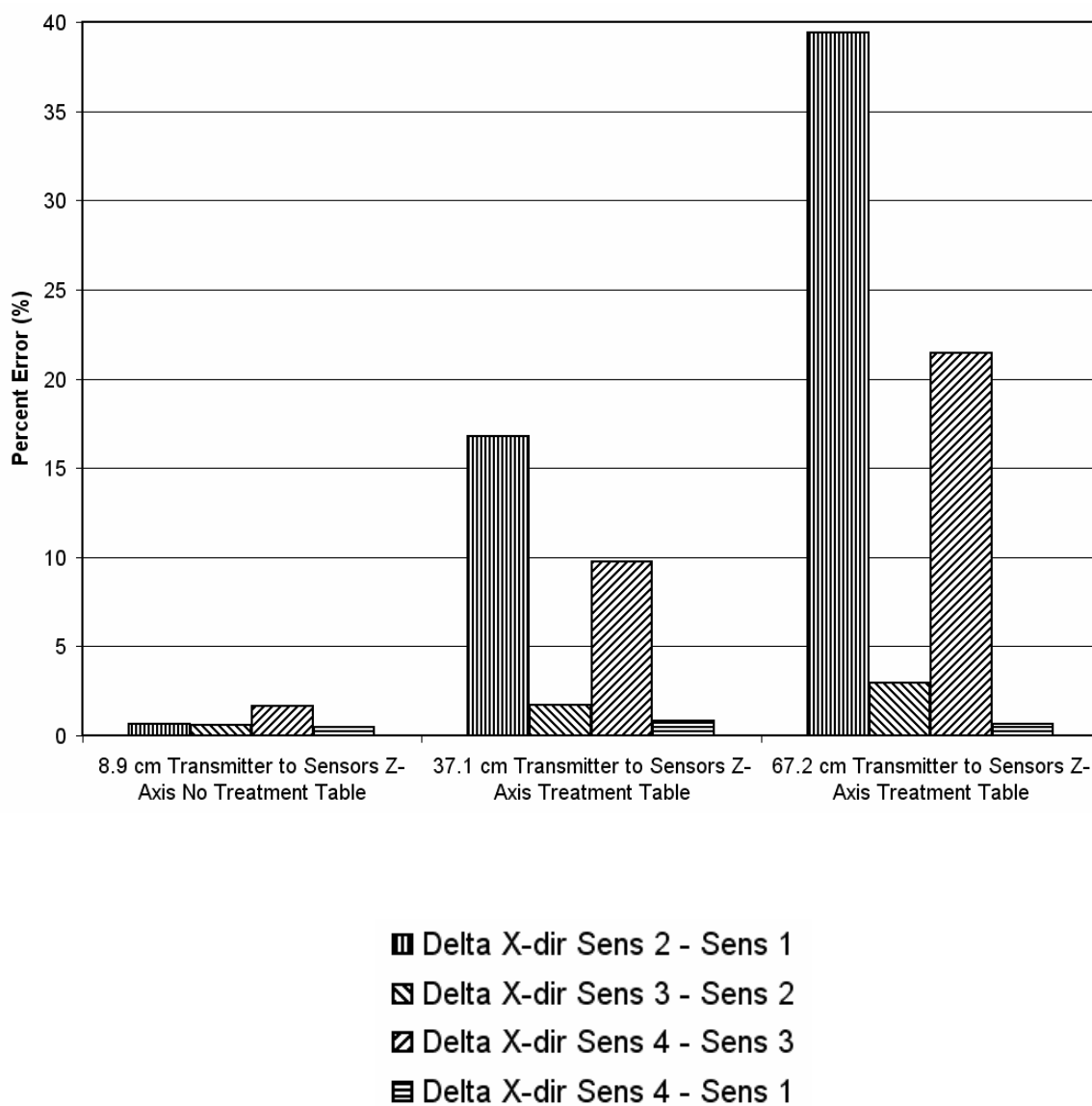


Figure 13-b: Comparison of Polhemus Transmitter Height in Relation to Percent Error of Measured Distance in Y-Axis to Data Collected for Sensors

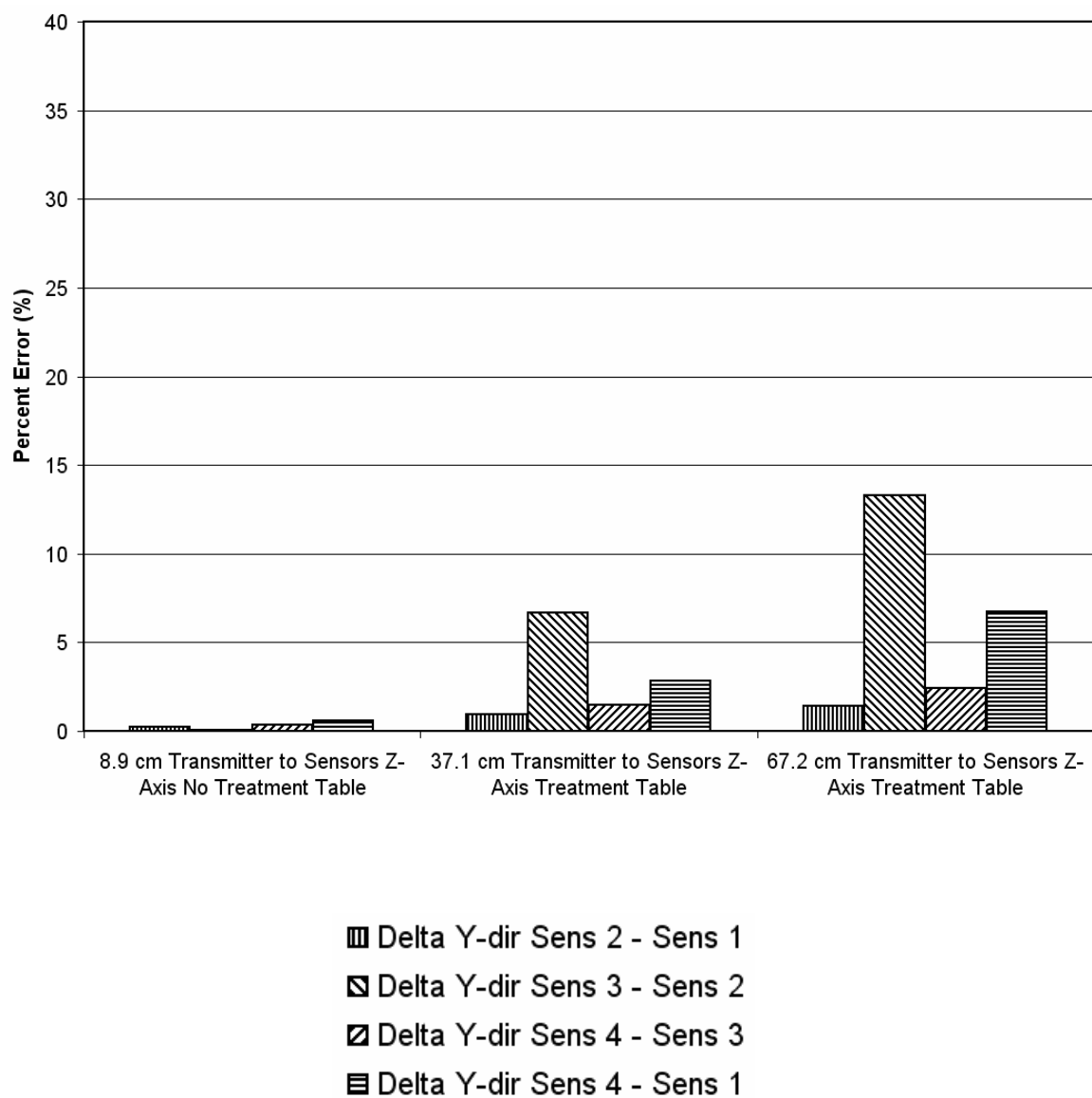
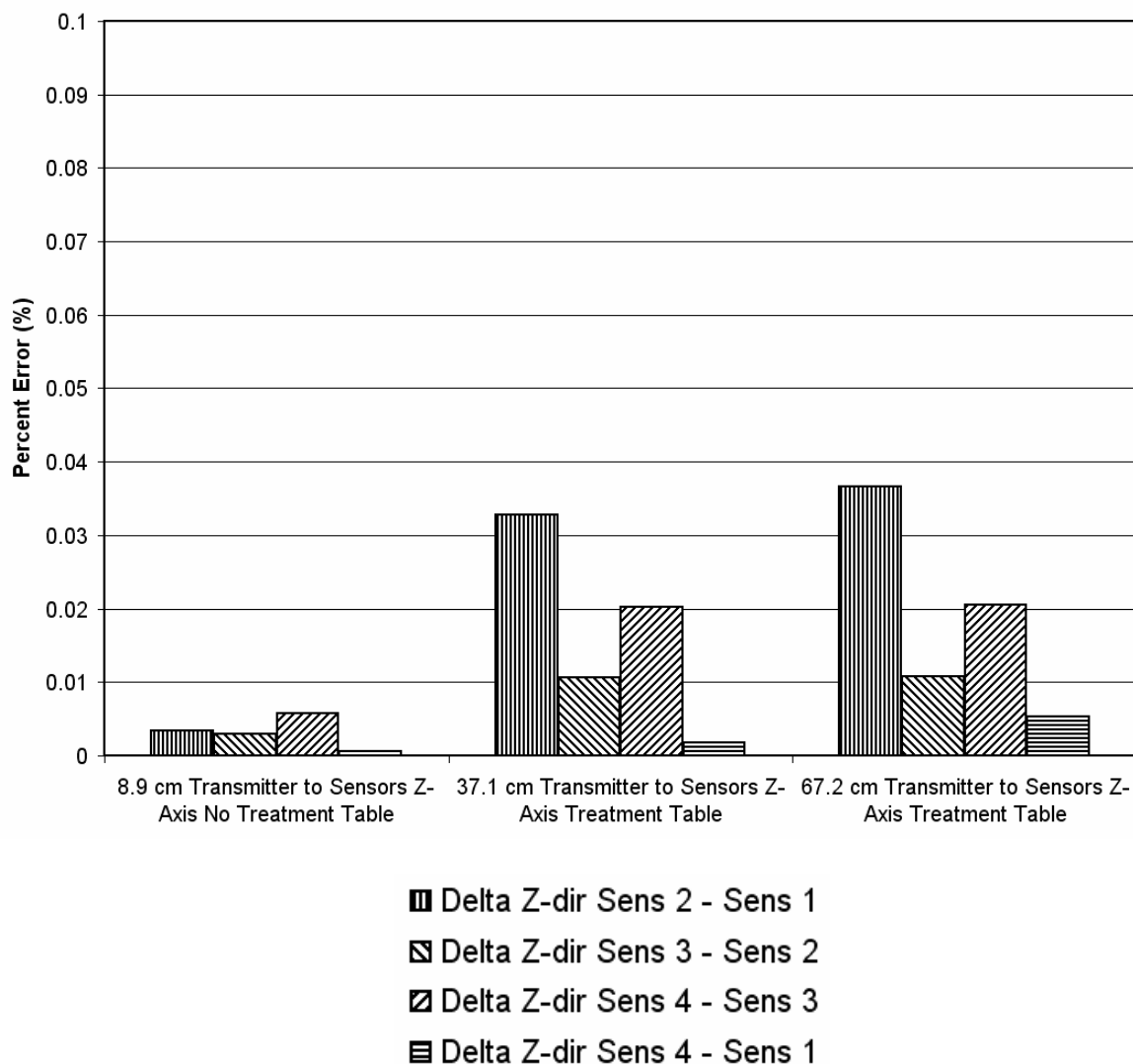


Figure 13-c: Comparison of Polhemus Transmitter Height in Relation to Percent Error of Measured Distance in Z-Axis to Data Collected for Sensors



The influence of the table on spatial accuracy measuring the 12.7 x 15.2 cm grid of the Polhemus system is apparent in all three axes by the significant increase in error shown in Figures 13 a-c. The transmitter positioned at 8.9cm with out potential interference, metallic materials or electromagnetic waves from the motor, demonstrates the accuracy of the Polhemus system. The best compromise in the experimental setting was achieved with the

transmitter positioned 37.1 cm above the CPM table surface. There, the maximum error measured was 17% in the X-axis, 7% for Y-axis and 3.5% for Z-axis. The movement to be measured was that of a subject's lower body and table surface actuated by the cam-push rod mechanism bending the table at its hinge in a 2D rotation. Based on the error factors, an optimal position was determined and the hinge direction parallel to the transmitter X-axis. This orientation and positioning minimized error with maximum uncertainty being 7%.

Accelerometry

The linear accelerometer, mounted on the pendulum attached to the moving table surface, remained oriented in the vertical direction, measuring vertical acceleration. Table motions measured by the Polhemus magnetic sensor were numerically differentiated twice and contrasted with accelerometer output for the test settings (0.2445 Hz and 0.5 Hz) under varied table loads. The ability of the instrumented table to generalize to the commercial tables in clinical use was evaluated by overlaying acceleration profiles obtained by testing 8 separate tables. Each commercial table was tested at the intermediate and fast speed unloaded and loaded with 4.5 Kg, 9.1 Kg, and 13.6 Kg.

For the intermediate setting (0.245 Hz) the Polhemus sensor accelerations (the double differentiated) demonstrated a slight phase shift to the right in comparison to the direct acceleration value (Figure 14). At the higher setting (0.5 Hz), a nearly equal phase shift to the left was observed (Figure 15).

Figure 14: Linear Acceleration Profiles, Double Differentiated Marker Versus Accelerometer Output, for Intermediate Setting at 0.245 Hz.

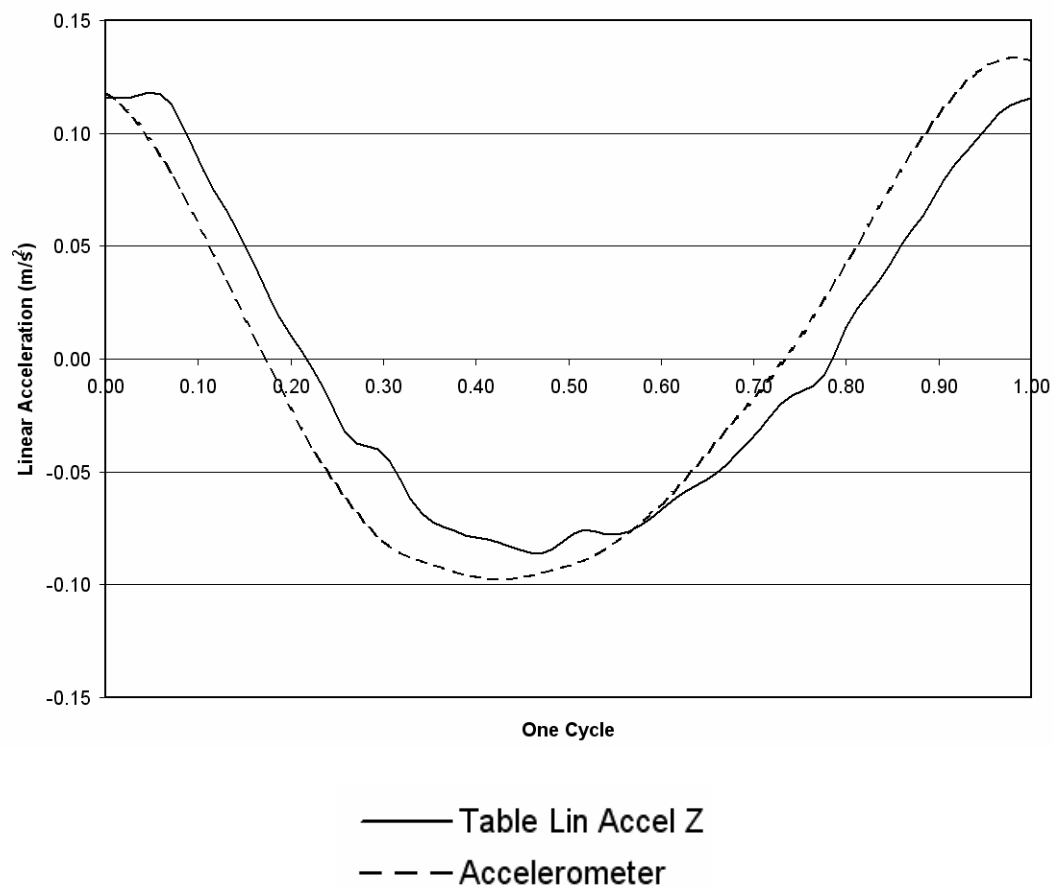
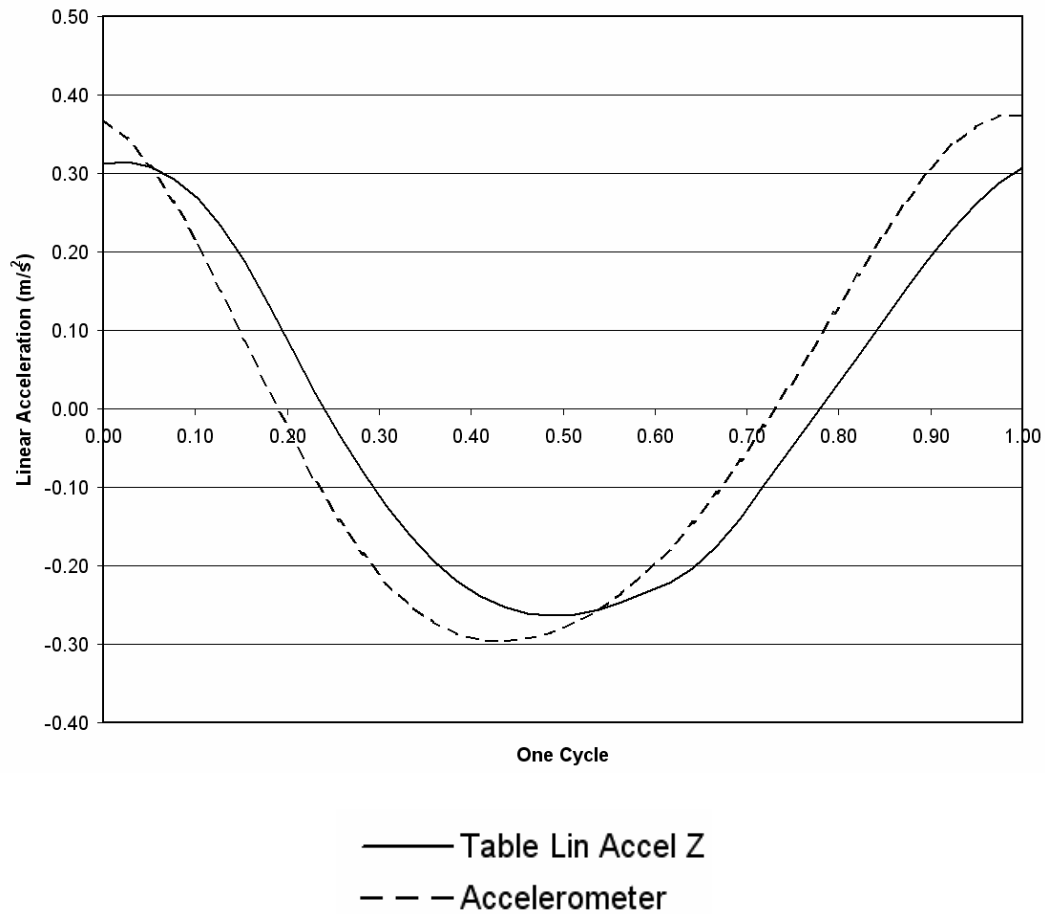
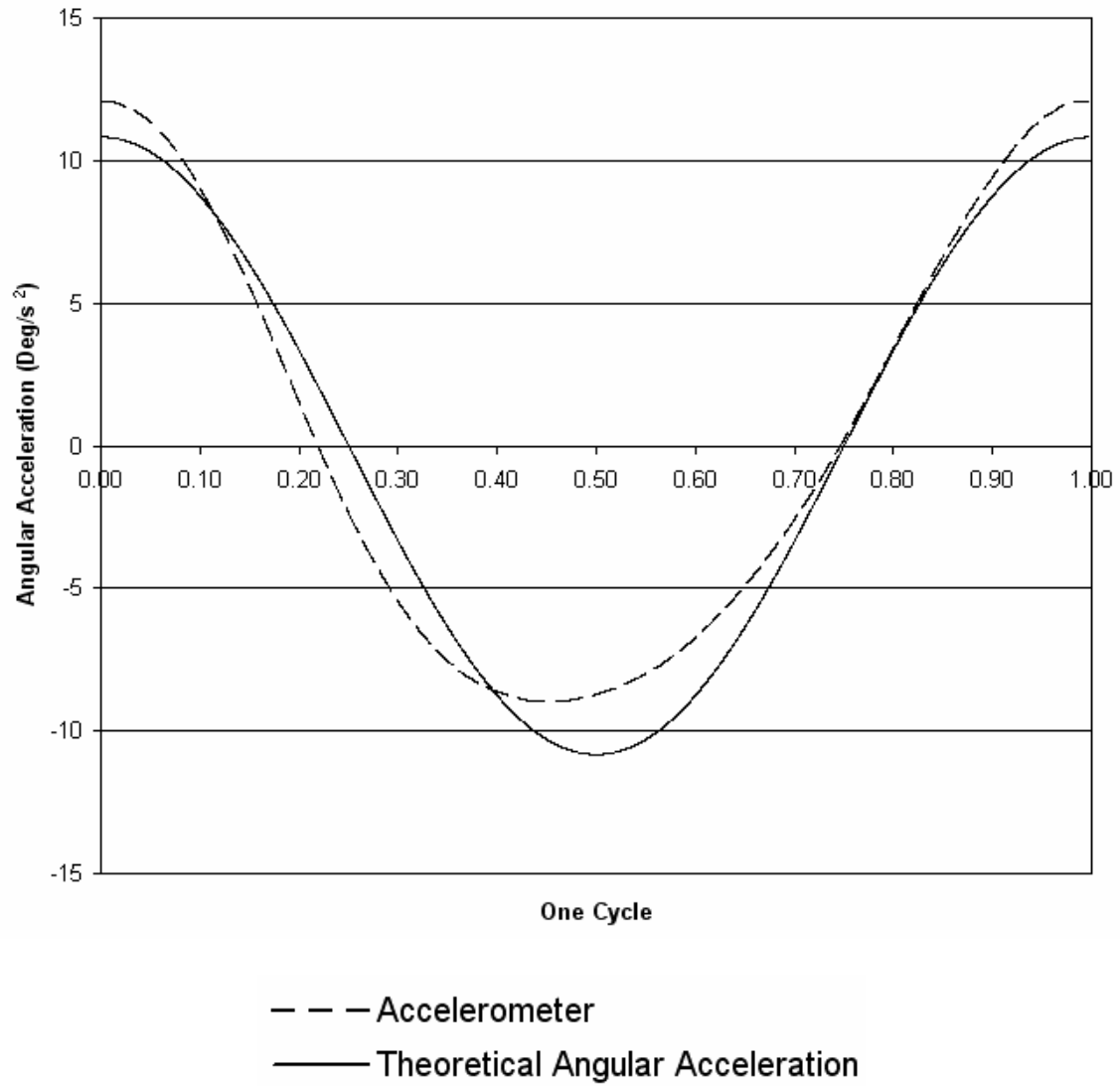


Figure 15: Linear Acceleration Profiles, Double Differentiated Marker Versus Accelerometer Output for Higher Setting at 0.5 Hz.



Through numerical differentiation using a sine function, a simple theoretical model of table motion was created and used to validate angular accelerations derived from the linear accelerometer output (Figure 16). To determine the parameters for the theoretical sine wave, estimates for the period of table motion were made from the known amplitude of table displacement and by determining the time necessary to complete 3 cycles. Differences in curve shape reflect the mechanical offset of the cam drive mechanism that introduces a lag in motion as the table nears its peak displacement.

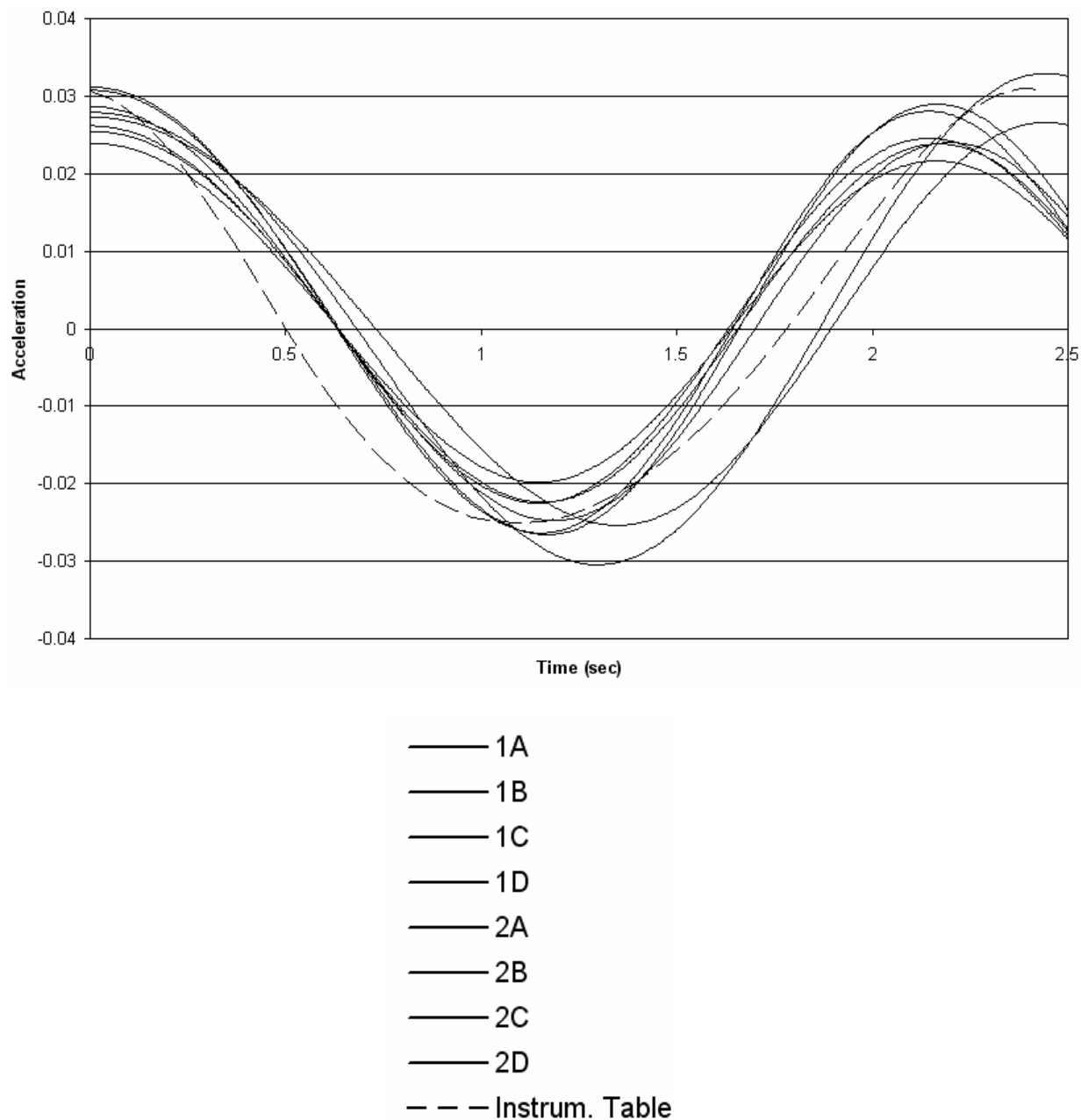
Figure 16: Theoretical Sine Function Estimation of the Table Angular Acceleration
Compared to the Calculated Angular Acceleration from the Linear
Accelerometer.



Generalizability of Table Motion

Representation of typical CPM dynamics by the instrumented treatment table presumes that there is consistency of periodic motion both within the instrumented table and across a sample of commercial tables. Consistency was evaluated by conducting a series of tests comparing the performance of the instrumented table and 8 commercial tables in clinical use under varying mass loads (0 Kg, 4.5 Kg, 9.1 Kg and 13.6 Kg) and various cycle frequencies (0.103 Hz, 0.245 Hz, 0.500 Hz). Figure 17 displays the performance of all eight tables at the highest setting and under a 13.6 Kg load. Acceleration profiles matched the instrumented table well, in general. Two tables showed significant phase shifting to the right.

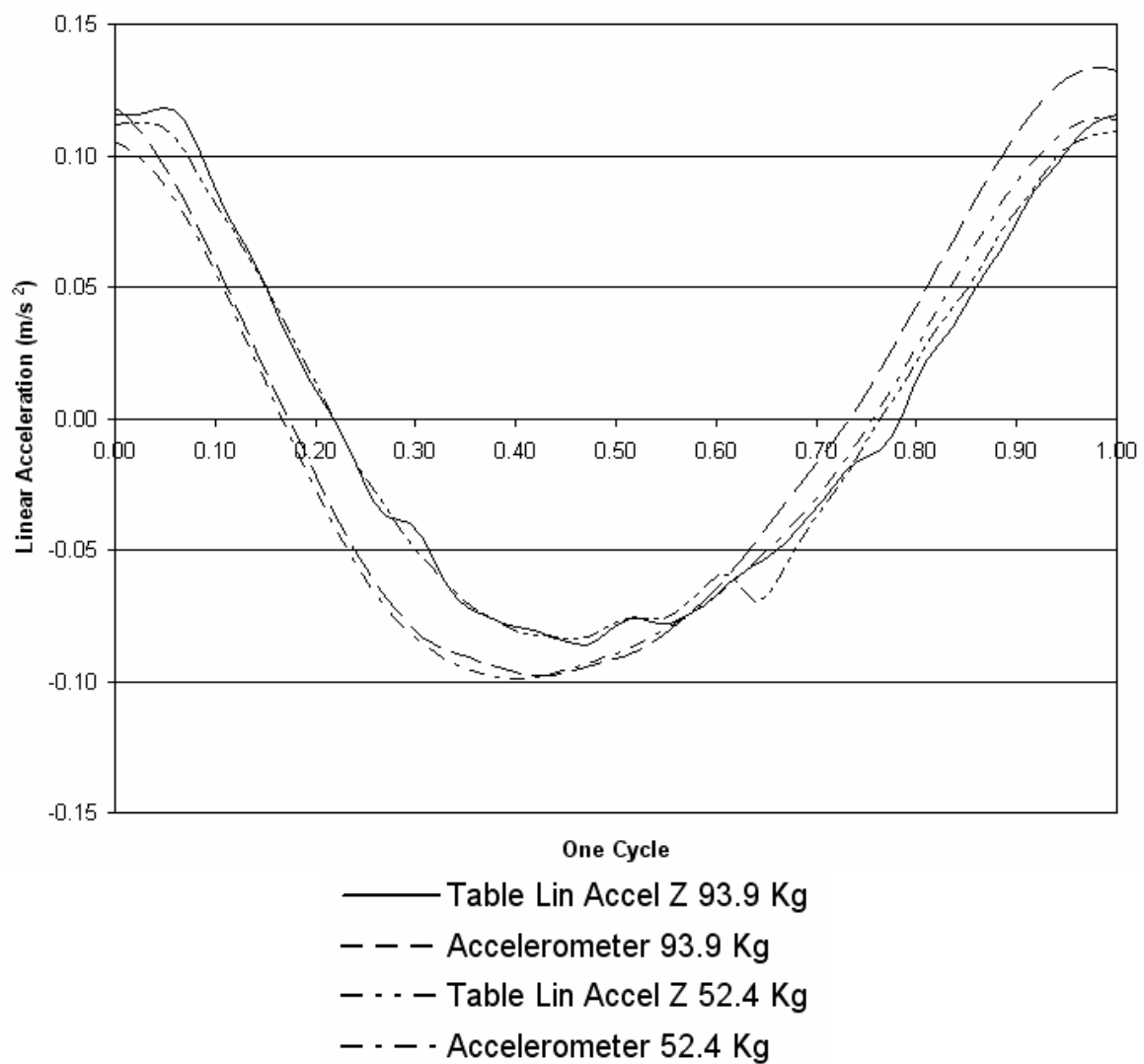
Figure 17: Acceleration Profiles Comparing Performance of Eight Commercial Tables with that of the Instrumented Table for this Study Set at Approximately 0.5 Hz.



Finally, effects of varying mass loads on the table mechanism were studied for any significant variation in performance as a result of different subject stature. Comparison of

the two subjects: height 186.7 cm and 157.5 cm, mass 93.9 Kg and 52.4 Kg, anterior-posterior 23 cm and 16 cm, and lateral 30 cm and 26 cm. Note the consistent phase lag in the differentiated position data (table lin accel) versus the smoother accelerometer output (Figure 18). No significant effects are observed from the difference in subject mass.

Figure 18: Data From the Subject in Figure 14 is Plotted in Conjunction with a Second Subject of Smaller Stature.



Uniaxial Load Cell

Factory calibration of the load cell was evaluated by comparing the output from a series of static loads applied in compression and in tension. Table 6 provides the comparison of in-line loading of the load cell and the force plate. The initial calibration setting provided for the load cell by the manufacturer showed an underestimate of the actual loads by 21.5% ($\pm 1.35\%$) difference in compression compared to the force plate. The calibration setting was adjusted and the static measurements were repeated yielding a percent difference of 0.72% ($\pm 0.9\%$). The difference between force plate and known loads was 0.5% ($\pm 0.6\%$). Load cell tensile test outputs were within 2.82 % of known values after recalibration.

The installed load cell in line with the drive train for the table motion yielded output differing from the known weights by an average of 16.8%, this is the proportion of load being borne by the hinge support. Dynamic tests were performed by activating cyclic table motion at medium speed with subjects of different stature.

Table 6: Comparison of Load Cell Output with Output From Factory Calibration, and

Following Adjusted Calibration with Known Static Loads Stacked In-Line on the Load Cell and Force Plate.

Weighed (N)	Force Plate	Load Cell (initial cal)	Load Cell (new cal)	Percent Difference from force plate with initial cal	Percent Difference from force plate with new cal
22.69	23.085	-27.465	-23.106	-18.971	-0.090
46.71	46.958	-57.236	-48.033	-21.887	-2.288
69.39	69.919	-85.932	-70.694	-22.903	-1.108
88.96	88.882	-107.823	-88.871	-21.309	0.013
111.65	111.745	-136.585	-112.293	-22.229	-0.490
135.67	135.816	-164.974	-136.333	-21.468	-0.380
			Average	-21.461	-0.724
			St. Dev.	1.347	0.862

Subjects

A total of nine volunteers meeting the entrance criteria agreed to participate in this study. Five (3 male, 2 female) were in the healthy group and four (3 male, 1 female) in the low back pain group. Altogether, subjects ranged in age from 29 to 50 years and had stature with a mean height of 177.0 cm (+/- 9.9 cm), mean weight of 92.2 Kg (+/- 44.2), and body surface area (BSA) 1.93 m² (+/- 0.25). The prior week pain scores by visual analogue scale (VAS) served as the baseline for each subject. Healthy patients reported a mean VAS of 0.4 (\pm 0.4) while LBP subjects listed a mean VAS of 6.2 (\pm 1.2). Little change in VAS was observed over the course of the test sequences, ranging from 0.1 to 0.2. One subject experienced an increase in discomfort of 2.4 points during the course of the test.

Validation of the Biomechanical Model

The passive loading of the L5/S1 disc from static postures and tasks is explicitly calculated with the commercial 3D biomechanical model, allowing for direct comparison with the estimates made for this study. The three standardized tasks (upright, weighted, and flexion) were selected to create a monotonically increasing load using symmetric postures. The estimates from both the 3D model and the 2D static model for this study were tested by Pearson-r correlation for comparability in response and Student – t test for systematic bias (Table 7). Excellent correlation was found for passive disc compression with $r^2 = 0.994$. A minimal systematic bias was found ($t = 4.012$, $p < 0.0005$) with the 2D static model underestimating the 3D model by 1.2%. For moment calculations, a slightly smaller correlation of $r^2 = 0.935$ was observed. However, no systematic bias was noted as the 2D model reproduced the 3D model estimates within 2% ($t = 0.416$, $p < 0.681$).

Table 7: Comparison of Mean Force and Moment Estimations Between the 3D Commercial Model and the 2D Static Model Developed for this Project.

	3D Commercial Model		2D Static Model		Difference In Means	t-statistic	p-value
	Mean	SD	Mean	SD			
Force	281.7 N	(55.5)	278.1 N	(55.8)	3.6 N	4.01	0.0005
Moment	32.5 Nm	(24.8)	32.9 Nm	(25.6)	0.53 Nm	0.416	0.681

MES-RMS Predicted Loads

Joint forces and moments are the main determinants, driving muscle response under static weight bearing conditions. Similarly, the joint loads are primarily a function of body segment geometry and postures for the structures supported by the joint under consideration. As a result, the active loads generated by the back muscles in the 3D model and the MES-RMS predicted loads for the equivalent muscle model should be comparable. Similarly, values recorded for healthy and low back pain groups should be essentially the same under non-painful weight-bearing tasks when they are normalized for stature (forces: weight and moments: height times weight) of the subject.

Regression of the calculated values for the muscle-generated spinal loads from the commercial 3D model with the MES-RMS mean values over the 10 second test interval of

the calibration tasks yielded predictive equations for both the healthy and low back pain volunteer groups and are given below.

$$\text{Healthy: Erector Spinae Muscle Load (N)} = -21.05 + 15.58 * \text{MES-RMS (mV)} \quad \text{Eq. 4.1}$$

$$\text{LBP: Erector Spinae Muscle Load (N)} = 147.05 + 8.51 * \text{MES-RMS (mV)} \quad \text{Eq. 4.2}$$

Multifidus muscle loads were computed by proportion of erector spinae muscle cross-sectional area (12.44%).

A strong correlation was observed between the 3D predicted erector spinae muscle load ($r^2 = 0.503$) and the MES-RMS predicted loads from the multifidus muscle that accounted for 92% of variation (R^2) in the data. An underestimation of the predicted muscle loads from the 3D model by the 2D model of 9.9 N was observed but was not statistically significant. When data was normalized for patient stature and contrasted between healthy and low back pain groups, the results were correlated ($r^2 = 0.533$) with 99% of the data variation taken into account.

Inverse Dynamics Model of CPM

Prone CPM loading of the spine is the algebraic sum of three components: 1) the upper body mass weight, 2) inertial loads caused by periodic motion to the lower body, and 3) the internally generated forces and moments from muscle action crossing the cutting plane

of the disc at L5/S1. Load-time histories provide a continuous representation of these actions over the time of each CPM period.

Some small variability in the consistency of CPM cycle timing was observed, necessitating the representation of parameters normalized to cycle period. All parameters were first represented in global coordinates at the force plate, combined as necessary and then estimated at the L5/S1 disc level through mathematical load transformation. The transformation is determining the loads in one coordinate system to a secondary coordinate system. There, the effective muscle action was taken into consideration and regression equation predictions of effective muscle load based on MES-RMS of the multifidus muscle were summed. The sum of the multifidus was used when determining the regression equation because the 3D program used the erector spinae as the summation of all posterior stabilizing muscles.

A key assumption for the validity of the present work is that the pivot for motion within the body lies within the L5/S1. Under these conditions, surface markers on either side of the pivot (lumbar vs. sacrum) should show little relative displacement while markers at greater distance will show displacements proportional to the length of the body. Lower body segments allow for comparison of relative movements. Figure 19 displays the motions of the markers on the lower body and the rigidly fixed pylon supporting the accelerometer. Table 8 uses the mean distance from the cephalad edge of the support surface for the lower body to the marker sites and the vertical displacement to calculate the maximum angular displacement. Excellent agreement between the angular displacement of the sacrum and

shank is observed indicating the approximate center of rotation lies between the sacral and lumbar markers.

Figure 19: Displacement of Lower Body Segments and Table in the Vertical (Z) Axis.

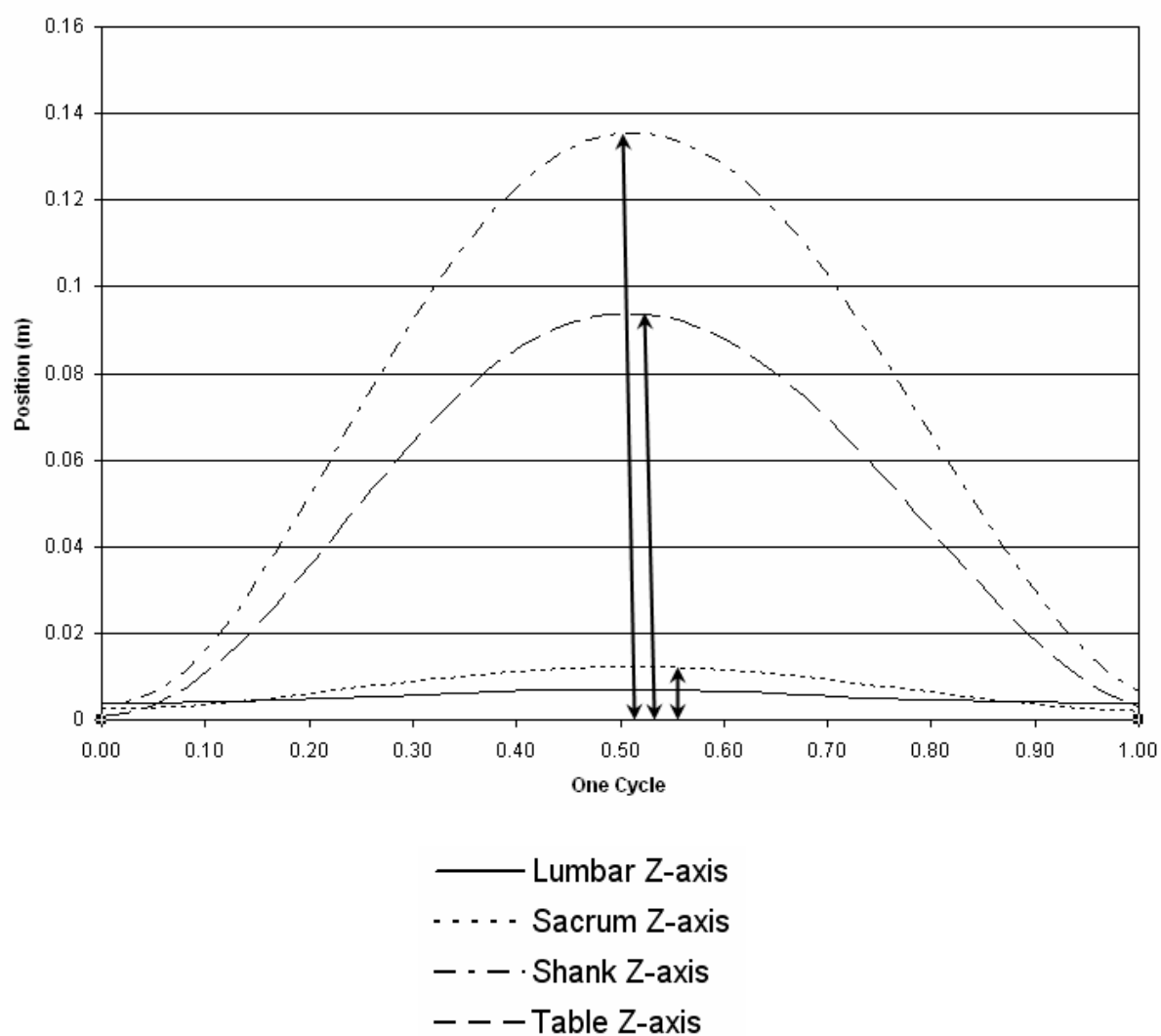


Table 8: Calculation of Table Angular Displacement From Peak Marker Vertical

Displacements and Mean Distance of Marker Site Along the Table Length (Y-Axis).

	Sacral Marker	Table Marker	Lower Leg Marker
Y-axis site	8.75 cm	54 cm	87 cm
Vertical displacement	1.4 cm	9.14 cm	9.46 cm
Calculated angle	8.8 °	9.1 °	9.5 °

Overview of MES-RMS Activity

Load transmission pathways during CPM are unknown. This work estimates the resulting load transmitted through the body's transverse cutting plane at the L5/S1 segment. However, awareness of how the muscles respond to the periodic motion may provide insights into the development of the transmitted load. For example, should all pelvic muscles be inactive, motions would be expected to occur at the sacroiliac and femoral joints as deformation of soft tissues occurs as the body bends, attenuating load transmitted to the L5/S1. At the opposite extreme, rigid contraction of pelvic and leg muscles would stiffen the pelvis and femoral joints, potentially promoting loading at the targeted disc. Quantitative evaluation of the lower body muscular actions is reserved for future applications. However, a general insight is available by observation of the qualitative description of muscle behaviors.

Three descriptors characterized the general behavior of muscles recorded during the CPM motions; cyclic, steady and bursting activity. Cyclic action showed regular patterns of increasing and decreasing activity, generally phase shifted with the table motions. Individual

muscles were observed to cycle in step with the table downward motion, associated with bending the spine in flexion while other muscles seemed to more consistently respond to upward motion that was associated with unbending of the spine. Steady myoelectric action was observed in other muscles that seemed to be nonresponsive to cycle motion and to maintain a continuous level of activity. Finally, a few muscles showed unpredictable and short lived bursting responses.

Variability was observed within individual muscles and across CPM conditions. The more consistent muscles were the multifidus and the hamstring groups, which tended to be either cyclic or continuous in response. The latissimus dorsi, a potential contributor to the loads acting on the lumbosacral spine, proved most difficult to characterize and to quantify as it was often dominated by heart beat artifact despite use of notch filtering and, in two subjects, had large artifacts rendering the data unusable. While the sample size was small, the group membership as a healthy subject or a low back pain subject did not appear to predict individual muscle response.

Regardless of no general muscle activation pattern, the potential loading effect from contraction of the muscles cross the cutting-plane at the L5/S1 disc. Table 9 shows the characterization of the multifidus muscle MES-RMS in the mean and the predicted equivalent spine loads across a typical cycle. The lag represents the percent of the cycle period to the appearance of the greatest MES-RMS signal amplitude. The low back pain group tended to peak earlier in the cycle than did the healthy group at lower CPM rates. At the higher rates, both groups responded similarly in the cycle. For all three conditions, the

peak activity generated a mean of 43.5% higher activation and corresponding predicted muscle tension.

Table 9: Greatest RMS Amplitude, Cycle Lag, and Predicted Load for Healthy and LBP Groups.

CPM Type	Lag (%Cycle Period)	RMS Amp (mV)	Predicted Multifidus Load (N)
Mean Intermed - Speed Healthy	41.63	18.785	33.82
Mean Intermed - Speed Med LBP	30.74	30.090	55.75
Mean High Speed Healthy	60.95	29.019	53.67
Mean High Speed LBP	65.50	40.748	76.42
Mean Intermed-Speed at 20 Degrees Healthy	58.40	21.161	38.43
Mean Intermed-Speed at 20 Degrees LBP	32.90	27.008	49.77

Figures 20 a – c show the range of cycle lag for greatest and least MES-RMS activity superimposed on a typical table cycle period. The range of cycle lags to greatest and least RMS is quite broad. In general, the higher rate of CPM is associated with slightly broader ranges than slower rates, which demonstrates greater variability within the groups. Greater depth of angular displacement during CPM tends to shift the range of cycle lag to the left.

Figure 20-a: Variability of Lag to Greatest and Least RMS Amp with Table Position Between Healthy and LBP Groups During CPM at Intermediate Speed.

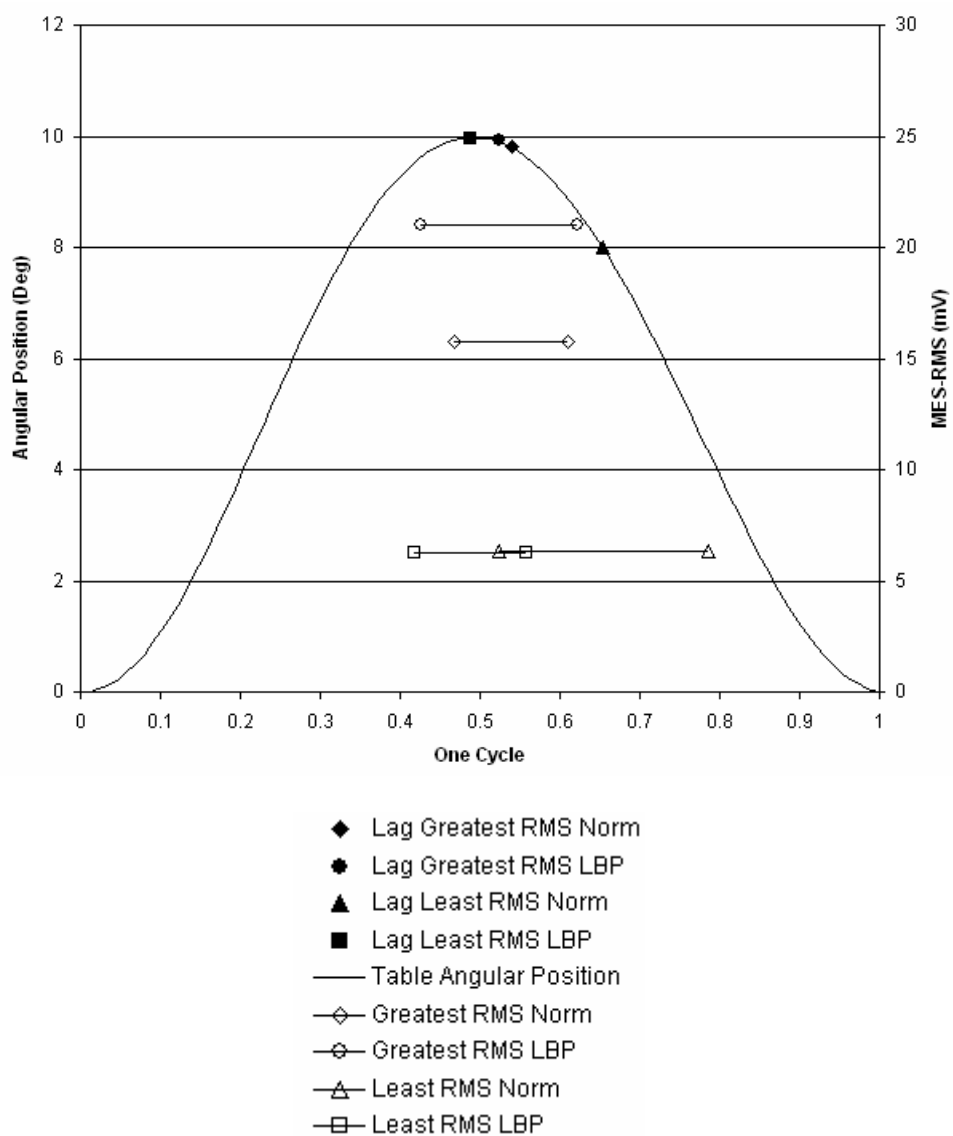


Figure 20-b: Variability of Lag to Greatest and Least RMS Amp with Table Position Between Healthy and LBP Groups During CPM at Fast Speed.

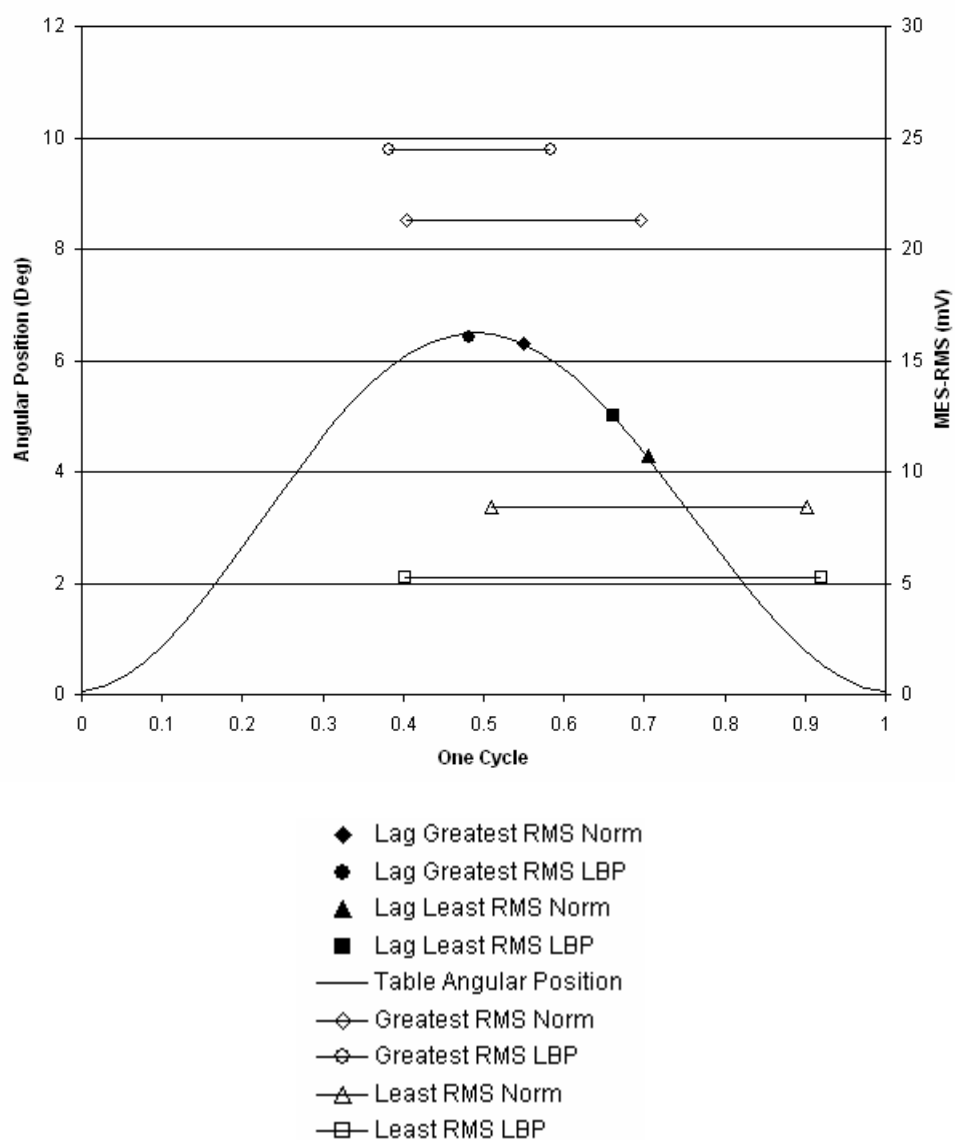
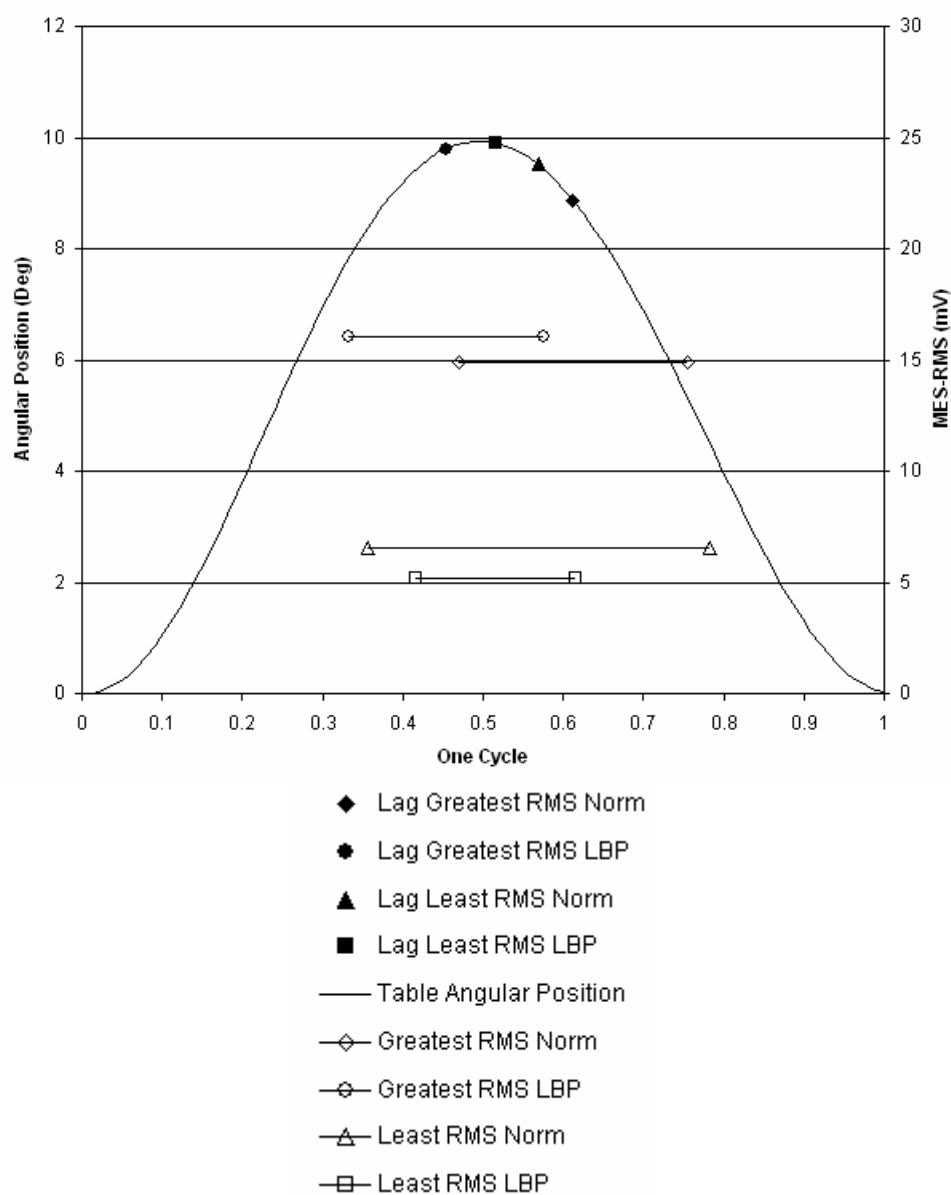


Figure 20-c: Variability of Lag to Greatest and Least RMS Amp with Table Position Between Healthy and LBP Groups During CPM at Intermediate Speed with 20 Degrees.



Perhaps more representative of the fact that the multifidus muscle activity varied with the phase of the table cycle but did not ever become silent is the total MES-RMS value per full cycle as given in Table 10. While variation is evident, continuous activity was observed across the cycle. Only the LBP group under the influence of higher rate CPM appeared to differ in its behavior over the period ($F_{\text{var}} = 0.01$).

Table 10: Mean MES-RMS Values per Full Cycle.

Group	CPM Med Multifidus		CPM Fast Multifidus		CPM 20Deg Multifidus	
	Mean	Std Dev	Mean	Std Dev	Mean	Std Dev
Healthy	0.8986	0.4554	0.5715	0.5113	0.8633	0.2867
LBP	0.9852	0.3020	0.4058	0.0861	0.6590	0.1354

F test on Variability*	2.27	35.26	4.48
p	NS	0.01	NS

Sub	CPM Med Multifidus		CPM Fast Multifidus		CPM 20Deg Multifidus	
	Mean	Std Dev	Mean	Std Dev	Mean	Std Dev
1	0.8482	0.1257	0.3349	0.0215	0.7646	0.0214
2	0.9019	0.0117	0.4316	0.0052	0.6114	0.0156
3	1.6527	0.1284	1.4793	0.0822	1.3585	0.3103
4	0.4788	0.0042	0.2552	0.0107	0.7958	0.0081
5	0.6117	0.0072	0.3565	0.0451	0.7864	0.0086
6	1.3194	0.3480	0.4440	0.1356	0.6369	0.0074
7	0.9048	0.0951	0.4578	0.0381	0.7844	0.0965
8	0.6101	0.0296	0.2769	0.0457	0.4780	0.0777
9	1.1064	0.3127	0.4445	0.0610	0.7368	0.1220

* From Mendenhall ³⁰

Low Back CPM Transmitted Loads

The effect of CPM on spinal tissues depends on the loads transmitted through them. The intended action is to distract and flex the spinal joints at the disc. Muscle action, if of

sufficient amplitude, could over power the input forces and moments resulting, in the extreme, with exactly the opposite effects. Similar influences of muscular loads have been observed with lumbar traction³¹ and in the predicted effects of muscle action during scoliosis bracing³². For CPM tested in the present work, the postures and motions are sagittally symmetric as is the input driving force from the table actuation. As expected from the symmetry, the only significant forces transmitted through the spine are in the y-z plane. Similarly, the only significant moments are about the transverse or x-axis. The total loads are the algebraic sum of motions of the lower body at different speeds, the body mass weight and the internal muscle generated forces that cross the cutting plane.

Figures 21 a-c show the load-time histories for the forces and moments transmitted through the spine at the L5/S1 junction for the healthy and LBP groups. The mean was calculated over ten cycles of each subject at the different CPM conditions. The mean of each subject was then used to calculate a grand mean and standard deviation at each time interval. Each illustration gives the group mean and standard deviation curves, over the CPM cycle, for the passive forces and moments, the active forces and moments superimposed on the table cyclic motion. The passive force and moment represent the action of the inertial loading from the lower body motions interacting with the upper body mass. The active elements are from the MES-RMS predicted muscle tensions. The total loads, not separately depicted, are the algebraic sums of the two sets of curves. It is important to note that while the figures cite the plotting of the active moments, the magnitudes of these are sufficiently small as to be illegible on a scale adequately large to contain the passive elements.

Clearly the active loads are a small contribution, in comparison to the passive loads, to the total transmitted force and moment. Based on these results, it appears that muscle action, while capable of attenuating the transmitted loads to a small degree, can be ignored as a practical matter. Perhaps the most characteristic feature of the MES-RMS predicted loads is the difference in pattern of activation in the mean between healthy and LBP subjects. At lower CPM rates, the muscles appear to deactivate as the torso bends for healthy subject whereas, for the LBP group, the activity remains relatively constant.

Figures 21 a-f all demonstrate a phase shift to the left for the peak loads in comparison to the peak position of the table motion. The phase shift arises from the fact that the loads applied by the CPM motions are a consequence of the accelerations applied to the lower body. Acceleration peaks always precede the peak of position showing, in this case as a phase shifted to the left.

The patterns of muscle activity observed were unexpected. In simple terms, muscle stretched at sufficient speed is expected to result in a reflex activation. In the data presented here, healthy subjects showed a decrease in muscle activity as the table moved from the horizontal position followed by increase again as the cycle period ended. Unhealthy subjects generally demonstrated lesser activity in comparison to the healthy groups at all phases of the motion cycle. In the mean, there was little change in activity regardless of table motion.

The final question of loading from the action of CPM is whether the transmitted loads can be accurately predicted from the subject's stature and the speed of motion application. Regressions were performed attempting to predict the passive transmitted force and moment magnitudes based on CPM speed setting and subject stature and accounting for group

membership. Based on the small sample size, the critical p-value for significance was accepted at 0.1 that, for larger samples, would be considered a trend.

Transmitted passive force magnitude was achieved with $R^2 = 0.654$ while moment magnitudes reached $R^2 = 0.302$. Table 11 lists the variable coefficients and probabilities. Both speed and mass (Kg) were significant contributors to the successful prediction ($p = 0.000$ & $p = 0.081$, respectively). In the case of the moments, only the body mass index ($BMI = \text{mass} * \text{height}$) was significant ($p = 0.040$).

Table 11: Regression Equation Coefficients and Associated Significance Values

	Force Magnitude	p-value	Moment Magnitude	p-value
CPM Speed	-15.92	0.081	-6.77	0.343
Mass or BMI	1.39	0.000	0.0024	0.040
Group	-2.64	0.764	-2.71	0.704
Constant	56.04	0.049	42.79	0.034

Figure 21-a: Intermediate Speed Grand Mean of Healthy Active and Passive Sagittal CPM

Loads 11.5 Degree Angular Motion.

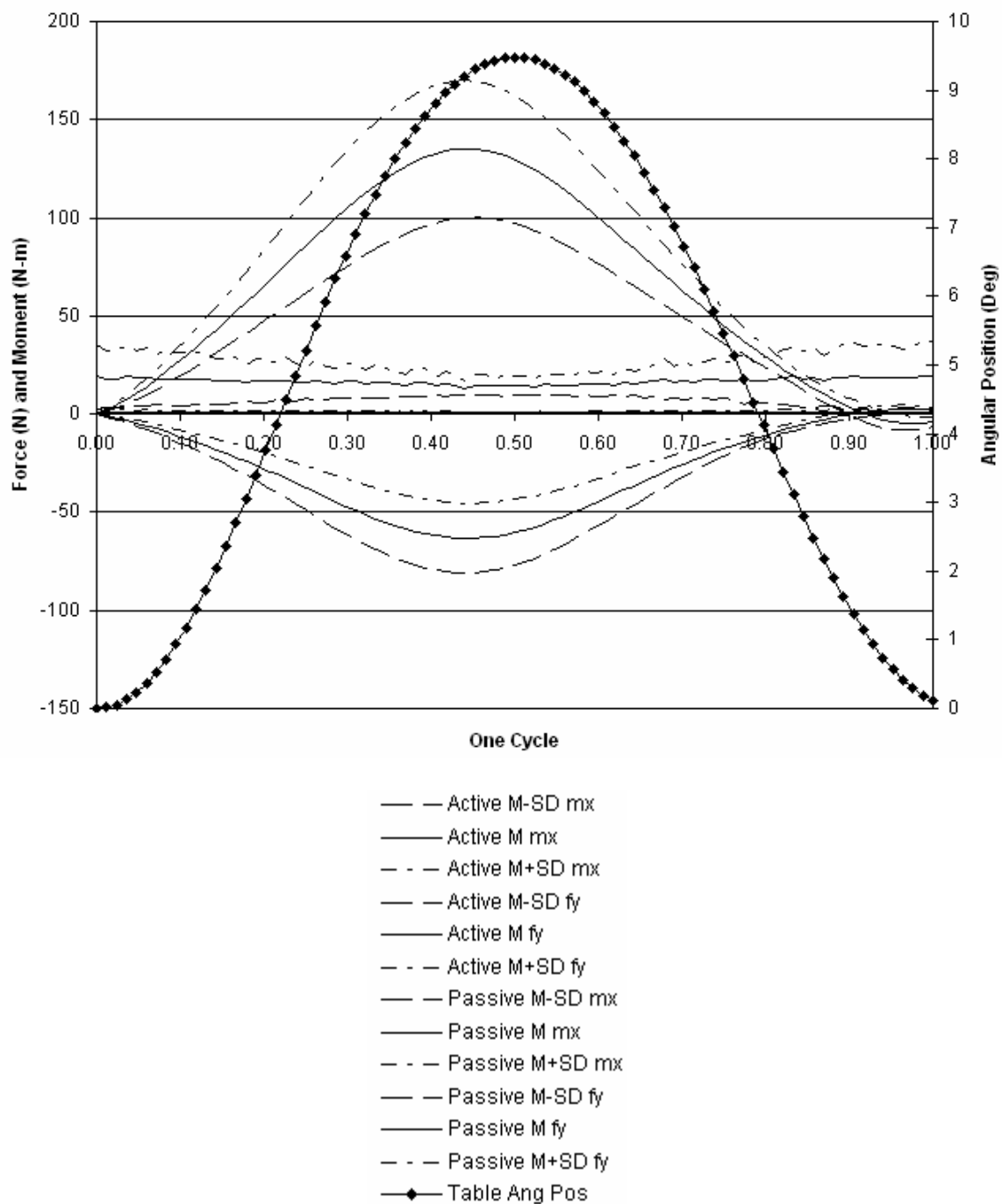


Figure 21-b: Intermediate Speed Grand Mean of LBP Active and Passive Sagittal CPM

Loads 11.5 Degree Angular Motion.

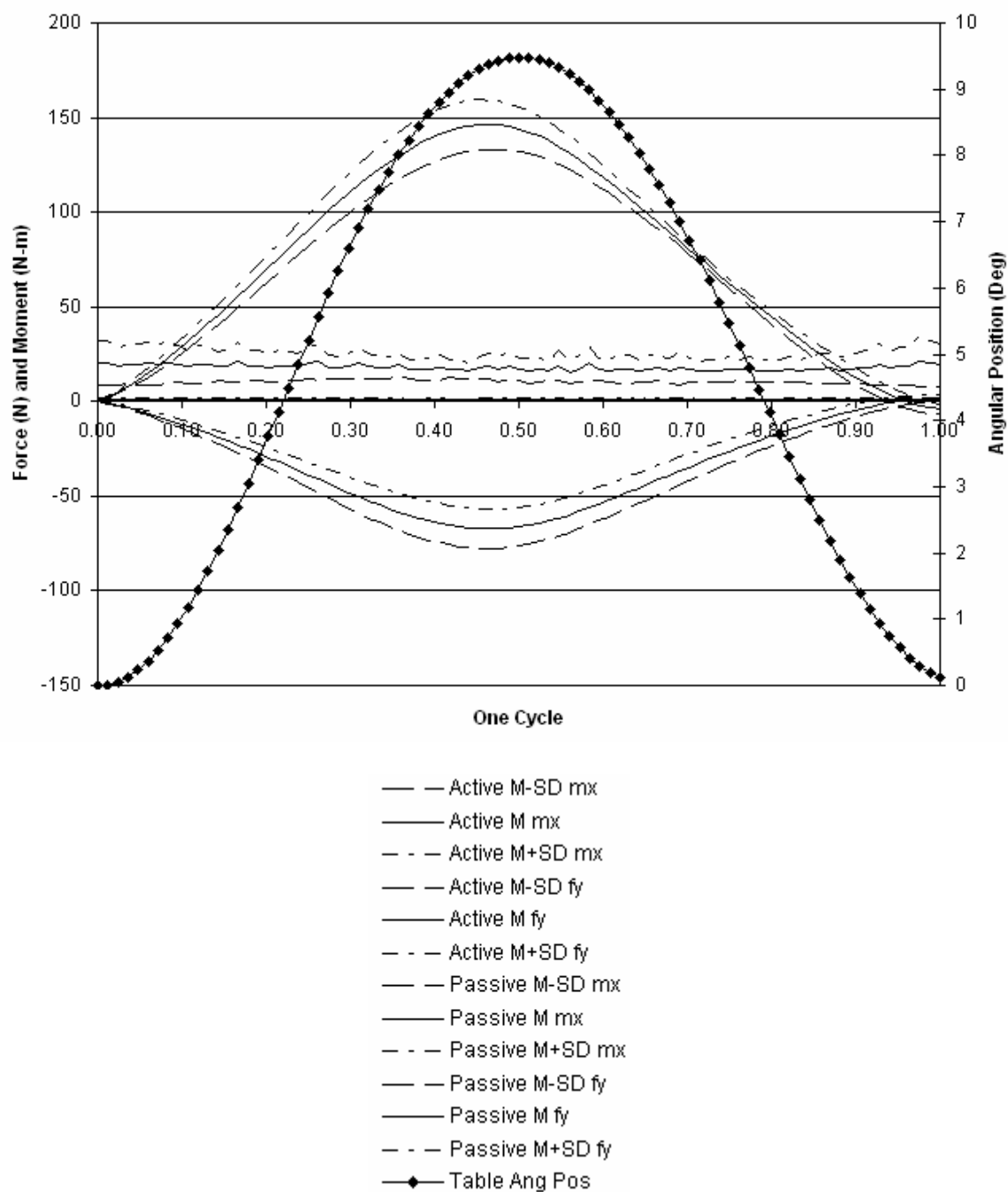


Figure 21-c: Fast Speed Grand Mean of Healthy Active and Passive Sagittal CPM Loads
11.5 Degree Angular Motion.

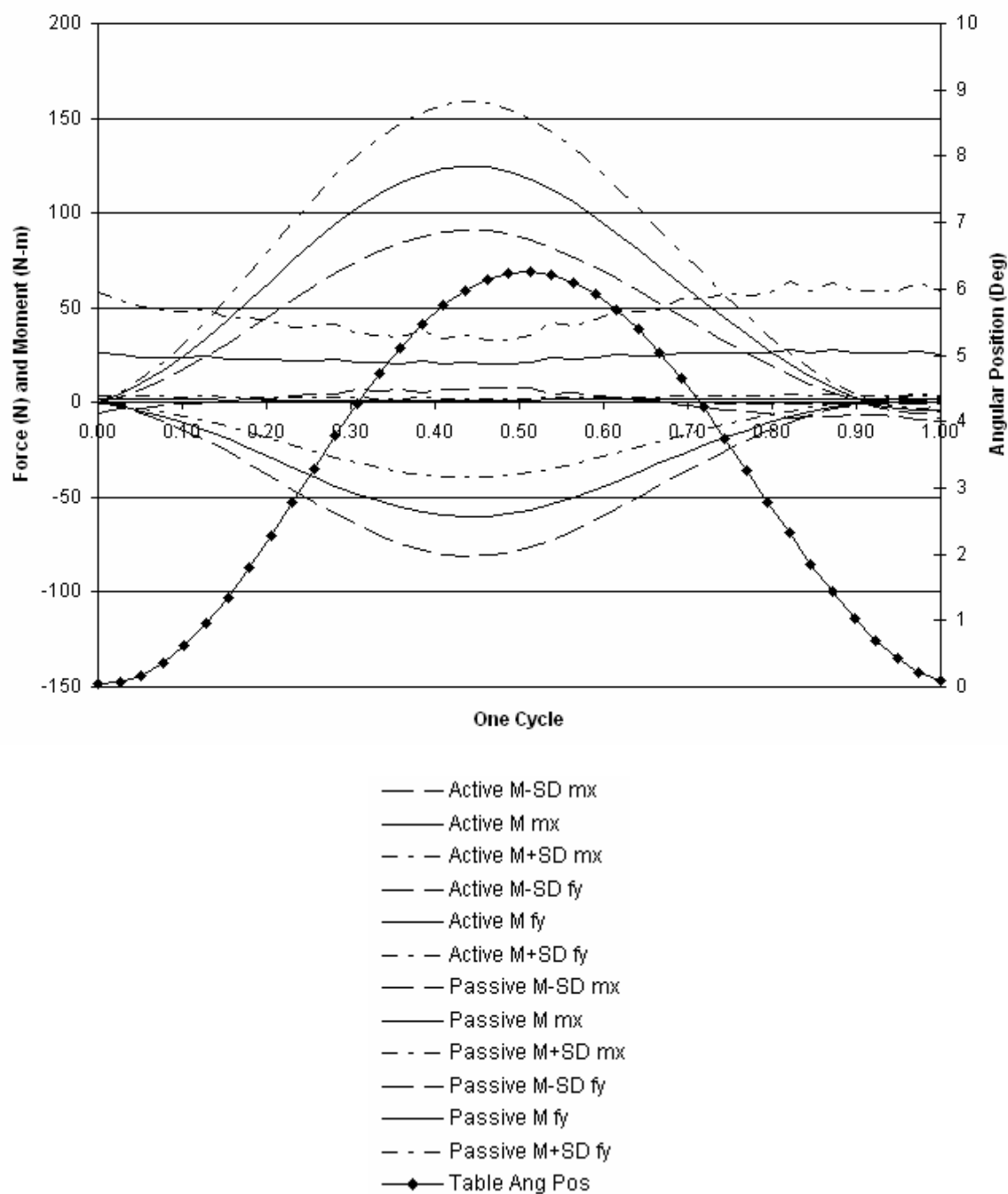


Figure 21-d: Fast Speed Grand Mean of LBP Active and Passive Sagittal CPM Loads 11.5

Degree Angular Motion.

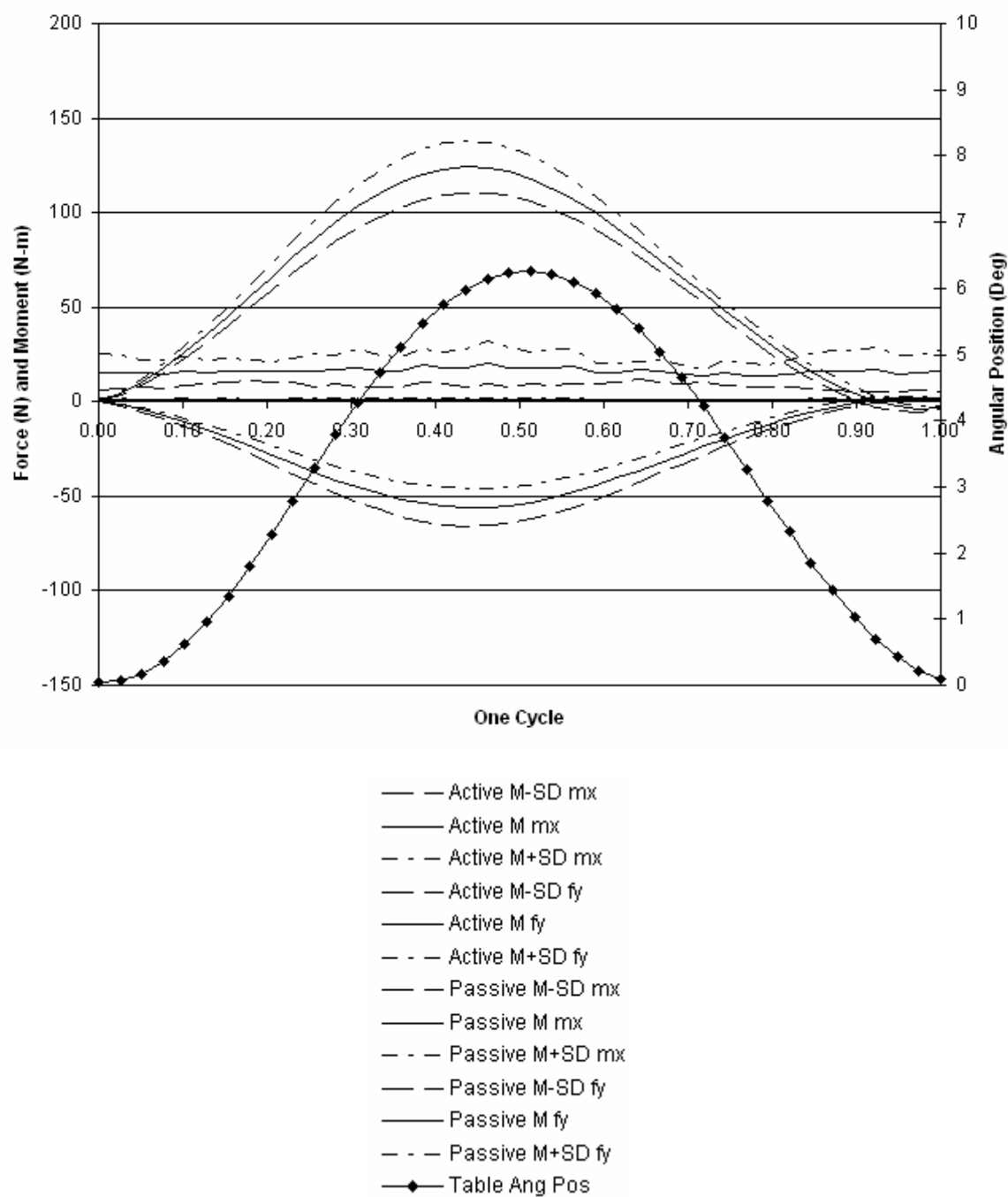


Figure 21-e: Intermediate Speed Grand Mean of Healthy Active and Passive Sagittal CPM

Loads at 20 Degree Angular Motion.

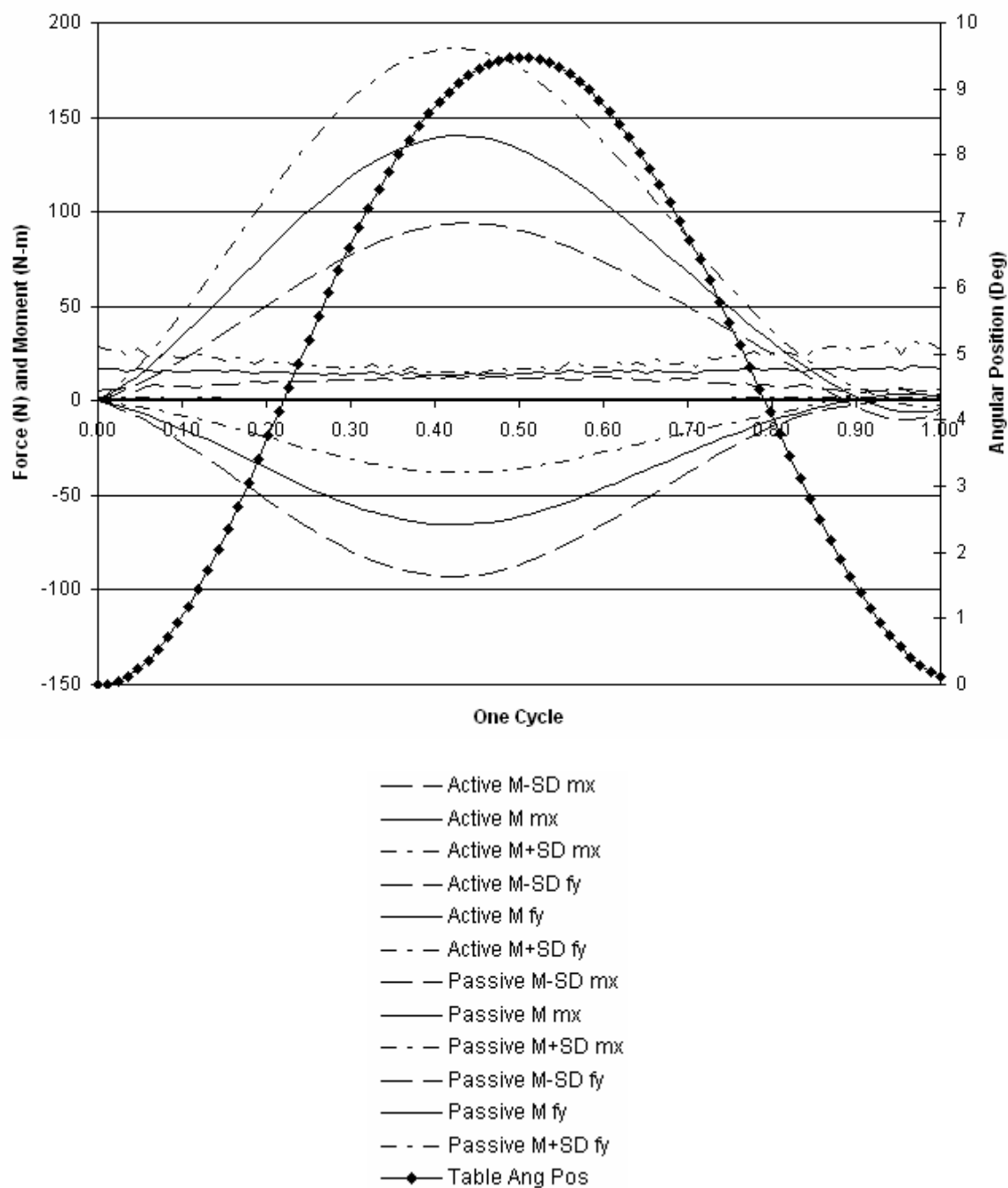
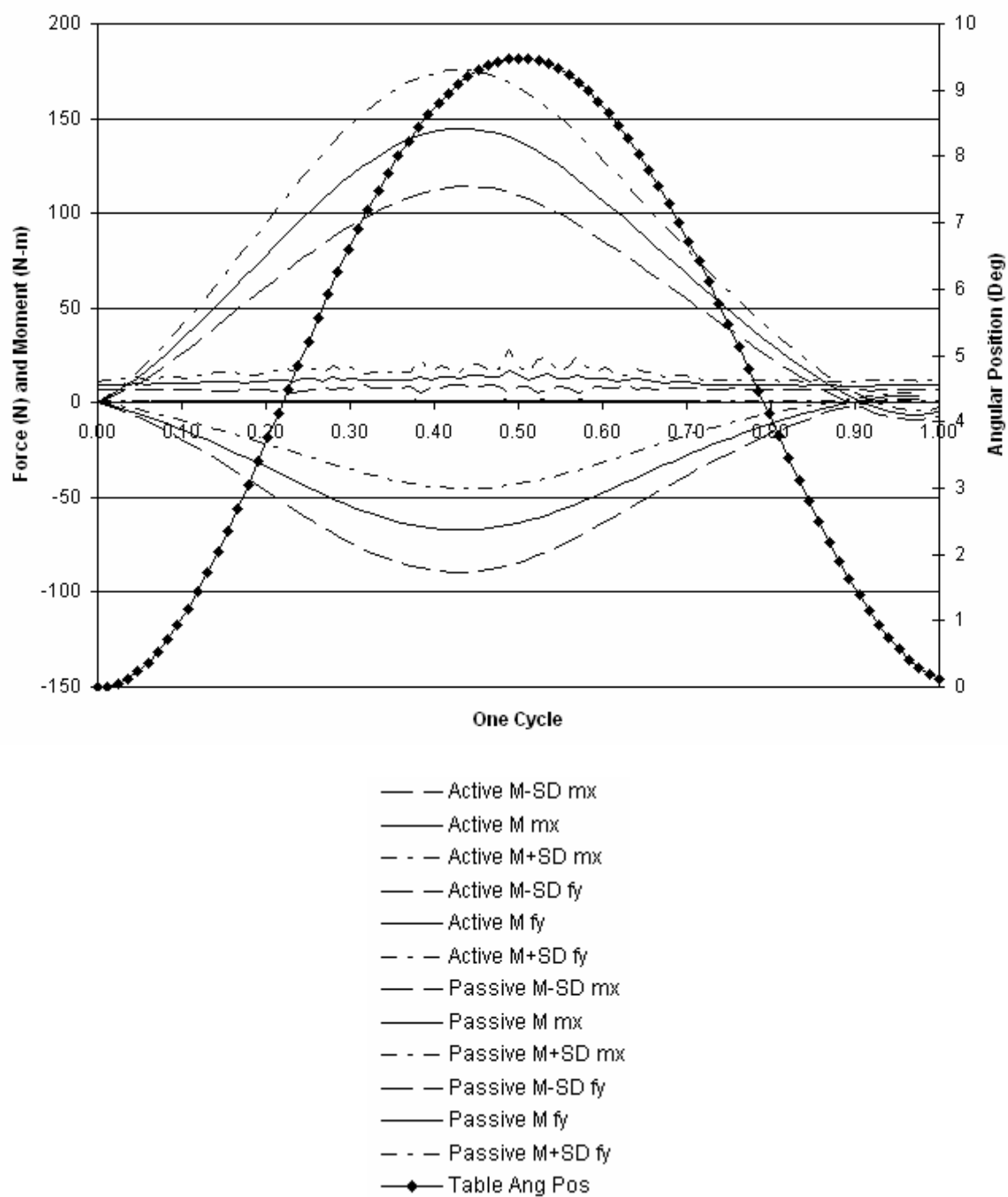
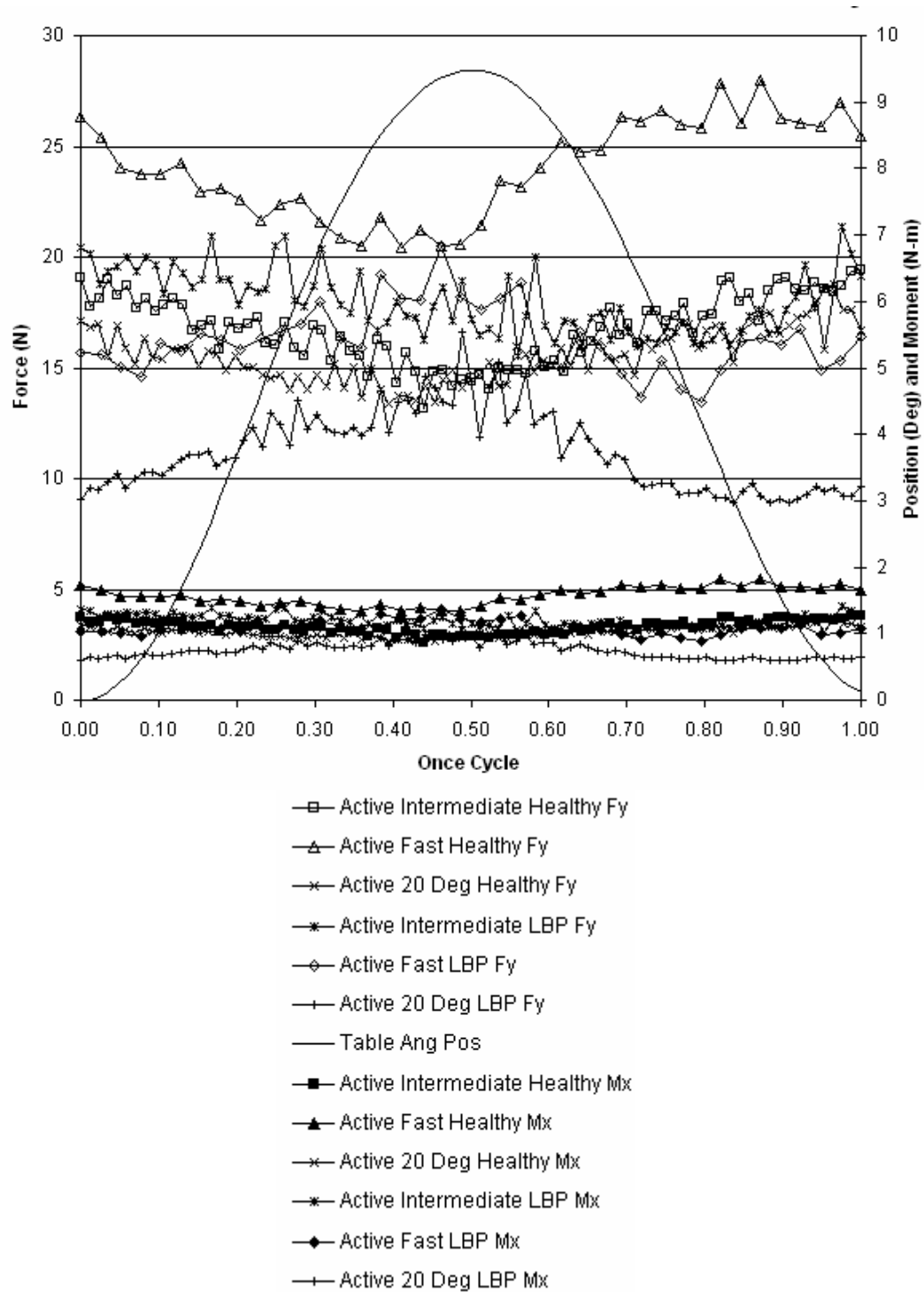


Figure 21-f: Intermediate Speed Grand Mean of LBP Active and Passive Sagittal CPM Loads
at 20 Degree Angular Motion.



The unknown factor in determining the total loads passing through the lumbar spine during CPM are the active loads. As shown in Figure 22, the estimated active forces and moments have a range of 9 N to 28 N and 0.6 Nm to 1.8 Nm for healthy and LBP groups respectively during the various CPM methods. The range of loads is minimal in comparison to the passive loads created by the motion of the table.

Figure 22: Active Loads for Healthy and LBP Groups During CPM at Intermediate Speed, Fast Speed, and Intermediate Speed at 20 Degrees.



CHAPTER FIVE

DISCUSSION

This work represents an extensive biomechanical study of recumbent CPM applied to the spine in patient class with reference to a healthy control population. It is intended to deal with challenges to procedural control and validity of clinical applications. The clinical intent of CPM is to engage joint motion without the influence of upright body weight, reduce stiffness around the joint from the accumulation of tissue swelling and edema, reduce muscle tension and promote healing. While this could not directly assess the physiological effects of CPM (beyond the scope of the study), the question of muscle activation is relevant. As noted for other spinal therapies, notably traction³¹ and scoliosis bracing³², the clinical observations and perceptions in forming the theoretical foundations, for patient management may be incorrect. For traction, the expected reduction in disc pressure was actually associated with an increase in disc pressure in every case, due to strong opposing muscle action. With scoliosis bracing, it had been presumed that the discomfort of the throat mold pressing upward against the larynx would induce volitional postural adaptations, producing muscle forces and moments that would be corrective in nature. Biomechanical models have shown that muscle action is capable of straightening curvature. It has also been shown that the amount of muscle action developed by bracing is negligible.

CPM for spine disorders has also been grounded on clinical knowledge and the extrapolation from earlier work in peripheral joints. Might it also be true that the intended muscle relaxation in this case is overwhelmed by reflex muscle tension caused by stretching?

CHAPTER SIX

CONCLUSIONS

As shown in Figures 17 a-c, the muscular response to CPM stimulation is varied in its timing and its amplitude. There appears to be no clear or useful pattern, at least within the constraints of this small sample. From Table 8 and Figures 18 a-c, there is a suggestion of more constant low grade muscle activity found in LBP subjects verse controls, particularly at higher rates of CPM. An unexpected result shown in Figures 18 and 19 in the healthy group is an increase in active forces during the initial and final four degrees of CPM cycle motion. Regardless, the main result of this work is that internally developed muscle tension does not appear to be sufficiently strong to confound the intended effects of CPM. A basic hypothesis of the mechanism in the use of CPM appears to be confirmed by the data presented here.

It may be a useful construct to apply cyclic, inertial loads to the spine. However, how to control those loads explicitly has not been a topic of study. This work asked an additional question as to whether the simple intuitive notion that passive loads transmitted through the spine might be a function of subject mass and cycle frequency or speed. Even for such a small sample, the data on transmitted forces strongly support that hypothesis. As shown in Table 8, the regression analysis demonstrates that both speed and, more so, body mass predict the passive transmitted force. Moments, however are not as clearly defined. Only the body mass index held influence on the transmitted moments, and then, at a much lower level of statistical significance. Given the absence of internal, active muscle forces of consequence, it may be possible for future investigations to help design control strategies that improve the efficiency and effectiveness of therapeutic load applications.

The sample population for this study was small and represents the study's greatest weakness. While the results appear to be consistent and numerically grounded, the sample may be a special case and not represent the general population of back pain sufferers. It is at least conceivable that there exist patients who have a more dramatic MES-RMS response to CPM. The data here would not generalize to that population under those conditions. Moreover, means to prospectively identify such cases remain to be determined.

CHAPTER SEVEN

RECOMMENDATIONS FOR FUTURE WORK

Future work should examine the current study's hypothesis in a larger population. This would determine if the results determined in our small population are generalizable.

The current work examined the loads induced on L5/S1 with symmetric loading. The treatment table has the capacity to induce eccentric loads by placing a subject in non-symmetric positions and applying CPM. Differential loading asymmetric positioning may have beneficial effects to be determined.

Clinical studies should be accomplished to examine the effects of CPM directly on patient symptoms and under distinct pathological conditions under alternate CPM conditions.

APPENDIX A
CONSENT FORM

Subject Consent To Be In Research

Title of Study:

Biomechanics of Continuous Passive Motion to the Lumbar Spine.

<u>Investigators</u>	<u>Office Phone</u>	<u>Night/Weekend Phone</u>
John J. Triano, DC, PhD. – Principal Investigator	972-608-5062	214-353-4323
Jennifer Diederich, MS(c)	972-608-5154	214-353-4323

You are being asked to be in a research study. Persons who are subjects in research have certain rights. These rights include your right to:

1. Be told about the nature and purpose of the research,
2. Be told about the procedures and any drug or device to be used in the research,
3. Be told about any discomforts and risks that could occur,
4. Be told about any benefits to the subject to be expected,
5. Be told about any other treatments, drugs, or devices that might be helpful to the subject,
6. Be told about any other medical treatments, if any, available to the subject during or after the research if problems arise,
7. Ask questions about the research,
8. Stop being in the study at any time,
9. Have a copy of the signed and dated consent form, and
10. To decide to be in the study or not to be in the study without pressure or untruths.

You have the right to privacy. All information that is obtained in connection with this study that relates to you personally will be kept private. Any information that comes from this study that has your name on it may be shown only to those carrying out the study, the sponsors of the study, the Presbyterian Hospital of Dallas Institutional Review Board (IRB) (described below) and your doctors. The Food and Drug Administration (FDA) of the U.S. government also may inspect all of the records of this study. If the results of this study are published, your name will not be used.

The records about your being in this study may be looked at by members and staff of the Presbyterian Hospital of Dallas IRB, and you may be asked questions by a member of that Committee about being in this study. If you wish, you may refuse to answer these questions. Your records may be chosen at random (as by drawing straws) for review by the IRB.

The researchers can tell you about treatment in case of problems from the research, which you should report to them promptly. Phone numbers where the researchers may be reached are listed on the top of this form. If you have questions about other treatment, drug, or device options appropriate for your case, at any time before or after becoming involved in this study, please speak

with one of the researchers. Because clinical situations vary among individuals, you may be referred back to the doctor in charge of your care for further consultation.

Be sure to ask the researchers any questions you have about the research or about your rights as a subject. If you have questions later, or if you wish to report a problem related to the research (besides telling the researcher), you may call the Presbyterian Hospital of Dallas IRB at 214/345-6901.

The Presbyterian Hospital of Dallas IRB has reviewed and approved this research based on certain laws about research in human subjects. Approval of this research by the Committee does not imply that the Committee is responsible for the conduct of this research or its results.

Being in this research is of your own free will. Choosing not to be in this study will involve no penalty or loss of benefits. If you decide to be in this research, you are free to withdraw at any time. If you withdraw from the study, you can still have standard treatment outside of the study.

The information on the next few pages tells you about the research and what you will be asked to do if you decide to be in the study. It also tells you about the risks and benefits of being in the study. Please read this form with care and feel free to ask questions.

Purpose:

The purpose for this study is to help determine the effect of continuous passive motion (CPM) on the low back. CPM uses a special table that will flex the low back with no physical effort by the patient. This study will help determine if the height and weight of a patient and speed of the table can be used to predict the impact CPM has on the spine. The study will also look at the effect CPM has on selected muscles of the back.

.

What You Will Be Asked To Do If You Are In This Study:

Patients who take part in the study may be healthy or have mechanical low back pain. Patients will be asked to perform three tasks: standing, bending, and holding weights. There will be four CPM tests. During these tests the patient will lie face down on the CPM treatment table. The table flexes the body at the waist a small amount (10 to 20 degrees). The study will last about an hour.

Research Procedures:

When you enter the study, you will be asked to meet with the patient coordinator to have the testing performed. The coordinator will review the procedure with you and have you answer questions about your back and any medications you may be taking. Sensors will be taped to your back and legs. These sensors will record your muscle activity during the three tasks. You will be asked to: 1) stand for 30 seconds, 2) bend forward 20 degrees for 30 seconds and 3) stand while holding a 3 pound weight in each hand with your arms extended in front of you. After completing these measurements you will lie face-down on a treatment table for four CPM tests. Additional sensors will be taped to your skin to record the position of your body. The tests will involve the table moving in small arcs to bend your lower back up to 20 degrees. After each test, you will be given a 5 minute rest period. During the rest time you may stand, bend or move. During all of these tests, your muscle activity and body movements will be recorded by the sensors taped to your skin.

Risks And Discomforts:

There is minimal risk associated with this study. You may feel short term discomfort related to the tasks. The feeling may be similar to discomfort you have during normal standing and bending during your day. You may also have some skin irritation from the tape used to attach the sensors to your body. If there are questions or if you have any problems from the test, you may contact the principal investigator by calling 972-608-5062.

Benefits:

Taking part in this study may not result in any direct benefit, if you are having mechanical low back pain. The benefit from the study is to generate data that will help future research on the treatment of low back pain.

Options To Being In The Study:

The other option to taking part in this study is to decline. Declining will not in any way affect your current or future care as a patient of the Texas Back Institute. Whether you decline or not, your standard care will continue as per your doctor's recommendations.

Withdrawal From Being In The Study:

It is not necessary that you take part in this study. Your taking part in this study is voluntary, and you may withdraw your consent and stop being this study at any time and for any reason without penalty. If you choose not to take part in the study, as a patient of the Texas Back Institute, the care given to you by your doctor will not change.

Cost Of Being In The Study:

There will be no additional charge to you for being in this study. However, normal billing for any office visit and treatment prescribed for you as a patient outside of this study will occur as if you were not part of a study.

New Findings:

Any new findings during the research which might affect your wanting to be in this study will be given to you.

Payment For Being In This Study:

The treatment you will receive is the same as if you were not a part of this study except for the addition of the one time testing. There is no payment for being in this study.

Consenting To Be In This Study:

You are deciding whether or not to be in this study. You should not sign until you understand all the information presented in this form and until all of your questions about this research have been answered. Signing this form shows that you have decided to be in this study, having read (or been read) the information given above.

1. I understand that this is a research study. ☐ Yes ☐ No
2. I understand the risks of being in this study. ☐ Yes ☐ No
3. I understand the length of time I will be in this study. ☐ Yes ☐ No
4. I understand the purpose and hoped-for outcomes of this study. ☐ Yes ☐ No
5. I understand that my being in this study is of my own free will. ☐ Yes ☐ No

If you did not answer “yes” to all of the above questions, please review being in this study again with the researcher. You should only sign this consent when you have answered “yes” to all of the questions above.

Signature Lines:

 Signature of Subject

 Date

 Printed Name of Subject

 Signature of Witness

 Date

 Printed Name of Witness

 Signature of Researcher

 Date

 Printed Name of Researcher

You Will Be Given A Copy Of This Consent Form To Keep

For use by interpreter:

I certify that I am fluent in the English language and in the _____ language. I have read and understood the preceding information and fully explained it to the patient/subject in his or her own language.

Signature of Interpreter

Date

APPENDIX B

MATLAB PROGRAMS

Description of MATLAB programs:

MATLAB Program 1: Program determines the EMG-RMS for each subject in calibration stances with a window of 50 ms. Secondly, a matrix is created containing all subjects' minimum, mean, maximum, and standard deviation calibration stances.

MATLAB Program 2: Program for performing RMS on the EMG and resampling the kinematic data. Program performs transformation on all the kinematic data from the Polhemus coordinate system to the global coordinate system.

MATLAB Program 3: Program for pre-processing the data: 1) zeroing position sensors; 2) calculate the angular position for the table sensor; 3) zeroing the accelerometer; 4) determine individual cycles; 5) truncate all data to end of first cycle and prior to last cycle; 6) sum muscle pair MES-RMS; 7) determine least and greatest MES-RMS for each cycle; 8) create matrix for each subject and CPM condition for multifidus lag and statistics

MATLAB Program 4: Program for determining the Grand Mean of variability at greatest and least Multifidus EMG RMS activity during CPM

MATLAB Program 5: Program calculates the total RMS per cycle per muscle pair

MATLAB Program 6: Calculating the loads at L5/S1 through equations for the cephalic section of the treatment table. Calculate passive loads with dynamic equations, active loads with regression equations, and the total loads are the sum of the passive and active loads. Program in entirety is shown below.

MATLAB Program 7: Program calculates a mean and mean +/- standard deviation for active, passive, and total loads for each subject

MATLAB Program 8: Program determines mean, mean-standard deviation, mean+standard deviation for active, passive, and total loads for healthy and LBP group.

MATLAB Program 9: Program calculates the mean, mean-standard deviation, mean+standard deviation for active, passive, and total loads for each subject at each interval.

MATLAB Program 10: Program calculates peak passive loads in healthy and LBP group for CPM conditions of intermediate speed, fast speed, and intermediate speed at 20 deg.

MATLAB program for calculating the loads at L5/S1 through equations for the cephalic section of the treatment table. Calculate passive loads with dynamic equations, active loads with regression equations, and the total loads are the sum of the passive and active loads.

```
clear all
```

```
% load c:\MATLAB6p5\work\analysis\sub1\CPMSlow\cor\datapercor120deg1.txt;
A1=datapercor1slow1;
% load c:\MATLAB6p5\work\analysis\sub1\CPMSlow\cor\datapercor2slow1.txt;
A2=datapercor2slow1;
% load c:\MATLAB6p5\work\analysis\sub1\CPMSlow\cor\datapercor3slow1.txt;
A3=datapercor3slow1;
% load c:\MATLAB6p5\work\analysis\sub1\CPMSlow\cor\datapercor4slow1.txt;
A4=datapercor4slow1;
% load c:\MATLAB6p5\work\analysis\sub1\CPMSlow\cor\datapercor5slow1.txt;
A5=datapercor5slow1;
% load c:\MATLAB6p5\work\analysis\sub1\CPMSlow\cor\datapercor6slow1.txt;
A6=datapercor6slow1;
% load c:\MATLAB6p5\work\analysis\sub1\CPMSlow\cor\datapercor7slow1.txt;
A7=datapercor7slow1;

% load c:\MATLAB6p5\work\analysis\sub1\CPMMed\cor\datapercor1med1.txt;
A1=datapercor1med1;
% load c:\MATLAB6p5\work\analysis\sub1\CPMMed\cor\datapercor2med1.txt;
A2=datapercor2med1;
% load c:\MATLAB6p5\work\analysis\sub1\CPMMed\cor\datapercor3med1.txt;
A3=datapercor3med1;
% load c:\MATLAB6p5\work\analysis\sub1\CPMMed\cor\datapercor4med1.txt;
A4=datapercor4med1;
% load c:\MATLAB6p5\work\analysis\sub1\CPMMed\cor\datapercor5med1.txt;
A5=datapercor5med1;
% load c:\MATLAB6p5\work\analysis\sub1\CPMMed\cor\datapercor6med1.txt;
A6=datapercor6med1;
% load c:\MATLAB6p5\work\analysis\sub1\CPMMed\cor\datapercor7med1.txt;
A7=datapercor7med1;
% load c:\MATLAB6p5\work\analysis\sub1\CPMMed\cor\datapercor8med1.txt;
A8=datapercor8med1;
% load c:\MATLAB6p5\work\analysis\sub1\CPMMed\cor\datapercor9med1.txt;
A9=datapercor9med1;
% load c:\MATLAB6p5\work\analysis\sub1\CPMMed\cor\datapercor10med1.txt;
A10=datapercor10med1;
```

```

load c:\MATLAB6p5\work\analysis\sub1\CPMFast\cor\datapercor1fast1.txt;
A1=datapercor1fast1;
load c:\MATLAB6p5\work\analysis\sub1\CPMFast\cor\datapercor2fast1.txt;
A2=datapercor2fast1;
load c:\MATLAB6p5\work\analysis\sub1\CPMFast\cor\datapercor3fast1.txt;
A3=datapercor3fast1;
load c:\MATLAB6p5\work\analysis\sub1\CPMFast\cor\datapercor4fast1.txt;
A4=datapercor4fast1;
load c:\MATLAB6p5\work\analysis\sub1\CPMFast\cor\datapercor5fast1.txt;
A5=datapercor5fast1;
load c:\MATLAB6p5\work\analysis\sub1\CPMFast\cor\datapercor6fast1.txt;
A6=datapercor6fast1;
load c:\MATLAB6p5\work\analysis\sub1\CPMFast\cor\datapercor7fast1.txt;
A7=datapercor7fast1;
load c:\MATLAB6p5\work\analysis\sub1\CPMFast\cor\datapercor8fast1.txt;
A8=datapercor8fast1;
load c:\MATLAB6p5\work\analysis\sub1\CPMFast\cor\datapercor9fast1.txt;
A9=datapercor9fast1;
load c:\MATLAB6p5\work\analysis\sub1\CPMFast\cor\datapercor10fast1.txt;
A10=datapercor10fast1;

% load c:\MATLAB6p5\work\analysis\sub1\CPM20Deg\cor\datapercor120deg1.txt;
A1=datapercor120deg1;
% load c:\MATLAB6p5\work\analysis\sub1\CPM20Deg\cor\datapercor220deg1.txt;
A2=datapercor220deg1;
% load c:\MATLAB6p5\work\analysis\sub1\CPM20Deg\cor\datapercor320deg1.txt;
A3=datapercor320deg1;
% load c:\MATLAB6p5\work\analysis\sub1\CPM20Deg\cor\datapercor420deg1.txt;
A4=datapercor420deg1;
% load c:\MATLAB6p5\work\analysis\sub1\CPM20Deg\cor\datapercor520deg1.txt;
A5=datapercor520deg1;
% load c:\MATLAB6p5\work\analysis\sub1\CPM20Deg\cor\datapercor620deg1.txt;
A6=datapercor620deg1;
% load c:\MATLAB6p5\work\analysis\sub1\CPM20Deg\cor\datapercor720deg1.txt;
A7=datapercor720deg1;
% load c:\MATLAB6p5\work\analysis\sub1\CPM20Deg\cor\datapercor820deg1.txt;
A8=datapercor820deg1;
% load c:\MATLAB6p5\work\analysis\sub1\CPM20Deg\cor\datapercor920deg1.txt;
A9=datapercor920deg1;
% load c:\MATLAB6p5\work\analysis\sub1\CPM20Deg\cor\datapercor1020deg1.txt;
A10=datapercor1020deg1;

load c:\MATLAB6p5\work\analysis\stature.txt; Stature=stature;

```

```

SubNum=1
SubHtcm=Stature(SubNum,4);
SubMasskg=Stature(SubNum,5);
SubUBMasskgz=Stature(SubNum,8);
SubUBMasskg=[0;0;SubUBMasskgz];
SubLBMasskg=Stature(SubNum,9);
%
[a,b]=size(A1);

%
%Regression equation for converting RMS to load: 3D ES = c7 + b7*Calibrated EMG
(Multifidus)
%Percent cross-sectional area and load of erector spinae as multifidus is
%.1244%
percentmult=.1244
regintercept=-26.0538809
regxvariable=15586.31939

xzer=zeros(a,1);
zzer=zeros(a,1);
Ones=ones(a,1);
Zeros=zeros(a,1);

%%Force of Upper Body
Fubx=0
Fuby=0
Fubz=SubUBMasskg*6.81;
Fub=[Fubx;Fuby;Fubz];
rubx=0;
ruby=Stature(SubNum,14); %Determine if movement in y-dir enough for inclusion of
change per time
rubz=Stature(SubNum,22);
rub=[rubx;ruby;rubz];

%%rL vector from force plate to functional spine unit
rLx=0;
rLy=Stature(SubNum,15);
rLz=Stature(SubNum,23);
rL=[rLx;rLy;rLz];

%%Moment arm for Erector Spinae from 3DSSPP
ActiveMomArmz=Stature(SubNum,45);
ActiveMomArmy=Stature(SubNum,46);

```

```

ActiveMomArmz=Stature(SubNum,47);
ActiveMomArmxyz=[ActiveMomArmz;ActiveMomArmz;ActiveMomArmz];

%%Calculating the moment and loads at functional spine unit in respect of
%%the global coordinate axis of the force plate
for q=1:10;
    i=1
    if q==1
        ActiveLoadPeriodA1=(regintercept + regxvariable*A1(:,102))*percentmult;
        ActiveLoadA1t=[xzer ActiveLoadPeriodA1 zzer]'
        LumLinAccelxA1=xzer;
        LumLinAccelyA1=A1(:,28);
        LumLinAccelzA1=A1(:,29);
        LumLinAccelA1=[LumLinAccelxA1 LumLinAccelyA1 LumLinAccelzA1]';
        FPFxzerA1=(A1(:,83)-A1(1,83))';
        FPFyzerA1=(A1(:,84)-A1(1,84))';
        FPFzzerA1=(A1(:,85)-A1(1,85))';
        FPFmagzerA1=(A1(:,86)-A1(1,86))';
        FPMxzerA1=(A1(:,87)-A1(1,87))';
        FPMMyzerA1=(A1(:,88)-A1(1,88))';
        FPMzzerA1=(A1(:,89)-A1(1,89))';
        FPMmagzerA1=(A1(:,90)-A1(1,90))';
        RFPA1=[FPFxzerA1;FPFyzerA1;FPFzzerA1];
        MFPA1=[FPMxzerA1;FPMMyzerA1;FPMzzerA1];
        for i=1:a
            LumLinAccelUBMassA1(:,i)=LumLinAccelA1(:,i).*SubUBMasskg
            RLA1t(:,i)=LumLinAccelUBMassA1(:,i)-RFPA1(:,i);
            CrossrLRLA1(:,i)=cross(rL,RLA1t(:,i));
            CrossrUBlinaccelA1(:,i)=cross(rub,LumLinAccelUBMassA1(:,i));
            MLA1t(:,i)=-MFPA1(:,i) - CrossrLRLA1(:,i) - CrossrUBlinaccelA1(:,i);
            ActiveMomentxA1t(1,i)=ActiveMomArmxyz(3,1)*ActiveLoadA1t(2,i);
            i=i+1
        end
    end
    if q==2
        ActiveLoadPeriodA2=(regintercept + regxvariable*A2(:,102))*percentmult;
        ActiveLoadA2t=[xzer ActiveLoadPeriodA2 zzer]'
        LumLinAccelxA2=xzer;
        LumLinAccelyA2=A2(:,28);
        LumLinAccelzA2=A2(:,29);
        LumLinAccelA2=[LumLinAccelxA2 LumLinAccelyA2 LumLinAccelzA2]';
        FPFxzerA2=(A2(:,83)-A2(1,83))';
        FPFyzerA2=(A2(:,84)-A2(1,84))';
        FPFzzerA2=(A2(:,85)-A2(1,85))';

```

```

FPFmagzerA2=(A2(:,86)-A2(1,86))';
FPMxzerA2=(A2(:,87)-A2(1,87))';
FPMMyzerA2=(A2(:,88)-A2(1,88))';
FPMzzerA2=(A2(:,89)-A2(1,89))';
FPMmagzerA2=(A2(:,90)-A2(1,90))';
RFPA2=[FPFxzerA2;FPFyzerA2;FPFzzerA2];
MFPA2=[FPMxzerA2;FPMMyzerA2;FPMzzerA2];
for i=1:a
    LumLinAccelUBMassA2(:,i)=LumLinAccelA2(:,i).*SubUBMasskg
    RLA2t(:,i)=LumLinAccelUBMassA2(:,i)-RFPA2(:,i);
    CrossrLRLA2(:,i)=cross(rL,RLA2t(:,i));
    CrossrUBlinaccelA2(:,i)=cross(rub,LumLinAccelUBMassA2(:,i));
    MLA2t(:,i)=-MFPA2(:,i) - CrossrLRLA2(:,i) - CrossrUBlinaccelA2(:,i);
    ActiveMomentxA2t(1,i)=ActiveMomArmxyz(3,1)*ActiveLoadA2t(2,i);
    i=i+1
end
end
if q==3
    ActiveLoadPeriodA3=(regintercept + regxvariable*A3(:,102))*percentmult;
    ActiveLoadA3t=[xzer ActiveLoadPeriodA3 zzer]'
    LumLinAccelxA3=xzer;
    LumLinAccelyA3=A3(:,28);
    LumLinAccelzA3=A3(:,29);
    LumLinAccelA3=[LumLinAccelxA3 LumLinAccelyA3 LumLinAccelzA3]';
    FPFxzerA3=(A3(:,83)-A3(1,83))';
    FPFyzerA3=(A3(:,84)-A3(1,84))';
    FPFzzerA3=(A3(:,85)-A3(1,85))';
    FPFmagzerA3=(A3(:,86)-A3(1,86))';
    FPMxzerA3=(A3(:,87)-A3(1,87))';
    FPMMyzerA3=(A3(:,88)-A3(1,88))';
    FPMzzerA3=(A3(:,89)-A3(1,89))';
    FPMmagzerA3=(A3(:,90)-A3(1,90))';
    RFPA3=[FPFxzerA3;FPFyzerA3;FPFzzerA3];
    MFPA3=[FPMxzerA3;FPMMyzerA3;FPMzzerA3];
    for i=1:a
        LumLinAccelUBMassA3(:,i)=LumLinAccelA3(:,i).*SubUBMasskg
        RLA3t(:,i)=LumLinAccelUBMassA3(:,i)-RFPA3(:,i);
        CrossrLRLA3(:,i)=cross(rL,RLA3t(:,i));
        CrossrUBlinaccelA3(:,i)=cross(rub,LumLinAccelUBMassA3(:,i));
        MLA3t(:,i)=-MFPA3(:,i) - CrossrLRLA3(:,i) - CrossrUBlinaccelA3(:,i);
        ActiveMomentxA3t(1,i)=ActiveMomArmxyz(3,1)*ActiveLoadA3t(2,i);
        i=i+1
    end
end
end

```



```

if q==4
    ActiveLoadPeriodA4=(regintercept + regxvariable*A4(:,102))*percentmult;
    ActiveLoadA4t=[xzer ActiveLoadPeriodA4 zzer]';
    LumLinAccelxA4=xzer;
    LumLinAccelyA4=A4(:,28);
    LumLinAccelzA4=A4(:,29);
    LumLinAccelA4=[LumLinAccelxA4 LumLinAccelyA4 LumLinAccelzA4]';
    FPFxzerA4=(A4(:,83)-A4(1,83))';
    FPFyzerA4=(A4(:,84)-A4(1,84))';
    FPFzzerA4=(A4(:,85)-A4(1,85))';
    FPFmagzerA4=(A4(:,86)-A4(1,86))';
    FPMxzerA4=(A4(:,87)-A4(1,87))';
    FPMyzerA4=(A4(:,88)-A4(1,88))';
    FPMzzerA4=(A4(:,89)-A4(1,89))';
    FPMmagzerA4=(A4(:,90)-A4(1,90))';
    RFPA4=[FPFxzerA4;FPFyzerA4;FPFzzerA4];
    MFPA4=[FPMxzerA4;FPMyzerA4;FPMzzerA4];
    for i=1:a
        LumLinAccelUBMassA4(:,i)=LumLinAccelA4(:,i).*SubUBMasskg
        RLA4t(:,i)=LumLinAccelUBMassA4(:,i)-RFPA4(:,i);
        CrossrLRLA4(:,i)=cross(rL,RLA4t(:,i));
        CrossrUBlinaccelA4(:,i)=cross(rub,LumLinAccelUBMassA4(:,i));
        MLA4t(:,i)=-MFPA4(:,i) - CrossrLRLA4(:,i) - CrossrUBlinaccelA4(:,i);
        ActiveMomentxA4t(1,i)=ActiveMomArmxyz(3,1)*ActiveLoadA4t(2,i);
        i=i+1
    end
end
if q==5
    ActiveLoadPeriodA5=(regintercept + regxvariable*A5(:,102))*percentmult;
    ActiveLoadA5t=[xzer ActiveLoadPeriodA5 zzer]';
    LumLinAccelxA5=xzer;
    LumLinAccelyA5=A5(:,28);
    LumLinAccelzA5=A5(:,29);
    LumLinAccelA5=[LumLinAccelxA5 LumLinAccelyA5 LumLinAccelzA5]';
    FPFxzerA5=(A5(:,83)-A5(1,83))';
    FPFyzerA5=(A5(:,84)-A5(1,84))';
    FPFzzerA5=(A5(:,85)-A5(1,85))';
    FPFmagzerA5=(A5(:,86)-A5(1,86))';
    FPMxzerA5=(A5(:,87)-A5(1,87))';
    FPMyzerA5=(A5(:,88)-A5(1,88))';
    FPMzzerA5=(A5(:,89)-A5(1,89))';
    FPMmagzerA5=(A5(:,90)-A5(1,90))';
    RFPA5=[FPFxzerA5;FPFyzerA5;FPFzzerA5];
    MFPA5=[FPMxzerA5;FPMyzerA5;FPMzzerA5];

```

```

for i=1:a
    LumLinAccelUBMassA5(:,i)=LumLinAccelA5(:,i).*SubUBMasskg
    RLA5t(:,i)=LumLinAccelUBMassA5(:,i)-RFPA5(:,i);
    CrossrLRLA5(:,i)=cross(rL,RLA5t(:,i));
    CrossrUBlinaccelA5(:,i)=cross(rub,LumLinAccelUBMassA5(:,i));
    MLA5t(:,i)=-MFPA5(:,i) - CrossrLRLA5(:,i) - CrossrUBlinaccelA5(:,i);
    ActiveMomentxA5t(1,i)=ActiveMomArmxyz(3,1)*ActiveLoadA5t(2,i);
    i=i+1
end
end
if q==6
    ActiveLoadPeriodA6=(regintercept + regxvariable*A6(:,102))*percentmult;
    ActiveLoadA6t=[xzer ActiveLoadPeriodA6 zzer]'
    LumLinAccelxA6=xzer;
    LumLinAccelyA6=A6(:,28);
    LumLinAccelzA6=A6(:,29);
    LumLinAccelA6=[LumLinAccelxA6 LumLinAccelyA6 LumLinAccelzA6]';
    FPFxzerA6=(A6(:,83)-A6(1,83))';
    FPFyzerA6=(A6(:,84)-A6(1,84))';
    FPFzzerA6=(A6(:,85)-A6(1,85))';
    FPFmagzerA6=(A6(:,86)-A6(1,86))';
    FPMxzerA6=(A6(:,87)-A6(1,87))';
    FPMyzerA6=(A6(:,88)-A6(1,88))';
    FPMzzerA6=(A6(:,89)-A6(1,89))';
    FPMmagzerA6=(A6(:,90)-A6(1,90))';
    RFPA6=[FPFxzerA6;FPFyzerA6;FPFzzerA6];
    MFPA6=[FPMxzerA6;FPMyzerA6;FPMzzerA6];
    for i=1:a
        LumLinAccelUBMassA6(:,i)=LumLinAccelA6(:,i).*SubUBMasskg
        RLA6t(:,i)=LumLinAccelUBMassA6(:,i)-RFPA6(:,i);
        CrossrLRLA6(:,i)=cross(rL,RLA6t(:,i));
        CrossrUBlinaccelA6(:,i)=cross(rub,LumLinAccelUBMassA6(:,i));
        MLA6t(:,i)=-MFPA6(:,i) - CrossrLRLA6(:,i) - CrossrUBlinaccelA6(:,i);
        ActiveMomentxA6t(1,i)=ActiveMomArmxyz(3,1)*ActiveLoadA6t(2,i);
        i=i+1
    end
end
if q==7
    ActiveLoadPeriodA7=(regintercept + regxvariable*A7(:,102))*percentmult;
    ActiveLoadA7t=[xzer ActiveLoadPeriodA7 zzer]'
    LumLinAccelxA7=xzer;
    LumLinAccelyA7=A7(:,28);
    LumLinAccelzA7=A7(:,29);
    LumLinAccelA7=[LumLinAccelxA7 LumLinAccelyA7 LumLinAccelzA7]';

```

```

FPFxzerA7=(A7(:,83)-A7(1,83))';
FPFyzerA7=(A7(:,84)-A7(1,84))';
FPFzzerA7=(A7(:,85)-A7(1,85))';
FPFmagzerA7=(A7(:,86)-A7(1,86))';
FPMxzerA7=(A7(:,87)-A7(1,87))';
FPMyzerA7=(A7(:,88)-A7(1,88))';
FPMzzerA7=(A7(:,89)-A7(1,89))';
FPMmagzerA7=(A7(:,90)-A7(1,90))';
RFPA7=[FPFxzerA7;FPFyzerA7;FPFzzerA7];
MFPA7=[FPMxzerA7;FPMyzerA7;FPMzzerA7];
for i=1:a
    LumLinAccelUBMassA7(:,i)=LumLinAccelA7(:,i).*SubUBMasskg
    RLA7t(:,i)=LumLinAccelUBMassA7(:,i)-RFPA7(:,i);
    CrossrLRLA7(:,i)=cross(rL,RLA7t(:,i));
    CrossrUBlinaccelA7(:,i)=cross(rub,LumLinAccelUBMassA7(:,i));
    MLA7t(:,i)=-MFPA7(:,i) - CrossrLRLA7(:,i) - CrossrUBlinaccelA7(:,i);
    ActiveMomentxA7t(1,i)=ActiveMomArmxyz(3,1)*ActiveLoadA7t(2,i);
    i=i+1
end
end
if q==8
    ActiveLoadPeriodA8=(regintercept + regxvariable*A8(:,102))*percentmult;
    ActiveLoadA8t=[xzer ActiveLoadPeriodA8 zzer]'
    LumLinAccelxA8=xzer;
    LumLinAccelyA8=A8(:,28);
    LumLinAccelzA8=A8(:,29);
    LumLinAccelA8=[LumLinAccelxA8 LumLinAccelyA8 LumLinAccelzA8]';
    FPFxzerA8=(A8(:,83)-A8(1,83))';
    FPFyzerA8=(A8(:,84)-A8(1,84))';
    FPFzzerA8=(A8(:,85)-A8(1,85))';
    FPFmagzerA8=(A8(:,86)-A8(1,86))';
    FPMxzerA8=(A8(:,87)-A8(1,87))';
    FPMyzerA8=(A8(:,88)-A8(1,88))';
    FPMzzerA8=(A8(:,89)-A8(1,89))';
    FPMmagzerA8=(A8(:,90)-A8(1,90))';
    RFPA8=[FPFxzerA8;FPFyzerA8;FPFzzerA8];
    MFPA8=[FPMxzerA8;FPMyzerA8;FPMzzerA8];
    for i=1:a
        LumLinAccelUBMassA8(:,i)=LumLinAccelA8(:,i).*SubUBMasskg
        RLA8t(:,i)=LumLinAccelUBMassA8(:,i)-RFPA8(:,i);
        CrossrLRLA8(:,i)=cross(rL,RLA8t(:,i));
        CrossrUBlinaccelA8(:,i)=cross(rub,LumLinAccelUBMassA8(:,i));
        MLA8t(:,i)=-MFPA8(:,i) - CrossrLRLA8(:,i) - CrossrUBlinaccelA8(:,i);
        ActiveMomentxA8t(1,i)=ActiveMomArmxyz(3,1)*ActiveLoadA8t(2,i);
    end
end

```

```

        i=i+1
    end
end
if q==9
    ActiveLoadPeriodA9=(regintercept + regxvariable*A9(:,102))*percentmult;
    ActiveLoadA9t=[xzer ActiveLoadPeriodA9 zzer]';
    LumLinAccelxA9=xzer;
    LumLinAccelyA9=A9(:,28);
    LumLinAccelzA9=A9(:,29);
    LumLinAccelA9=[LumLinAccelxA9 LumLinAccelyA9 LumLinAccelzA9]';
    FPFxzerA9=(A9(:,83)-A9(1,83))';
    FPFyzerA9=(A9(:,84)-A9(1,84))';
    FPFzzerA9=(A9(:,85)-A9(1,85))';
    FPFmagzerA9=(A9(:,86)-A9(1,86))';
    FPMxzerA9=(A9(:,87)-A9(1,87))';
    FPMMyzerA9=(A9(:,88)-A9(1,88))';
    FPMzzerA9=(A9(:,89)-A9(1,89))';
    FPMmagzerA9=(A9(:,90)-A9(1,90))';
    RFPA9=[FPFxzerA9;FPFyzerA9;FPFzzerA9];
    MFPA9=[FPMxzerA9;FPMMyzerA9;FPMzzerA9];
    for i=1:a
        LumLinAccelUBMassA9(:,i)=LumLinAccelA9(:,i).*SubUBMasskg
        RLA9t(:,i)=LumLinAccelUBMassA9(:,i)-RFPA9(:,i);
        CrossrLRLA9(:,i)=cross(rL,RLA9t(:,i));
        CrossrUBlinaccelA9(:,i)=cross(rub,LumLinAccelUBMassA9(:,i));
        MLA9t(:,i)=-MFPA9(:,i) - CrossrLRLA9(:,i) - CrossrUBlinaccelA9(:,i);
        ActiveMomentxA9t(1,i)=ActiveMomArmxyz(3,1)*ActiveLoadA9t(2,i);
        i=i+1
    end
end
if q==10
    ActiveLoadPeriodA10=(regintercept + regxvariable*A10(:,102))*percentmult;
    ActiveLoadA10t=[xzer ActiveLoadPeriodA10 zzer]';
    LumLinAccelxA10=xzer;
    LumLinAccelyA10=A10(:,28);
    LumLinAccelzA10=A10(:,29);
    LumLinAccelA10=[LumLinAccelxA10 LumLinAccelyA10 LumLinAccelzA10]';
    FPFxzerA10=(A10(:,83)-A10(1,83))';
    FPFyzerA10=(A10(:,84)-A10(1,84))';
    FPFzzerA10=(A10(:,85)-A10(1,85))';
    FPFmagzerA10=(A10(:,86)-A10(1,86))';
    FPMxzerA10=(A10(:,87)-A10(1,87))';
    FPMMyzerA10=(A10(:,88)-A10(1,88))';
    FPMzzerA10=(A10(:,89)-A10(1,89))';

```

```

FPMmagzerA10=(A10(:,90)-A10(1,90))';
RFPA10=[FPFxzerA10;FPFyzerA10;FPFzzerA10];
MFPA10=[FPMxzerA10;FPMyzerA10;FPMzzerA10];
for i=1:a
    LumLinAccelUBMassA10(:,i)=LumLinAccelA10(:,i).*SubUBMasskg
    RLA10t(:,i)=LumLinAccelUBMassA10(:,i)-RFPA10(:,i);
    CrossrLRLA10(:,i)=cross(rL,RLA10t(:,i));
    CrossrUBlinaccelA10(:,i)=cross(rub,LumLinAccelUBMassA10(:,i));
    MLA10t(:,i)=-MFPA10(:,i) - CrossrLRLA10(:,i) - CrossrUBlinaccelA10(:,i);
    ActiveMomentxA10t(1,i)=ActiveMomArmxyz(3,1)*ActiveLoadA10t(2,i);
    i=i+1
end
end
q=q+1;
end
momentloadFPfsuA1=[MLA1t;RLA1t]
momentloadFPfsuA2=[MLA2t;RLA2t]
momentloadFPfsuA3=[MLA3t;RLA3t]
momentloadFPfsuA4=[MLA4t;RLA4t]
momentloadFPfsuA5=[MLA5t;RLA5t]
momentloadFPfsuA6=[MLA6t;RLA6t]
momentloadFPfsuA7=[MLA7t;RLA7t]
momentloadFPfsuA8=[MLA8t;RLA8t]
momentloadFPfsuA9=[MLA9t;RLA9t]
momentloadFPfsuA10=[MLA10t;RLA10t]

%%
% save
c:\MATLAB6p5\work\analysis\sub1\CPMSlow\cor\fsuMomentsLoadspretranscorA1slow1.t
xt momentloadFPfsuA1 -ascii -tabs
% save
c:\MATLAB6p5\work\analysis\sub1\CPMSlow\cor\fsuMomentsLoadspretranscorA2slow1.t
xt momentloadFPfsuA2 -ascii -tabs
% save
c:\MATLAB6p5\work\analysis\sub1\CPMSlow\cor\fsuMomentsLoadspretranscorA3slow1.t
xt momentloadFPfsuA3 -ascii -tabs
% save
c:\MATLAB6p5\work\analysis\sub1\CPMSlow\cor\fsuMomentsLoadspretranscorA4slow1.t
xt momentloadFPfsuA4 -ascii -tabs
% save
c:\MATLAB6p5\work\analysis\sub1\CPMSlow\cor\fsuMomentsLoadspretranscorA5slow1.t
xt momentloadFPfsuA5 -ascii -tabs

```

```

% save
c:\MATLAB6p5\work\analysis\sub1\CPMSlow\cor\fsuMomentsLoadspretranscorA6slow1.t
xt momentloadFPfsuA6 -ascii -tabs
% save
c:\MATLAB6p5\work\analysis\sub1\CPMSlow\cor\fsuMomentsLoadspretranscorA7slow1.t
xt momentloadFPfsuA7 -ascii -tabs

% save
c:\MATLAB6p5\work\analysis\sub1\CPMMed\cor\fsuMomentsLoadspretranscorA1med1.txt
momentloadFPfsuA1 -ascii -tabs
% save
c:\MATLAB6p5\work\analysis\sub1\CPMMed\cor\fsuMomentsLoadspretranscorA2med1.txt
momentloadFPfsuA2 -ascii -tabs
% save
c:\MATLAB6p5\work\analysis\sub1\CPMMed\cor\fsuMomentsLoadspretranscorA3med1.txt
momentloadFPfsuA3 -ascii -tabs
% save
c:\MATLAB6p5\work\analysis\sub1\CPMMed\cor\fsuMomentsLoadspretranscorA4med1.txt
momentloadFPfsuA4 -ascii -tabs
% save
c:\MATLAB6p5\work\analysis\sub1\CPMMed\cor\fsuMomentsLoadspretranscorA5med1.txt
momentloadFPfsuA5 -ascii -tabs
% save
c:\MATLAB6p5\work\analysis\sub1\CPMMed\cor\fsuMomentsLoadspretranscorA6med1.txt
momentloadFPfsuA6 -ascii -tabs
% save
c:\MATLAB6p5\work\analysis\sub1\CPMMed\cor\fsuMomentsLoadspretranscorA7med1.txt
momentloadFPfsuA7 -ascii -tabs
% save
c:\MATLAB6p5\work\analysis\sub1\CPMMed\cor\fsuMomentsLoadspretranscorA8med1.txt
momentloadFPfsuA8 -ascii -tabs
% save
c:\MATLAB6p5\work\analysis\sub1\CPMMed\cor\fsuMomentsLoadspretranscorA9med1.txt
momentloadFPfsuA9 -ascii -tabs
% save
c:\MATLAB6p5\work\analysis\sub1\CPMMed\cor\fsuMomentsLoadspretranscorA10med1.t
xt momentloadFPfsuA10 -ascii -tabs

save
c:\MATLAB6p5\work\analysis\sub1\CPMFast\cor\fsuMomentsLoadspretranscorA1fast1.txt
momentloadFPfsuA1 -ascii -tabs
save
c:\MATLAB6p5\work\analysis\sub1\CPMFast\cor\fsuMomentsLoadspretranscorA2fast1.txt
momentloadFPfsuA2 -ascii -tabs

```

```

save
c:\MATLAB6p5\work\analysis\sub1\CPMFast\cor\fsuMomentsLoadspretranscorA3fast1.txt
momentloadFPfsuA3 -ascii -tabs
save
c:\MATLAB6p5\work\analysis\sub1\CPMFast\cor\fsuMomentsLoadspretranscorA4fast1.txt
momentloadFPfsuA4 -ascii -tabs
save
c:\MATLAB6p5\work\analysis\sub1\CPMFast\cor\fsuMomentsLoadspretranscorA5fast1.txt
momentloadFPfsuA5 -ascii -tabs
save
c:\MATLAB6p5\work\analysis\sub1\CPMFast\cor\fsuMomentsLoadspretranscorA6fast1.txt
momentloadFPfsuA6 -ascii -tabs
save
c:\MATLAB6p5\work\analysis\sub1\CPMFast\cor\fsuMomentsLoadspretranscorA7fast1.txt
momentloadFPfsuA7 -ascii -tabs
save
c:\MATLAB6p5\work\analysis\sub1\CPMFast\cor\fsuMomentsLoadspretranscorA8fast1.txt
momentloadFPfsuA8 -ascii -tabs
save
c:\MATLAB6p5\work\analysis\sub1\CPMFast\cor\fsuMomentsLoadspretranscorA9fast1.txt
momentloadFPfsuA9 -ascii -tabs
save
c:\MATLAB6p5\work\analysis\sub1\CPMFast\cor\fsuMomentsLoadspretranscorA10fast1.tx
t momentloadFPfsuA10 -ascii -tabs

% save
c:\MATLAB6p5\work\analysis\sub1\CPM20Deg\cor\fsuMomentsLoadspretranscorA120deg
1.txt momentloadFPfsuA1 -ascii -tabs
% save
c:\MATLAB6p5\work\analysis\sub1\CPM20Deg\cor\fsuMomentsLoadspretranscorA220deg
1.txt momentloadFPfsuA2 -ascii -tabs
% save
c:\MATLAB6p5\work\analysis\sub1\CPM20Deg\cor\fsuMomentsLoadspretranscorA320deg
1.txt momentloadFPfsuA3 -ascii -tabs
% save
c:\MATLAB6p5\work\analysis\sub1\CPM20Deg\cor\fsuMomentsLoadspretranscorA420deg
1.txt momentloadFPfsuA4 -ascii -tabs
% save
c:\MATLAB6p5\work\analysis\sub1\CPM20Deg\cor\fsuMomentsLoadspretranscorA520deg
1.txt momentloadFPfsuA5 -ascii -tabs
% save
c:\MATLAB6p5\work\analysis\sub1\CPM20Deg\cor\fsuMomentsLoadspretranscorA620deg
1.txt momentloadFPfsuA6 -ascii -tabs

```

```
% save
c:\MATLAB6p5\work\analysis\sub1\CPM20Deg\cor\fsuMomentsLoadspretranscorA720deg
1.txt momentloadFPfsuA7 -ascii -tabs
% save
c:\MATLAB6p5\work\analysis\sub1\CPM20Deg\cor\fsuMomentsLoadspretranscorA820deg
1.txt momentloadFPfsuA8 -ascii -tabs
% save
c:\MATLAB6p5\work\analysis\sub1\CPM20Deg\cor\fsuMomentsLoadspretranscorA920deg
1.txt momentloadFPfsuA9 -ascii -tabs
% save
c:\MATLAB6p5\work\analysis\sub1\CPM20Deg\cor\fsuMomentsLoadspretranscorA1020de
g1.txt momentloadFPfsuA10 -ascii -tabs
```

```
time=A1(:,1);
```

```
%Transformation of the loads and moments at the force plate to spine unit
```

```
%of L5/S1
```

```
%%Vector from the spine unit to force plate in Lumbar coordinate axis
```

```
LrxFP=0
```

```
LryFP=Stature(SubNum,15);
```

```
LrzFP=Stature(SubNum,23);
```

```
LrFP=[LrxFP;LryFP;LrzFP];
```

```
R=[-1 0 0;0 -1 0;0 0 1]
```

```
n=R(1,:);
```

```
o=R(2,:);
```

```
a=R(3,:);
```

```
%%Cross product of vector Spine functional unit to force plate and Rotation
```

```
%matrix
```

```
crossLrFPn=cross(LrFP,n)
```

```
crossLrFPo=cross(LrFP,o)
```

```
crossLrFPa=cross(LrFP,a)
```

```
LrFPcrossR=[crossLrFPn; crossLrFPo; crossLrFPa]
```

```
zer3by3=zeros(3,3);
```

```
T=[R LrFPcrossR;zer3by3 R] %Load and Moment Transformation matrix from Force Plate
to Functional Spine Unit
```

```
A1MomentLoad=[MLA1t;RLA1t];
```

```
A2MomentLoad=[MLA2t;RLA2t];
```

```
A3MomentLoad=[MLA3t;RLA3t];
```

```
A4MomentLoad=[MLA4t;RLA4t];
```

```
A5MomentLoad=[MLA5t;RLA5t];
```

```
A6MomentLoad=[MLA6t;RLA6t];
```



```

A7MomentLoad=[MLA7t;RLA7t];
A8MomentLoad=[MLA8t;RLA8t];
A9MomentLoad=[MLA9t;RLA9t];
A10MomentLoad=[MLA10t;RLA10t];

%%Loop for performing the transformation from the force plate axis to the
%%lumbar axis
[c,d]=size(A1MomentLoad)
i=1
for i=1:d
    TransMLRLA1(:,i)=T*A1MomentLoad(:,i)
    TransMLRLA2(:,i)=T*A2MomentLoad(:,i);
    TransMLRLA3(:,i)=T*A3MomentLoad(:,i);
    TransMLRLA4(:,i)=T*A4MomentLoad(:,i);
    TransMLRLA5(:,i)=T*A5MomentLoad(:,i);
    TransMLRLA6(:,i)=T*A6MomentLoad(:,i);
    TransMLRLA7(:,i)=T*A7MomentLoad(:,i);
    TransMLRLA8(:,i)=T*A8MomentLoad(:,i);
    TransMLRLA9(:,i)=T*A9MomentLoad(:,i);
    TransMLRLA10(:,i)=T*A10MomentLoad(:,i);
    i=i+1
end
PassiveMomentLoadLA1=TransMLRLA1';
PassiveMomentLoadLA2=TransMLRLA2';
PassiveMomentLoadLA3=TransMLRLA3';
PassiveMomentLoadLA4=TransMLRLA4';
PassiveMomentLoadLA5=TransMLRLA5';
PassiveMomentLoadLA6=TransMLRLA6';
PassiveMomentLoadLA7=TransMLRLA7';
PassiveMomentLoadLA8=TransMLRLA8';
PassiveMomentLoadLA9=TransMLRLA9';
PassiveMomentLoadLA10=TransMLRLA10';

zerom=zeros(d,1)';

%%Creating matrix of the active loads and moments for determining the total
%%load at the functional spine unit
ActiveMomentLoadA1=[ActiveMomentxA1t;zerom;zerom;ActiveLoadA1t]'
ActiveMomentLoadA2=[ActiveMomentxA2t;zerom;zerom;ActiveLoadA2t]'
ActiveMomentLoadA3=[ActiveMomentxA3t;zerom;zerom;ActiveLoadA3t]'
ActiveMomentLoadA4=[ActiveMomentxA4t;zerom;zerom;ActiveLoadA4t]'
ActiveMomentLoadA5=[ActiveMomentxA5t;zerom;zerom;ActiveLoadA5t]';

```

```
ActiveMomentLoadA6=[ActiveMomentxA6t;zerom;zerom;ActiveLoadA6t]';
ActiveMomentLoadA7=[ActiveMomentxA7t;zerom;zerom;ActiveLoadA7t]';
ActiveMomentLoadA8=[ActiveMomentxA8t;zerom;zerom;ActiveLoadA8t]';
ActiveMomentLoadA9=[ActiveMomentxA9t;zerom;zerom;ActiveLoadA9t]';
ActiveMomentLoadA10=[ActiveMomentxA10t;zerom;zerom;ActiveLoadA10t]';
```

```
%%Total Load and Moment for cephalic table section
```

```
TotalLoadCephalicA1=PassiveMomentLoadLA1 + ActiveMomentLoadA1
TotalLoadCephalicA2=PassiveMomentLoadLA2 + ActiveMomentLoadA2;
TotalLoadCephalicA3=PassiveMomentLoadLA3 + ActiveMomentLoadA3;
TotalLoadCephalicA4=PassiveMomentLoadLA4 + ActiveMomentLoadA4;
TotalLoadCephalicA5=PassiveMomentLoadLA5 + ActiveMomentLoadA5;
TotalLoadCephalicA6=PassiveMomentLoadLA6 + ActiveMomentLoadA6;
TotalLoadCephalicA7=PassiveMomentLoadLA7 + ActiveMomentLoadA7;
TotalLoadCephalicA8=PassiveMomentLoadLA8 + ActiveMomentLoadA8;
TotalLoadCephalicA9=PassiveMomentLoadLA9 + ActiveMomentLoadA9;
TotalLoadCephalicA10=PassiveMomentLoadLA10 + ActiveMomentLoadA10;
```

```
%%Creating a matrix of the active, passive, and total load at functional
```

```
%%spine unit
```

```
ActPasTotMomentsLoadsA1=[time ActiveMomentLoadA1 PassiveMomentLoadLA1
TotalLoadCephalicA1];
ActPasTotMomentsLoadsA2=[time ActiveMomentLoadA2 PassiveMomentLoadLA2
TotalLoadCephalicA2];
ActPasTotMomentsLoadsA3=[time ActiveMomentLoadA3 PassiveMomentLoadLA3
TotalLoadCephalicA3];
ActPasTotMomentsLoadsA4=[time ActiveMomentLoadA4 PassiveMomentLoadLA4
TotalLoadCephalicA4];
ActPasTotMomentsLoadsA5=[time ActiveMomentLoadA5 PassiveMomentLoadLA5
TotalLoadCephalicA5];
ActPasTotMomentsLoadsA6=[time ActiveMomentLoadA6 PassiveMomentLoadLA6
TotalLoadCephalicA6];
ActPasTotMomentsLoadsA7=[time ActiveMomentLoadA7 PassiveMomentLoadLA7
TotalLoadCephalicA7];
ActPasTotMomentsLoadsA8=[time ActiveMomentLoadA8 PassiveMomentLoadLA8
TotalLoadCephalicA8];
ActPasTotMomentsLoadsA9=[time ActiveMomentLoadA9 PassiveMomentLoadLA9
TotalLoadCephalicA9];
ActPasTotMomentsLoadsA10=[time ActiveMomentLoadA10 PassiveMomentLoadLA10
TotalLoadCephalicA10];
```

```
% save
```

```
c:\MATLAB6p5\work\analysis\sub1\CPMSlow\cor\fsuMomentsLoadsactpastotcorA1slow1.t
xt ActPasTotMomentsLoadsA1 -ascii -tabs
```

```
% save
c:\MATLAB6p5\work\analysis\sub1\CPMSlow\cor\fsuMomentsLoadsactpastotcorA2slow1.t
xt ActPasTotMomentsLoadsA2 -ascii -tabs
% save
c:\MATLAB6p5\work\analysis\sub1\CPMSlow\cor\fsuMomentsLoadsactpastotcorA3slow1.t
xt ActPasTotMomentsLoadsA3 -ascii -tabs
% save
c:\MATLAB6p5\work\analysis\sub1\CPMSlow\cor\fsuMomentsLoadsactpastotcorA4slow1.t
xt ActPasTotMomentsLoadsA4 -ascii -tabs
% save
c:\MATLAB6p5\work\analysis\sub1\CPMSlow\cor\fsuMomentsLoadsactpastotcorA5slow1.t
xt ActPasTotMomentsLoadsA5 -ascii -tabs
% save
c:\MATLAB6p5\work\analysis\sub1\CPMSlow\cor\fsuMomentsLoadsactpastotcorA6slow1.t
xt ActPasTotMomentsLoadsA6 -ascii -tabs
% save
c:\MATLAB6p5\work\analysis\sub1\CPMSlow\cor\fsuMomentsLoadsactpastotcorA7slow1.t
xt ActPasTotMomentsLoadsA7 -ascii -tabs

% save
c:\MATLAB6p5\work\analysis\sub1\CPMMed\cor\fsuMomentsLoadsactpastotcorA1med1.t
xt ActPasTotMomentsLoadsA1 -ascii -tabs
% save
c:\MATLAB6p5\work\analysis\sub1\CPMMed\cor\fsuMomentsLoadsactpastotcorA2med1.t
xt ActPasTotMomentsLoadsA2 -ascii -tabs
% save
c:\MATLAB6p5\work\analysis\sub1\CPMMed\cor\fsuMomentsLoadsactpastotcorA3med1.t
xt ActPasTotMomentsLoadsA3 -ascii -tabs
% save
c:\MATLAB6p5\work\analysis\sub1\CPMMed\cor\fsuMomentsLoadsactpastotcorA4med1.t
xt ActPasTotMomentsLoadsA4 -ascii -tabs
% save
c:\MATLAB6p5\work\analysis\sub1\CPMMed\cor\fsuMomentsLoadsactpastotcorA5med1.t
xt ActPasTotMomentsLoadsA5 -ascii -tabs
% save
c:\MATLAB6p5\work\analysis\sub1\CPMMed\cor\fsuMomentsLoadsactpastotcorA6med1.t
xt ActPasTotMomentsLoadsA6 -ascii -tabs
% save
c:\MATLAB6p5\work\analysis\sub1\CPMMed\cor\fsuMomentsLoadsactpastotcorA7med1.t
xt ActPasTotMomentsLoadsA7 -ascii -tabs
% save
c:\MATLAB6p5\work\analysis\sub1\CPMMed\cor\fsuMomentsLoadsactpastotcorA8med1.t
xt ActPasTotMomentsLoadsA8 -ascii -tabs
```

```

% save
c:\MATLAB6p5\work\analysis\sub1\CPMMed\cor\fsuMomentsLoadsactpastotcorA9med1.t
xt ActPasTotMomentsLoadsA9 -ascii -tabs
% save
c:\MATLAB6p5\work\analysis\sub1\CPMMed\cor\fsuMomentsLoadsactpastotcorA10med1.
txt ActPasTotMomentsLoadsA10 -ascii -tabs

save
c:\MATLAB6p5\work\analysis\sub1\CPMFast\cor\fsuMomentsLoadsactpastotcorA1fast1.txt
ActPasTotMomentsLoadsA1 -ascii -tabs
save
c:\MATLAB6p5\work\analysis\sub1\CPMFast\cor\fsuMomentsLoadsactpastotcorA2fast1.txt
ActPasTotMomentsLoadsA2 -ascii -tabs
save
c:\MATLAB6p5\work\analysis\sub1\CPMFast\cor\fsuMomentsLoadsactpastotcorA3fast1.txt
ActPasTotMomentsLoadsA3 -ascii -tabs
save
c:\MATLAB6p5\work\analysis\sub1\CPMFast\cor\fsuMomentsLoadsactpastotcorA4fast1.txt
ActPasTotMomentsLoadsA4 -ascii -tabs
save
c:\MATLAB6p5\work\analysis\sub1\CPMFast\cor\fsuMomentsLoadsactpastotcorA5fast1.txt
ActPasTotMomentsLoadsA5 -ascii -tabs
save
c:\MATLAB6p5\work\analysis\sub1\CPMFast\cor\fsuMomentsLoadsactpastotcorA6fast1.txt
ActPasTotMomentsLoadsA6 -ascii -tabs
save
c:\MATLAB6p5\work\analysis\sub1\CPMFast\cor\fsuMomentsLoadsactpastotcorA7fast1.txt
ActPasTotMomentsLoadsA7 -ascii -tabs
save
c:\MATLAB6p5\work\analysis\sub1\CPMFast\cor\fsuMomentsLoadsactpastotcorA8fast1.txt
ActPasTotMomentsLoadsA8 -ascii -tabs
save
c:\MATLAB6p5\work\analysis\sub1\CPMFast\cor\fsuMomentsLoadsactpastotcorA9fast1.txt
ActPasTotMomentsLoadsA9 -ascii -tabs
save
c:\MATLAB6p5\work\analysis\sub1\CPMFast\cor\fsuMomentsLoadsactpastotcorA10fast1.t
xt ActPasTotMomentsLoadsA10 -ascii -tabs

% save
c:\MATLAB6p5\work\analysis\sub1\CPM20Deg\cor\fsuMomentsLoadsactpastotcorA120de
g1.txt ActPasTotMomentsLoadsA1 -ascii -tabs
% save
c:\MATLAB6p5\work\analysis\sub1\CPM20Deg\cor\fsuMomentsLoadsactpastotcorA220de
g1.txt ActPasTotMomentsLoadsA2 -ascii -tabs

```

```
% save
c:\MATLAB6p5\work\analysis\sub1\CPM20Deg\cor\fsuMomentsLoadsactpastotcorA320deg1.txt ActPasTotMomentsLoadsA3 -ascii -tabs
% save
c:\MATLAB6p5\work\analysis\sub1\CPM20Deg\cor\fsuMomentsLoadsactpastotcorA420deg1.txt ActPasTotMomentsLoadsA4 -ascii -tabs
% save
c:\MATLAB6p5\work\analysis\sub1\CPM20Deg\cor\fsuMomentsLoadsactpastotcorA520deg1.txt ActPasTotMomentsLoadsA5 -ascii -tabs
% save
c:\MATLAB6p5\work\analysis\sub1\CPM20Deg\cor\fsuMomentsLoadsactpastotcorA620deg1.txt ActPasTotMomentsLoadsA6 -ascii -tabs
% save
c:\MATLAB6p5\work\analysis\sub1\CPM20Deg\cor\fsuMomentsLoadsactpastotcorA720deg1.txt ActPasTotMomentsLoadsA7 -ascii -tabs
% save
c:\MATLAB6p5\work\analysis\sub1\CPM20Deg\cor\fsuMomentsLoadsactpastotcorA820deg1.txt ActPasTotMomentsLoadsA8 -ascii -tabs
% save
c:\MATLAB6p5\work\analysis\sub1\CPM20Deg\cor\fsuMomentsLoadsactpastotcorA920deg1.txt ActPasTotMomentsLoadsA9 -ascii -tabs
% save
c:\MATLAB6p5\work\analysis\sub1\CPM20Deg\cor\fsuMomentsLoadsactpastotcorA1020deg1.txt ActPasTotMomentsLoadsA10 -ascii -tabs
```

```
KinFPLCAccelEMGLMLumA1=[A1 ActPasTotMomentsLoadsA1(:,2:19)];
KinFPLCAccelEMGLMLumA2=[A2 ActPasTotMomentsLoadsA2(:,2:19)];
KinFPLCAccelEMGLMLumA3=[A3 ActPasTotMomentsLoadsA3(:,2:19)];
KinFPLCAccelEMGLMLumA4=[A4 ActPasTotMomentsLoadsA4(:,2:19)];
KinFPLCAccelEMGLMLumA5=[A5 ActPasTotMomentsLoadsA5(:,2:19)];
KinFPLCAccelEMGLMLumA6=[A6 ActPasTotMomentsLoadsA6(:,2:19)];
KinFPLCAccelEMGLMLumA7=[A7 ActPasTotMomentsLoadsA7(:,2:19)];
KinFPLCAccelEMGLMLumA8=[A8 ActPasTotMomentsLoadsA8(:,2:19)];
KinFPLCAccelEMGLMLumA9=[A9 ActPasTotMomentsLoadsA9(:,2:19)];
KinFPLCAccelEMGLMLumA10=[A10 ActPasTotMomentsLoadsA10(:,2:19)];
```

```
%Plotting passive moments and loads at functional spine unit
subplot(5,2,1);
plotyy(time(:,1),KinFPLCAccelEMGLMLumA1(:,14),time(:,1),KinFPLCAccelEMGLMLumA1(:,105:116))
title('Period 1 Moments Loads')
subplot(5,2,2);
plotyy(time(:,1),KinFPLCAccelEMGLMLumA2(:,14),time(:,1),KinFPLCAccelEMGLMLumA2(:,105:116))
```

```

title('Period 2 Moments Loads')
subplot(5,2,3);
plotyy(time(:,1),KinFPLCAcceleMGLMLumA3(:,14),time(:,1),KinFPLCAcceleMGLMLu
mA3(:,105:116))
title('Period 3 Moments Loads')
subplot(5,2,4);
plotyy(time(:,1),KinFPLCAcceleMGLMLumA4(:,14),time(:,1),KinFPLCAcceleMGLMLu
mA4(:,105:116))
title('Period 4 Moments Loads')
subplot(5,2,5);
plotyy(time(:,1),KinFPLCAcceleMGLMLumA5(:,14),time(:,1),KinFPLCAcceleMGLMLu
mA5(:,105:116))
title('Period 5 Moments Loads')
subplot(5,2,6);
plotyy(time(:,1),KinFPLCAcceleMGLMLumA6(:,14),time(:,1),KinFPLCAcceleMGLMLu
mA6(:,105:116))
title('Period 6 Moments Loads')
subplot(5,2,7);
plotyy(time(:,1),KinFPLCAcceleMGLMLumA7(:,14),time(:,1),KinFPLCAcceleMGLMLu
mA7(:,105:116))
title('Period 7 Moments Loads')
subplot(5,2,8);
plotyy(time(:,1),KinFPLCAcceleMGLMLumA8(:,14),time(:,1),KinFPLCAcceleMGLMLu
mA8(:,105:116))
title('Period 8 Moments Loads')
subplot(5,2,9);
plotyy(time(:,1),KinFPLCAcceleMGLMLumA9(:,14),time(:,1),KinFPLCAcceleMGLMLu
mA9(:,105:116))
title('Period 9 Moments Loads')
subplot(5,2,10);
plotyy(time(:,1),KinFPLCAcceleMGLMLumA10(:,14),time(:,1),KinFPLCAcceleMGLMLu
mA10(:,105:116))
title('Period 10 Moments Loads')
%saveas(gcf,'PosActPassMomLoadSlowSub1')
%saveas(gcf,'PosActPassMomLoadMedSub1')
saveas(gcf,'PosActPassMomLoadFastSub1')
%saveas(gcf,'PosActPassMomLoad20DegSub1')

% save
c:\MATLAB6p5\work\analysis\sub1\CPMSlow\cor\kinfplcaccelemgfsumomloadcorA1slow1
.txt KinFPLCAcceleMGLMLumA1 -ascii -tabs
% save
c:\MATLAB6p5\work\analysis\sub1\CPMSlow\cor\kinfplcaccelemgfsumomloadcorA2slow1
.txt KinFPLCAcceleMGLMLumA2 -ascii -tabs

```

```
% save
c:\MATLAB6p5\work\analysis\sub1\CPMSlow\cor\kinfplcaccelemgsumomloadcorA3slow1
.txt KinFPLCAcceleMGLMLumA3 -ascii -tabs
% save
c:\MATLAB6p5\work\analysis\sub1\CPMSlow\cor\kinfplcaccelemgsumomloadcorA4slow1
.txt KinFPLCAcceleMGLMLumA4 -ascii -tabs
% save
c:\MATLAB6p5\work\analysis\sub1\CPMSlow\cor\kinfplcaccelemgsumomloadcorA5slow1
.txt KinFPLCAcceleMGLMLumA5 -ascii -tabs
% save
c:\MATLAB6p5\work\analysis\sub1\CPMSlow\cor\kinfplcaccelemgsumomloadcorA6slow1
.txt KinFPLCAcceleMGLMLumA6 -ascii -tabs
% save
c:\MATLAB6p5\work\analysis\sub1\CPMSlow\cor\kinfplcaccelemgsumomloadcorA7slow1
.txt KinFPLCAcceleMGLMLumA7 -ascii -tabs

% save
c:\MATLAB6p5\work\analysis\sub1\CPMMed\cor\kinfplcaccelemgsumomloadcorA1med1.
txt KinFPLCAcceleMGLMLumA1 -ascii -tabs
% save
c:\MATLAB6p5\work\analysis\sub1\CPMMed\cor\kinfplcaccelemgsumomloadcorA2med1.
txt KinFPLCAcceleMGLMLumA2 -ascii -tabs
% save
c:\MATLAB6p5\work\analysis\sub1\CPMMed\cor\kinfplcaccelemgsumomloadcorA3med1.
txt KinFPLCAcceleMGLMLumA3 -ascii -tabs
% save
c:\MATLAB6p5\work\analysis\sub1\CPMMed\cor\kinfplcaccelemgsumomloadcorA4med1.
txt KinFPLCAcceleMGLMLumA4 -ascii -tabs
% save
c:\MATLAB6p5\work\analysis\sub1\CPMMed\cor\kinfplcaccelemgsumomloadcorA5med1.
txt KinFPLCAcceleMGLMLumA5 -ascii -tabs
% save
c:\MATLAB6p5\work\analysis\sub1\CPMMed\cor\kinfplcaccelemgsumomloadcorA6med1.
txt KinFPLCAcceleMGLMLumA6 -ascii -tabs
% save
c:\MATLAB6p5\work\analysis\sub1\CPMMed\cor\kinfplcaccelemgsumomloadcorA7med1.
txt KinFPLCAcceleMGLMLumA7 -ascii -tabs
% save
c:\MATLAB6p5\work\analysis\sub1\CPMMed\cor\kinfplcaccelemgsumomloadcorA8med1.
txt KinFPLCAcceleMGLMLumA8 -ascii -tabs
% save
c:\MATLAB6p5\work\analysis\sub1\CPMMed\cor\kinfplcaccelemgsumomloadcorA9med1.
txt KinFPLCAcceleMGLMLumA9 -ascii -tabs
```

```

% save
c:\MATLAB6p5\work\analysis\sub1\CPMMed\cor\kinfplcaccelemgfsumomloadcorA10med
1.txt KinFPLCAcceleMGLMLumA10 -ascii -tabs

save
c:\MATLAB6p5\work\analysis\sub1\CPMFast\cor\kinfplcaccelemgfsumomloadcorA1fast1.t
xt KinFPLCAcceleMGLMLumA1 -ascii -tabs
save
c:\MATLAB6p5\work\analysis\sub1\CPMFast\cor\kinfplcaccelemgfsumomloadcorA2fast1.t
xt KinFPLCAcceleMGLMLumA2 -ascii -tabs
save
c:\MATLAB6p5\work\analysis\sub1\CPMFast\cor\kinfplcaccelemgfsumomloadcorA3fast1.t
xt KinFPLCAcceleMGLMLumA3 -ascii -tabs
save
c:\MATLAB6p5\work\analysis\sub1\CPMFast\cor\kinfplcaccelemgfsumomloadcorA4fast1.t
xt KinFPLCAcceleMGLMLumA4 -ascii -tabs
save
c:\MATLAB6p5\work\analysis\sub1\CPMFast\cor\kinfplcaccelemgfsumomloadcorA5fast1.t
xt KinFPLCAcceleMGLMLumA5 -ascii -tabs
save
c:\MATLAB6p5\work\analysis\sub1\CPMFast\cor\kinfplcaccelemgfsumomloadcorA6fast1.t
xt KinFPLCAcceleMGLMLumA6 -ascii -tabs
save
c:\MATLAB6p5\work\analysis\sub1\CPMFast\cor\kinfplcaccelemgfsumomloadcorA7fast1.t
xt KinFPLCAcceleMGLMLumA7 -ascii -tabs
save
c:\MATLAB6p5\work\analysis\sub1\CPMFast\cor\kinfplcaccelemgfsumomloadcorA8fast1.t
xt KinFPLCAcceleMGLMLumA8 -ascii -tabs
save
c:\MATLAB6p5\work\analysis\sub1\CPMFast\cor\kinfplcaccelemgfsumomloadcorA9fast1.t
xt KinFPLCAcceleMGLMLumA9 -ascii -tabs
save
c:\MATLAB6p5\work\analysis\sub1\CPMFast\cor\kinfplcaccelemgfsumomloadcorA10fast1.
txt KinFPLCAcceleMGLMLumA10 -ascii -tabs

% save
c:\MATLAB6p5\work\analysis\sub1\CPM20Deg\cor\kinfplcaccelemgfsumomloadcorA120d
eg1.txt KinFPLCAcceleMGLMLumA1 -ascii -tabs
% save
c:\MATLAB6p5\work\analysis\sub1\CPM20Deg\cor\kinfplcaccelemgfsumomloadcorA220d
eg1.txt KinFPLCAcceleMGLMLumA2 -ascii -tabs
% save
c:\MATLAB6p5\work\analysis\sub1\CPM20Deg\cor\kinfplcaccelemgfsumomloadcorA320d
eg1.txt KinFPLCAcceleMGLMLumA3 -ascii -tabs

```



```
% save
c:\MATLAB6p5\work\analysis\sub1\CPM20Deg\cor\kinfplcaccelemgfsumomloadcorA420d
eg1.txt KinFPLCAcceleMGLMLumA4 -ascii -tabs
% save
c:\MATLAB6p5\work\analysis\sub1\CPM20Deg\cor\kinfplcaccelemgfsumomloadcorA520d
eg1.txt KinFPLCAcceleMGLMLumA5 -ascii -tabs
% save
c:\MATLAB6p5\work\analysis\sub1\CPM20Deg\cor\kinfplcaccelemgfsumomloadcorA620d
eg1.txt KinFPLCAcceleMGLMLumA6 -ascii -tabs
% save
c:\MATLAB6p5\work\analysis\sub1\CPM20Deg\cor\kinfplcaccelemgfsumomloadcorA720d
eg1.txt KinFPLCAcceleMGLMLumA7 -ascii -tabs
% save
c:\MATLAB6p5\work\analysis\sub1\CPM20Deg\cor\kinfplcaccelemgfsumomloadcorA820d
eg1.txt KinFPLCAcceleMGLMLumA8 -ascii -tabs
% save
c:\MATLAB6p5\work\analysis\sub1\CPM20Deg\cor\kinfplcaccelemgfsumomloadcorA920d
eg1.txt KinFPLCAcceleMGLMLumA9 -ascii -tabs
% save
c:\MATLAB6p5\work\analysis\sub1\CPM20Deg\cor\kinfplcaccelemgfsumomloadcorA1020
deg1.txt KinFPLCAcceleMGLMLumA10 -ascii -tabs
```

BIBLIOGRAPHY

1. Salter RB. The biologic concept of continuous passive motion of synovial joints. The first 18 years of basic research and its clinical application. Clin Orthop 1989;242:12-25.
2. O' Driscoll SW, Kumar A, and Salter RB. The effect of the volume of effusion, joint position and continuous passive motion on intraarticular pressure in the rabbit knee. J Rheumatol 1983;10:360-3.
3. Coutts R.D. A Conversation with Richard D. Coutts, MD – Continuous Passive Motion in the Rehabilitation of the Total Knee Patient, Its Role and Effect. Orthopaedic Review 1986;15:126-34.
4. Salter RB, Simmonds DF, Malcom BW, Rumgle EJ, MacMichael D, and Clenents ND. The Biological Effect of Continuous Passive Motion on the Healing of Full Thickness Defects in Articular Cartilage. JBJS 1980;62A:1232-51.
5. O' Driscoll SW and Giori NJ. Continuous passive motion (CPM): theory and principles of clinical application. J Rehabil Res Dev 2000;37:179-88.
6. Triano .J. Biomechanics of spinal manipulation. The Spine 2001;1:121-30.
7. White AA, Panjabi M.M. Clinical Biomechanics of the Spine. Second ed. Philadelphia: J.B.Lippincott Company, 1990:49.
8. Panjabi MM. The Stabilizing System of the Spine. Part I. Function, Dysfunction, Adaptation, and Enhancement. J Spinal Disord 1992;5:383-9.
9. Pope MH and DeVocht J.W. The clinical relevance of biomechanics. Neurological clinics of North America 1999;17:17-40.

10. van Deursen DL, Lingsfeld M, Snijders CJ, Evers JJM, and Gordon MJ.
Mechanical effects of continuous passive motion on the lumbar spine in seating. *J Biomech* 2000;33:695-700.
11. Reinecke SM, Hazard R.G., and Coleman K. Continuous passive motion in seating: a new strategy against low back pain. *J Spinal Disord* 1994;7:29-35.
12. Triano J and Schultz AB. Loads transmitted during lumbosacral spinal manipulative therapy. *Spine* 1997;22:1955-64.
13. Bergmark, A. Mechanical stability of the human lumbar spine. 1-85. 1987. Lund University, Department of Solid Mechanics.
14. White A., Panjabi M.M. *Clinical Biomechanics of the Spine*. 2nd ed. Philadelphia: J.B. Lippincott, 1990.
15. White AA, Panjabi MM. *Clinical biomechanics of the spine*, ed 2. 2nd ed. Philadelphia: JB Lippincott, 1999.
16. Frymoyer JW, Nachemson A. Natural History of Low Back Disorders. In: Frymoyer JW, ed. *The Adult Spine Principles and Practice*. New York: Raven Press, 1991:1537-50.
17. O' Driscoll SW, Kumar A, and Salter RB. The Effect of Continuous Passive Motion on the Clearance of a Hemarthrosis from a Synovial Joint: An Experimental Investigation in the Rabbit. *Clinical Orthopaedics and Related Research*. 1983;176:305.
18. Rogers CM and Triano J.J. Biomechanical measure validation for spinal manipulation in clinical settings. *JMPT* 2003;26:539-48.

19. Bennett W.S. Control and measurement of unintentional electromagnetic radiation. New York: John Wiley & Sons, Inc., 1997.
20. Finneran MT. Physiologic imaging of the low back: Normative values for large array surface electromyography. Disability 2001;August:15-21.
21. Pease WS, Clairmont AC, and Finneran MT. Large array surface electromyography in acute low back pain: A preliminary analysis. Spine 2004;In submission.
22. Chaffin D.B., Andersson G.B. Occupational Biomechanics. 2nd ed. New York: John Wiley & Sons Inc., 1991:215-39.
23. Chaffin DB. Biomechanical Modeling for Simulation of 3D Static Human Excerptions. Computer Applications in Ergonomics, Occupational Safety and Health. London: Elsevier Publishers, 1992.
24. McGill S.M. A Myoelectrically Based Dynamic Three-Dimensional Model To Predict Loads On Lumbar Spine Tissues During Lateral Bending. J Biomech 1992;25:395-414.
25. Schultz A.B., Andersson G.B.J., Haderspeck K., Ortengren R., Nordin M., and Bjork B. Analysis and measurement of lumbar trunk loads in tasks involving bends and twists. J Biomechanics 1982;15:669-75.
26. Delagi EF, Iazzetti J, Perotto A, Morrison D. . Anatomic Guide for the Electromyographer: The Limbs. Springfield: Charles C. Thomas, 1981.

27. Regents of UofM. 3D Static Strength Prediction Program Manual. Regents of UofM. (4.3). 2005. Ann Arbor, MI, University of Michigan. Ref Type: Serial (Book, Monograph)
28. Anderson CK, Chaffin DB, and Herrin GD. A Study of Lumbosacral Orientation under Varied Static Loads. *Spine* 1986;11:456-62.
29. Chaffin D.B., Andersson G. Occupational biomechanics. New York: John Wiley & Sons, 1984:182-7.
30. Mendenhall W, Beaver RJ, Beaver BM. Introduction to Probability and Statistics. 11th ed. Pacific Grove, CA: Tomson Brooks/Cole, 2003.
31. Andersson G.B., Schultz A.B., and Nachemson A.L. Intervertebral Disc Pressures During Traction. *Scan Dj Rehabil Med Suppl* 1983;9:88-91.
32. Wynarski GT and Schultz A.B. Optimization of skeletal configuration: studies of scoliosis correction biomechanics. *J Biomech* 1991;24:720-32.

VITAE

Jennifer Marie Diederich was born in Aurora, Illinois, on June 30, 1974, the daughter of Nancy Jean White and John Arthur Diederich. Jennifer received her Bachelor of Science in Mechanical Engineering from the Oklahoma State University in May 1998. Upon graduation she entered the aeronautical industry at Lockheed Martin in the F-22 program. In the fall of 1999 she began graduate studies in Biomedical Engineering and focused on biomechanics of the spine at the Texas Back Institute. In 2003 she started as a Biomechanical Engineer at Innovative Spinal Technologies; a company developing spine related technology. She was awarded the Master of Science degree from the Joint Biomedical Engineering Program at The University of Texas Southwestern Medical School and The University of Texas at Arlington in May, 2005.

Permanent Address: 6820 North Preston Road Apt. 616

Plano, TX 75024